Marine terminating ice-stream retreat within the Eyjafjarðaráll basin, North Iceland; documented by multibeam bathymetric and high-resolution Chirp reflection data

Bailey OConnell

Faculty of Earth Sciences
University of Iceland
2020

Marine terminating ice-stream retreat within the Eyjafjarðaráll basin, North Iceland; documented by multibeam bathymetric and high-resolution Chirp reflection data

Bailey OConnell

60 ECTS thesis submitted in partial fulfillment of a
Magister Scientiarum degree in Earth Sciences

MS Committee
Bryndís Brandsdóttir
Ásta Rut Hjartardóttir

Master's Examiner
Ívar Örn Benediktsson

Faculty of Earth Sciences
School of Engineering and Natural Sciences
University of Iceland
Reykjavik, June 2020

Marine ice-stream retreat within the Eyjafjarðaráll basin, North Iceland; documented by multibeam bathymetric and high-resolution Chirp reflection data

Marine glacial features offshore North Iceland
60 ECTS thesis submitted in partial fulfillment of a *Magister Scientiarum* degree in Earth Sciences

Faculty of Earth Sciences
School of Engineering and Natural Sciences
University of Iceland
Sturlugata 7
101, Reykjavik
Iceland

Telephone: 525 4000

Bibliographic information:
Bailey OConnell, 2020, Marine ice-stream retreat within the Eyjafjarðaráll basin, North Iceland; documented by multibeam bathymetric and high-resolution Chirp reflection data, Master’s thesis, Faculty of Earth Sciences, University of Iceland, pp. 85.

Printing: June 2020
Reykjavik, Iceland, June 2020

Abstract

The behavior and retreat of the Icelandic Ice Sheet (IIS) is not well understood and research done on the shelf can help refine ice sheet models. Multibeam bathymetric maps and Chirp shallow-reflection data offshore N-Iceland provide some answers to long-standing questions about the extent of the Iceland ice sheet during the Last Glacial Maximum (LGM) and early deglaciation of the Eyjafjarðaráll ice stream. The glacially eroded Eyjafjarðaráll rift basin (EB) is ~80 km NS and 15-20 km wide EW and made up of complex extensional (normal) and transform (strike-slip) faults draped by ice-marginal and subglacial sedimentary features, megascale glacial lineations (MSGLs), moraines, eskers, and unidentified complex till ridge features, which have not been previously described in literature, possibly representing a push moraine or lateral crevasse-squeeze ridges. These features reflect the past ice flow directions of at least two major ice streams, from Skagafjörður into Skagafjarðardjúp and from Eyjafjörður into the southern Eyjafjarðaráll basin. These ice streams merged in the northern Eyjafjarðaráll basin, where the more prominent Skagafjörður ice stream deflected the Eyjafjarðaráll ice stream. The megaflutes are orientated parallel to the direction of the major basins and the Kolbeinsey Ridge indicating that the ice streams were topographically constrained. Similar lineations are also present within Skjálfandadjúp, east of Eyjafjarðaráll. The highly reflective V-shaped ridges are characterized by elongated “V-shape” formations with an average width of 300-500 m and an average length ranging from 400-1500 m, at a depth of 320-450 meters b.s.l. opening towards the flow direction of the main ice stream. The ridges change direction gradually, along with the basin curvature, from NNW-SSE in the southern part of the basin rotating to NNE-SSW, parallel to a 10 km long lateral moraine, which most likely separated two main ice streams. These ridges have not been identified elsewhere. The seafloor also bears ample scars made by icebergs from the IIS during the last Glacial as well as postglacial icebergs from the Greenland Ice Sheet (GIS). The faults present in the EB cut through the glacial features, indicating extensional activity within the EB after the deposition of the glacial features and throughout Holocene based on sedimentary structures and current seismicity. Analysis of the landsystems found throughout EB are useful to refine models of the IIS and could place the terminal position of several ice streams further offshore than previously thought.

Útdráttur

Fjölgeislamælingar af hafsbotninum ásamt há-upplausnar endurkastsmælingum úti fyrir Norðurlandi hafa varpað nýju ljósi á útbreiðslu og hörfunarsögu skriðjökla ísaldar. Ummerki jöklunar á svæðinu endurspegla skrið Skagafjarðarjökla norður í Skagafjarðardjúp, Eyjafjarðarjökla norður í Eyjafjarðarál og jökla frá Skjálfandaflóa norður í Skjálfandadjúp. Jökulkembur sýna að þessir megin jöklar sameinuðust og runnu saman a.m.k. 100 km út á landgrunnið, að sunnanverðum Kolbeinseyjarhrygg. Margbreytileg ummerki jöklunar má greina á hafsbotni í hinum ~80 km langa og 15-20 km breiða Eyjafjarðarál; þar liggja jökulgarðar af ýmsu tagi, jökulkembur og sérkennilegir V-laga hryggir eru sums staðar sundurskornir af miklum misgengjum. Landgrunnið er einnig alsett ísjakarákum, sumar hugsanlega frá ísaldarlokum. Misgengin endurspegla gliðnunar- (siggengi) og skerhreyfingar (sniðgengi) eftir að jöklar hurfu af svæðinu. Myndunarsaga V-laga hryggjanna er aðalumfangsefni þessa verkefnis. Hryggirnir eru að meðaltali 400-1500 m langir, 300-500 m breiðir, og mynda öfugt-V eftir skriðstefnu jökulsins. Lega hryggjanna eftir bugðum Eyjafjarðaráls endurspeglar einnig breytingar í skriðstefnu jökulsins. Hryggirnir stefna NNV-SSA í sunnanverðum Eyjafjarðarál en NNA-SSV í honum norðanverðum, þar sem þeir liggja samsíða um 10 km langrar jaðarurðar. Stefnubreytingin í norðanveðrum Eyjafjarðarál er líklega tilkomin vegna samruna skriðjökulsins úr Skagafjarðardjúpi við jökulinn í Eyjafjarðarál, sem ætla má, út frá landslagi, að hafi verið mun minni. Endurkastsmælingar sýna að V-laga hryggirnir eru úr hörðu efni (með háan endurkastsstuðul) og að þá er einnig að finna undir lausum setlögum í botni álsins. Sambærilegum V-laga jarðmyndunum hefur ekki verið lýst annars staðar frá. Hryggirnir eru líklegast myndaðir við framskrið jökuljaðarsins og hugsanlega tengdir aflögun á botnseti jökulsins upp í botnsprungur undan skriðþunga hans. Hliðar þeirra eru stundum mislangar og tengjast jökulkembum eða jaðargörðum sem liggja eftir skriðstefnu jökulsins.

Table of Contents

List of Figures

List of Tables

Abbreviations

CSR: Crevasse Squeeze Ridge

DL: Dalvík Lineation

E: Eyjafjarðaráll

EB: Eyjafjarðaráll Basin

EP: Eurasian Plate

GIS: Greenland Ice Sheet

GOR: Grímsey Oblique Ridge

GZW: Grounding Zone Wedge

HFF: Húsavík Flatey Fault

IIS: Icelandic Ice Sheet

KR: Kolbeinsey Ridge

LGM: Last Glacial Maximum

MSGL: Megascale Glacial Lineation

NAP: North American Plate

NGRIP: North Greenland Ice Core Project

NVZ: Northern Volcanic Zone

TFZ: Tjörnes Fracture Zone

Acknowledgements

I would like to thank my supervisors, Bryndís Brandsdóttir and Ásta Rut Hjartardóttir for our weekly meetings, whether they were in person or online. Thank you for all the books and literature you sent to me and for your help whenever I ran into a GIS problem or needed help in figure making. Thank you for your feedback and comments throughout the process of writing my thesis.

I would also like to thank my family and friends for their constant positivity, and mental and emotional support throughout my studies and thesis writing. You all believed in me when everything felt impossible. So thank you mom, dad, Joy, Kristján, Maria, Kyle, Michael, Carly, Dave, and everyone else.

1 Introduction

Ice streams are corridors of fast flowing ice extending from ice sheets and a large source of mass removal from ice sheets (Bennett, 2003; Morgan et al., 1982; Rignot et al., 2011; Spagnolo et al., 2014). Ice streams can flow up to 1000s of meters per year. Winsborrow et al., (2010) suggested a hierarchy of controls that influence the location of ice streams, though many studies (Alley et al., 1986; Engelhardt and Kamb, 1997; Tulaczyk et al., 2001) suggest the primary factor for ice stream formation is a soft sedimentary bed (Spagnolo et al., 2014). Examples of modern ice streams can be found in Antarctica (Joughin et al., 1999; Rignot et al., 2011), Svalbard, and Greenland (Joughin et al., 2010), where they account for 90% of mass loss in Antarctica and 50% mass loss in Greenland (Bamber et al., 2010; van den Broeke et al., 2009; Margold et al., 2015). Modern ice streams are difficult to study due to the inaccessibility of the ice-bed interface, so research done on paleo-ice streams is valuable in understanding modern ice stream areas (Winsborrow et al., 2004; Spagnolo et al., 2014).

Glacial landforms are indicators of paleo ice sheet extent and behavior, however, the conditions under which specific landforms and landform assemblages form can be very unique (Stokes and Clark, 1999; Ó Cofaigh, et al. 2002). Offshore Iceland, paleo-ice stream landforms are being researched as analogues to modern ice streams (e.g. Principato et al., 2016). The insular shelf of Iceland has been incised by ice streams through repeated glaciations, represented by fjords around most of its coastline (Figure 1). At the Last Glacial Maximum (LGM, ~23kya), the Icelandic Ice Sheet (IIS) terminated in the ocean and has been considered to have reached as far as the shelf break (Pétursson et al., 2015). A paleo ice stream extended past Grímsey, an island 40 km offshore north Iceland, during the LGM (Einarsson, 1967; Norðdahl, 1991; Pétursson, 2015; Patton et al., 2017). Tephrochronological data from a 37 m long MD99-2275 (MD-75) marine sediment core within the Skjálfandi basin, ~21 km east of Eyjafjarðaráll (Søndergaard, 2005; Gudmundsdóttir, 2010) indicates that ice streams on the NE-Iceland shelf retreated beyond the shoreline, by 14-15 kya (Magnúsdóttir et al., 2015).

Multibeam bathymetric mapping has revealed offshore marine glacial landforms which call for refined models of the extent and behavior of individual ice streams from the IIS at the LGM and the following period of rapid retreat (Pétursson et al., 2015; Patton et al., 2017). Eyjafjarðaráll is the seaward extension of the ~60 km long fjord Eyjafjörður. The ~85 km long N-S and 10-20 km wide Eyjafjarðaráll has been eroded by large ice streams from Eyjafjörður and Skagafjörður and faulted by tectonics related to the Tjörnes fracture zone, a transform zone which connects the Northern Volcanic Rift Zone with the Kolbeinsey ridge to its north (Einarsson, 2008). Evidence of the Eyjafjarðaráll paleo-ice stream is found on the sea floor in the form of megascale glacial lineations, moraines, eskers, and V-shaped ridges, seemingly associated with grounding zone wedges.

This thesis aims to describe and identify landform assemblages in the Eyjafjarðaráll basin (EB), North Iceland, specifically the V-shaped ridges which thus far seem to be unique to this location. I hypothesize the V-shaped ridges' origin and attempt to further understand the extent and behavior of the ice streams in North Iceland as indicated by these features. The presence of other glacial features seen in the EB are described as well with reference to the characteristics of individual ice streams. How far north did the ice stream extend at the LGM? What evidence do we see in the landform assemblages that shows us that the retreat of the ice stream was step like? How many grounding areas do we see?

Tectonics within the Eyjafjarðaráll Basin and along the Húsavík-Flatey Faults (HFF) will be minimally discussed, mostly where it is necessary in the description of the glacial features.

1.1 Regional Setting

Iceland is located on the Mid-Atlantic Ridge within the North Atlantic Ocean, straddling the arctic circle. It has been shaped over the past >15 million years by a volcanism and repeated glaciations to create a unique location for studying the glacial history of the Arctic (Geirsdóttir and Eiríksson, 1994, 1996; Geirsdóttir, 2004; Geirsdóttir et al., 2007; Eiríksson, 2008; Sigmundsson et al., 2018). Iceland was created from a combination of the magmatism of the Mid-Atlantic Ridge and a mantle plume fed hot spot located below the crust, thus making the island oldest in the eastern and western most extensions and youngest within the Neovolcanic zone (Figure 2) (Geirsdóttir et al., 2007; Einarsson, 2008; Sigmundsson et al., 2018). It is predominately basaltic, with small percentages (>5%) of rhyolite and andesite also present (Sigmundsson et al., 2018).

Iceland´s volcanism has had a large impact on the glaciations which have occurred there. Firstly, the geothermal activity, which is concurrent with Iceland's volcanically active zone, control on the basal motion of glaciers is high in Iceland relative to other landmasses hosting glaciers and ice sheets, i.e. Greenland and Antarctica (Bourgeois et al., 2000; Hubbard et al., 2006). Secondly, volcanism is affected by the isostatic depression and rebound which occurs with the advancement and retreat of large ice sheets. This combination of volcanism and geothermal activity in turn results in decoupling and fast flow of outlet glaciers and ice streams, and rapid potential destabilization and break-up of the ice streams (Hubbard et al., 2006).

Part of the mid-Atlantic plate boundary is exposed subaerially on the surface of Iceland, dividing the island between the North American Plate (NAP) to the west and the Eurasian Plate (EP) to the east, which govern the general spreading process in Iceland (Sigmundsson, 2018). On land, the boundary between the plates is known as the Northern Volcanic Zone (NVZ) which connects to the TFZ, one of two seismically active transform zones in Iceland, to the north. The TFZ extends through Eyjafjörður and connects to the Kolbeinsey Ridge (KR) just north of EB (Einarsson, 1991, 2008; Hjartardóttir et al., 2015; Sigmundsson 2018). The TFZ is seismically active, along three major NW trending seismic zones: the Dalvík lineament (DL), the Grímsey Oblique Rift (GOR) and the Húsavík-Flatey Fault System (HFF) (Einarsson, 2008; Stefánsson et al., 2008). Of these three components, the HFF runs through the southern EB (Figure 1) which has resulted in widespread faulting and fissures throughout the basin.

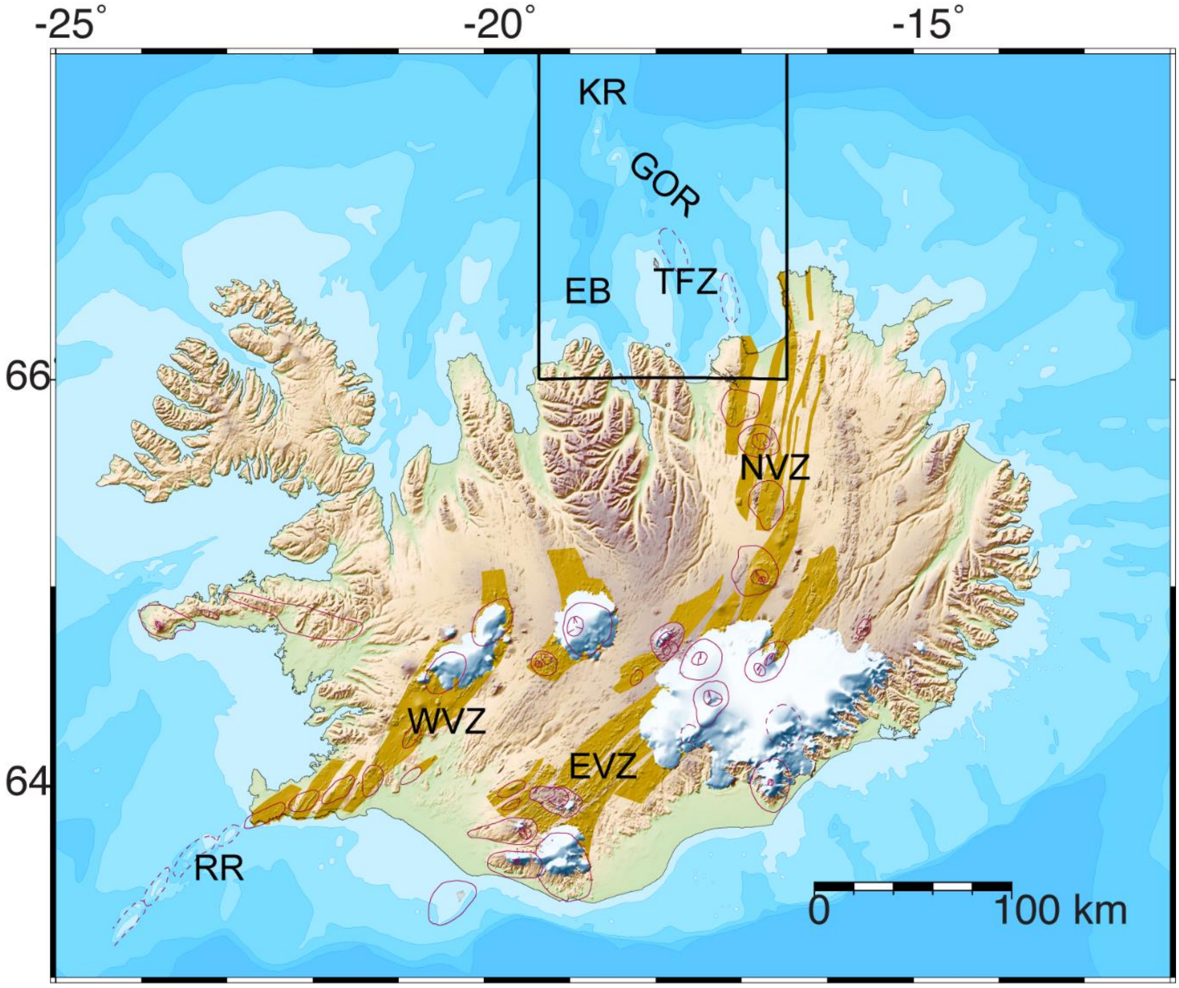

Figure 1. *Map of Iceland and tectonic connection to the plate boundary (Einarsson and Sæmundsson, 1987).The map has a black box around the study area, the Eyjafjarðaráll (EB) and Skjálfandadjúp rift basins, Labels are shown for the Northern Volcanic Zone (NVZ), the*

Kolbeinsey Ridge (KR), Grímsey Oblique Ridge (GOR), Tjörnes Fracture Zone (TFZ), Western Volcanic Zone (WVZ) Eastern Volcanic Zone (EVZ), and Reykjanes Ridge (RR),

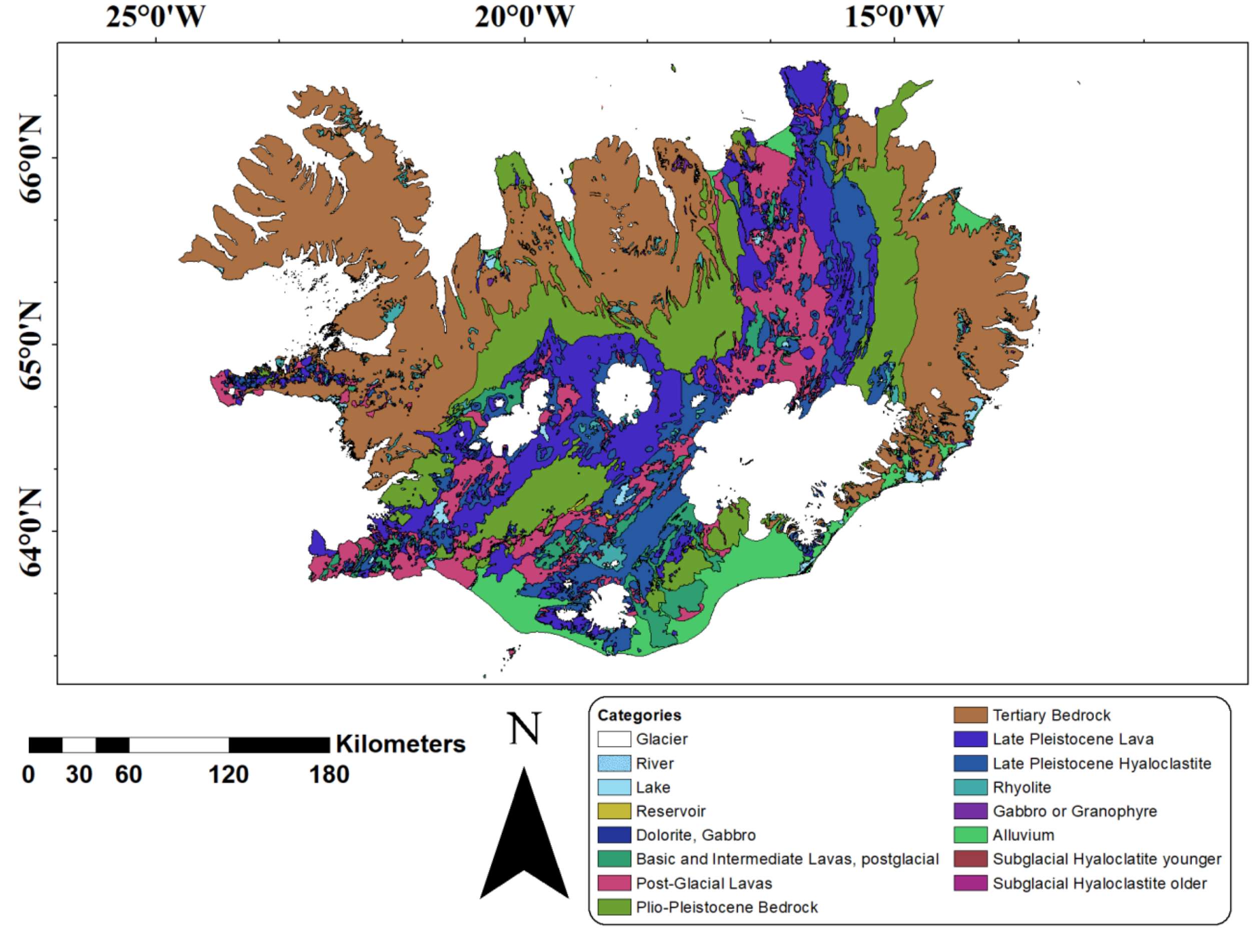

Figure 2. Geological map of Iceland. (Jóhannesson, H. and Sæmundsson, K., 1998.)

1.2 Glacial history

Iceland has experienced multiple glaciations throughout its history which have shaped the landscape both on- and offshore. Iceland began to experience glaciations about 3.8 mya on local mountain massifs and the oldest regional glaciation began at 2.5 mya, but glaciers existed possibly as early as 7 mya in high relief mountainous areas and volcanic centers (Eiríksson, 2008, Sigmundsson et al., 2018). Iceland has experienced up to 20 glaciations since the onset of glaciation (Geirsdóttir et al., 2007; Sigmundsson, 2018). The most recent glaciation, the Weichselian, began approximately 100 kya, reaching its maximum extent approximately 25-21 kya at the LGM and ending approximately 10 kya (Hubbard et al., 2006; Geirsdóttir et al., 2007; Ingólfsson et al., 2010; Patton et al., 2017).

During the LGM, Iceland was considered to have been covered continuously by an ice sheet which in parts exceeded 2000 m in thickness (Norðdahl et al., 2008) and at the peak of the

LGM, the ice sheet is thought to have extended as far out as the shelf surrounding Iceland and was in fact largely marine-based (Figure 3) (Geirsdóttir, 2004; Patton et al., 2017). In north Iceland, evidence such as till deposits and glacial striae indicate that this ice sheet extended past Grímsey island, which lies 40 km offshore (Figure 4, Norðdahl et al., 2008) and further north to the southern Kolbeinsey Ridge (Patton et al., 2017). Compared to the southern Iceland shelf, north Iceland troughs tend to be of a greater width, length, and depth which is attributed to a more convergent flow pattern of ice streams causing higher ice velocities and flux (Clark and Spagnolo, 2016), but higher sedimentation closer to the ice margin could also be a factor as well as narrower shelf edge, i.e. offshore calving of the broad S-Iceland ice stream (Figure 3).

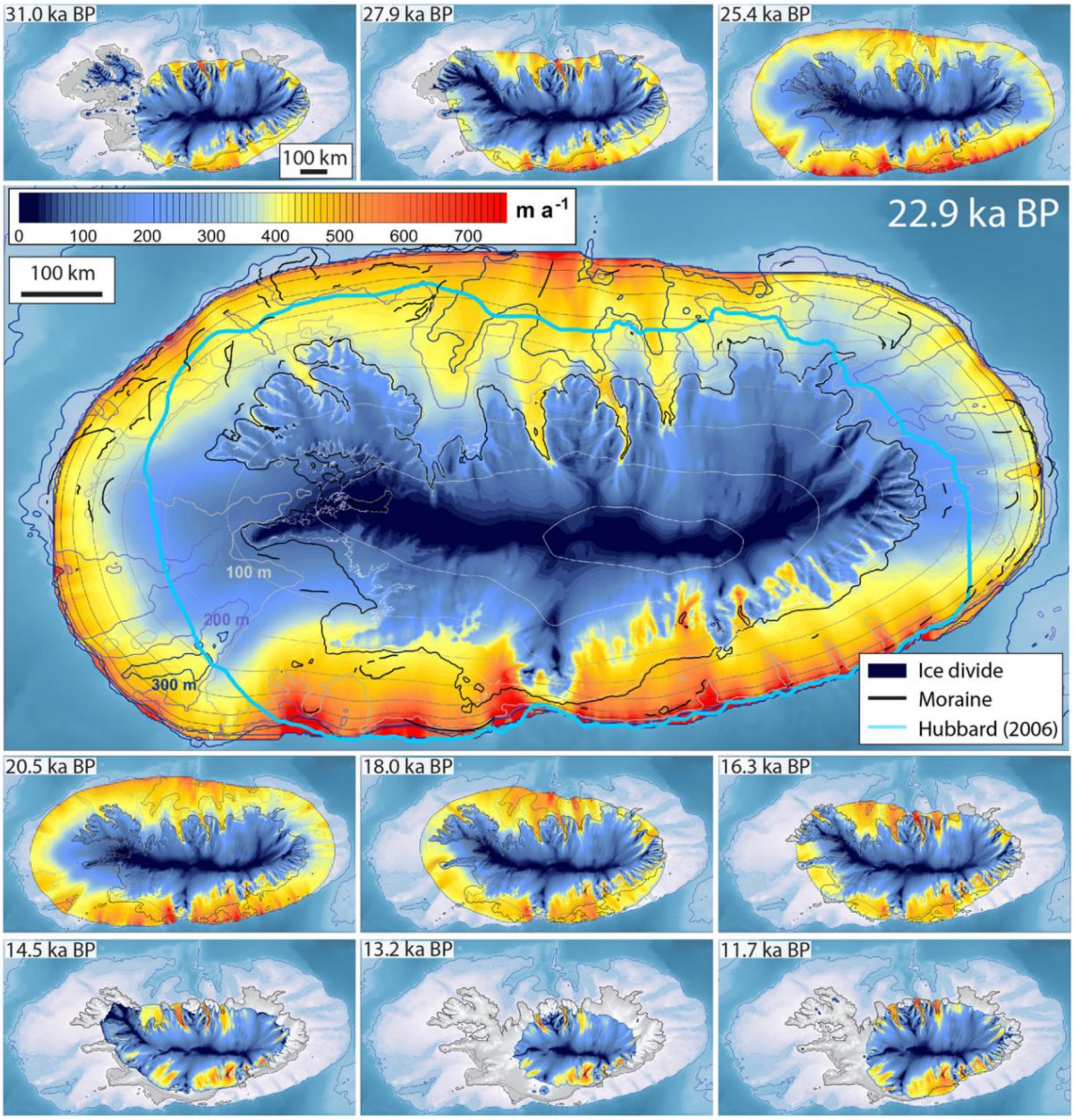

Figure 3. Modelled ice velocities and extent of the IIS as determined by Patton et al., 2017 and Hubbard et al., 2006 (blue line). Note maximum extent of the IIS offshore N-Iceland at 22.9 ka BP, covering the southern part of the Kolbeinsey Ridge.

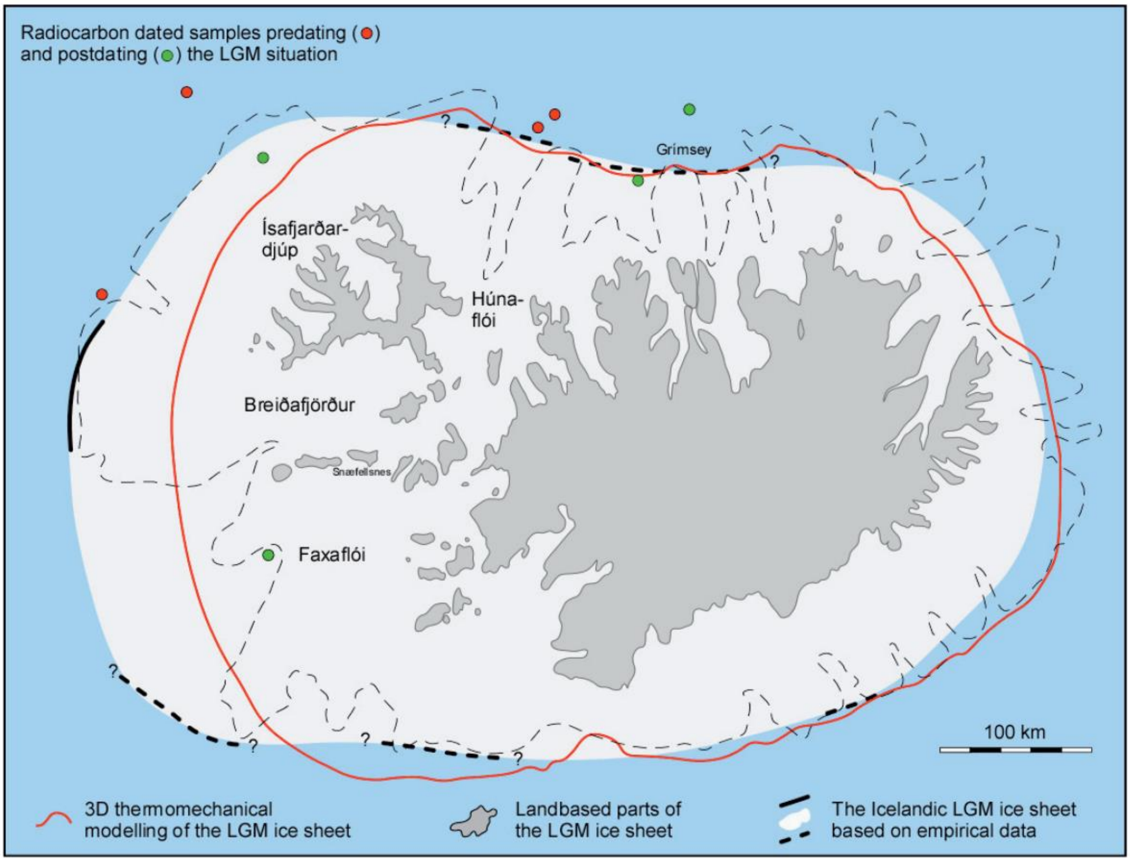

Figure 4. The extent of the Iceland ice sheet at the Last Glacial Maximum , based on geophysical evidence along with radiocarbon dates. From Norðdahl et al., (2008).

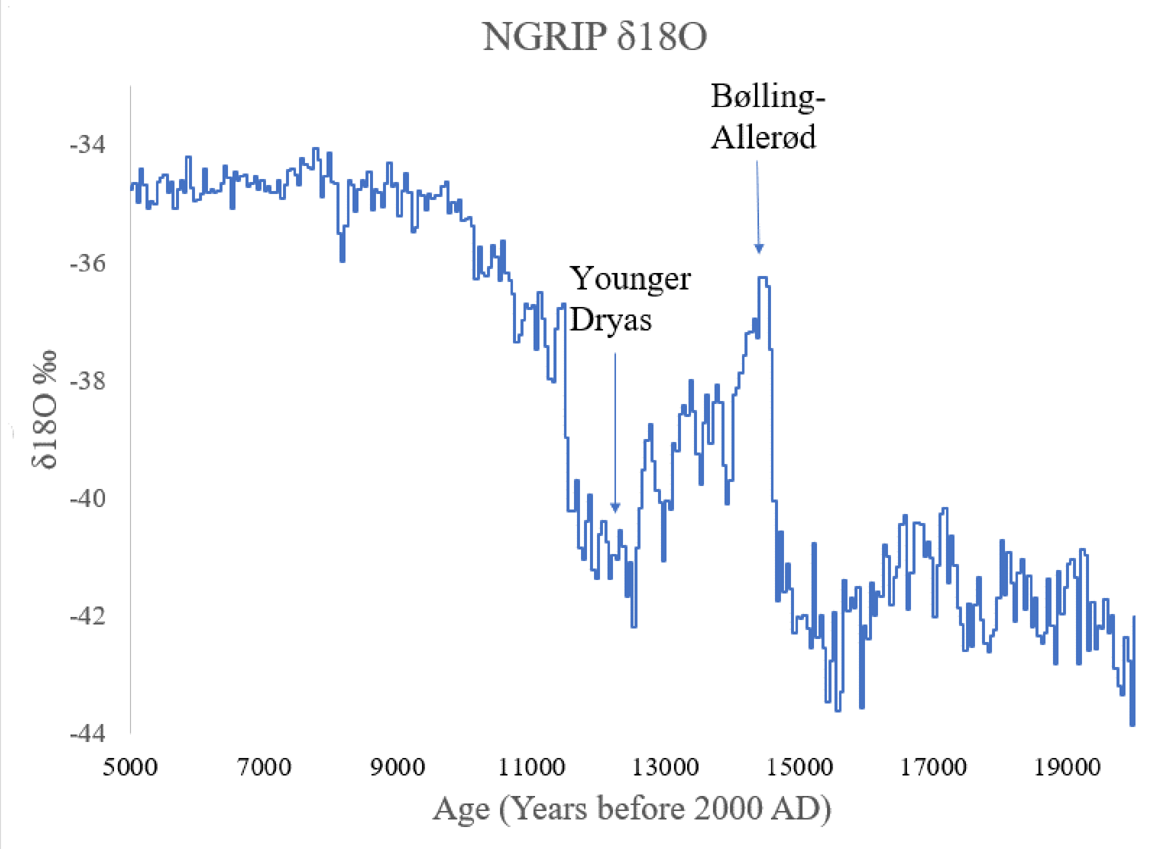

Figure 5. $\delta^{18}O$ data collected from the NGRIP ice core in Greenland, used for climate reconstruction. Higher values are correlated with warmer temperatures and vice versa. Note the increase in $\delta^{18}O$ values during the Bølling-Allerød period and subsequent lower $\delta^{18}O$ values during the Younger Dryas period, and finally the sharp increase after the Younger Dryas, marking the beginning of the Holocene. Data from North Greenland Ice Core Project members (2004).

The retreat of the IIS is considered to have been rapid and step-like, caused by a rapid rise in the eustatic sea level and the northward retreat of the Polar Front between 18.6 and 15 kya (Figure 3, panels 6-8; Geirsdóttir et al., 2007; 2009; Norðdahl and Ingólfsson, 2015; Patton et al., 2017; Pétursson et al., 2015). This was followed by a period of warming known as the Bølling-Allerød interstitial between approximately 14.7 and 13 kya (Figure 3, panels 8 and 9; Ingólfsson et al., 2010). Sedimentological analysis show that the ice margin had retreated from the N-Iceland insular shelf by approximately 13 kya, in past the present coastline in the northeast and southwest of Iceland in early Bølling time (Principato et al., 2005; Norðdahl et al., 2008; Geirsdóttir et al., 2009; Ingólfsson et al., 2010), indicating that any exposed subglacial features are over 13 thousand years old. A lack of further age constraining data within subglacial features in the EB make it impossible to state an exact age of formation.

The Younger Dryas, between ~12.7 and ~11 kya, (Figure 5) was a period of cooling following the Bølling-Allerød interstitial. The Younger Dryas readvancement of the IIS in several areas, has been debated (Geirsdóttir et al., 2007; Ingólfsson et al., 2010). Based on Patton et al., (2017) the IIS position was located within Eyjafjörður at 13.2 ka and extended to the mouth of the fjord at the end of the Younger Dryas (Figure 3). The presence of the Saksunarvatn tephra layer in lake sediments in the Fnjóskadalur valley, east of inner Eyjafjörður was ice-free area by the time of the eruption, approximately 12.1 kya BP, though there is evidence for an outlet glacier within Eyjafjörður at this time, reaching the island of Hrísey (Norðdahl and Hafliðason, 1992; Ingólfsson et al., 2010; Pétursson et al., 2015).

Four glacier readvancements have been suggested between the onset of the Bølling-Allerød and the end of the Younger Dryas (Geirsdóttir et al., 2007), including one prominent advancement between 11.5 and 10.1 ka which resulted in the formation of the Búði moraines in Southern Iceland (Hjartarson and Ingólfsson, 1988; Geirsdóttir et al., 1997, 2000, 2007), and up to 7 moraines created during a short lived glacial readvances (Jóhannesson, 1985; Axelsdóttir, 2002; Norðdahl and Pétursson, 2005; Norðdahl, et al. 2008; Ingólfsson, et al. 2010). The younger, inner moraine being radiocarbon dated to approx. 11.2 kya (Norðdahl, et al. 2008; Ingólfsson, et al. 2010). By this time, the IIS began a very rapid retreat up until it was completely broken apart, at 8.7 kya (Kaldal and Víkingsson, 1991; Ingólfsson, et al. 2010).

Research regarding the extent of the IIS in the LGM is sparse and reliant on limited empirical data which has been collected over the past three decades. Offshore data is especially sparse (Norðdahl, 1991; Andrews et al., 2000; Norðdahl et al., 2008; Ingólfsson et al., 2010; Patton et al., 2017). A reconstruction of the IIS at various stages between 31 and 11.7 kya modelled by Patton, et al. (2017) shows the hypothesized extent of the ice sheet as determined by factors such as topography, geothermal heat flux, and precipitation and compared to the extent of the IIS as seen in Hubbard et al., (2006), (Figure 3).

In the early 2000s, bathymetric surveys offshore north Iceland for research on the tectonics of the TFZ and HFF have also furthered our knowledge of the extent of the IIS in the region at the LGM, indicating that individual ice streams extended from the IIS into the basins the Eyjafjarðaráll, Skjálfandi, and Öxarfjörður basins at the LGM, (Figure 1). In the Eyjafjarðaráll basin, evidence of the extent and direction of the ice flow coming from the IIS, is recorded through mega scale glacial lineations (MSGLs), moraines, crag-and-tails, iceberg scours, and unknown V-shaped ridges. Unravelling the glacial retreat and understanding the formation of these features are the focus of this thesis.

1.3 Glacial features glossary

In this section is a glossary of glacial features is provided to give details and background on the various landforms which will be discussed in the results section.

1.3.1 Megascale Glacial Lineations

The term megascale glacial lineation was first used in Clark (1993) to describe elongated structures composed of sediment formed subglacially and typically under fast flow conditions, such as those seen in ice streams and or during surge events in surging glaciers (Clark, 1993; Clark et al., 2003; King et al., 2009; Ó Cofaigh et al., 2013; Streuff et al., 2015). MSGLs have a typical length:width ratio greater than 15:1 (Bell et al., 2016) and form parallel to ice flow direction (Clark, 1993). MSGLs typically range from 6 – 100 km in length, and 200 – 1300 m in width, with spacing from 200 m – 5 km (Clark et al., 2003).

Understanding the processes by which MSGLs form can further our understanding of ice-stream flow mechanisms (Ó Cofaigh et al., 2003). Whether the formation of MSGLs is by ridge building or by groove carving is not completely understood as we have yet to observe their formation (Tulaczyk et al., 2001; Clark et al., 2003). The groove carving theory states that elongated grooves are carved into the soft sediment by bumps in the ice base, which results in sediment deformation into ridges (Clark et al., 2003). Another theory suggests a non-Newtonian rheology and a transverse secondary flow in the basal ice (Schoof and Clarke, 2008). Shaw et al., (2008) suggest a meltwater origin for MSGLs based on evidence from the Antarctic shelf ice streams.

Examples of MSGLs are seen in paleo-glacial landscapes across the world, for example Canada (Bennett et al., 2016; MacLean et al., 2016), Svalbard (Dowdeswell et al., 2010;), Antarctica (Bart and Owolana, 2012; Livingstone et al., 2013), and Greenland (Slabon et al., 2016). MSGLs can also be found in modern glacial environments, for example the Mertz Trough in East Antarctica (McMullen et al., 2016) and the Whillans Ice Plain in West Antarctica (Barcheck et al., 2019) where their formation is linked to rapid ice flow. King et al., 2009 investigates modern MSGLs found beneath the Rutford Ice stream, where the data suggests that neither the groove carving nor the meltwater flood hypothesis explains the rapid creation of MSGLs here.

MSGLs are found in several locations within the Eyjafjarðaráll Basin.

1.3.2 Moraines and Grounding Zone Wedges

The ice margin is the area where the ice front meets the foreground, and significant sediment exchange occurs leading to the creation of ice marginal landforms (Bennett, 2011). Ice marginal landforms is a term used to describe landforms which form at the ice margin, including grounding zone wedges and moraines. Due to the relative inaccessibility of sub marine ice margins, it is hard to directly observe the processes which are occurring there (Dowdeswell and Powell, 1996; Dowdeswell and Fugelli, 2012).

The grounding zone of an ice sheet is the area where the contact between the ice sheet and the underlying substrate ends and the ice sheet begins to float (Figure 6) (Batchelor & Dowdeswell, 2015). A grounding zone wedge is a mound formed at the grounding zone of an ice sheet/ice shelf system, composed mainly of dipping diamicton beds overlain by a sheet of diamicton composed of subglacial till (Bell et al., 2017). GZWs are typically asymmetrical with the ice-distal side being steeper and the ice-proximal side being more gradual (Batchelor and Dowdeswell, 2016). The typical size of GZWs ranges from 5-20 km long, 50-100m thick, and 10s of kms wide, and the dimensions are reliant on the sediment flux, duration of the ice stand still, ice stream width, and sub-ice cavity shape (Dowdeswell and Fugelli, 2012). GZWs are used as evidence of episodic rather than chaotic ice sheet retreat as GZWs form during episodes of stand still lasting decades to centuries during the overall retreat of the ice sheet (Batchelor and Dowdeswell, 2015; Dowdeswell and Fugelli, 2012). Seismic reflection data shows that the inside of a GZW is most typically semitransparent to chaotic due to the low seismically reflective glacial debris which makes up a GZW (Dowdeswell and Fugelli, 2012).

A moraine is a mound or ridge composed of unsorted, unstratified glaciogenic sediment that is mainly till and is formed mostly by direct contact with glacial ice (Bell et al., 2017). There are many different types of moraines, including terminal, recessional, medial, shear, lateral, De Geer, ribbed, and push moraines, all of which differ from one another in genesis and location relative to the glacier. Of these, push moraines appear to be the most common type of moraine in EB.

Push moraines are very useful diagnostic features, as their characteristics are dependent on many glacial and material properties such as temperature, velocity, hydrology, and shear strength (Johnson et al., 2013; Bennett, 2001). Push moraines have a variety of definitions, from a formal term restricted to describing moraines created through sediment bulldozing at the ice margin, excluding glaciotectonic thrusting as a main source of formation, to a less formal catch-all term for ice marginal ridges formed through the deformation of ice, sediment, and/or rock (Kalin, 1971; Boulton, 1986; Evans, 1989; Etzelmuller et al., 1996; Benn and Evans, 1998; Boulton et al., 1999; Bennett, 2001). In general, push moraine is a term used to describe ridges created through minor readvances in an ice sheet (Winklemann et al., 2010). They exist on a morphological continuum ranging from small, discrete ridges indicative of seasonal readvances to wide, multi-crested ridges indicative of a more sustained readvancement of the ice margin. The genesis of push moraines formed terrestrially and subaqueously are similar (Bennett, 2001). Push moraines are most easily identified by their internal deformation structures, which is typically ramp-like, having a steeper ice distal side and gentler ice proximal side (Winklemann et al., 2010).

Ice stream lateral moraines (ISLM) are built up at the lateral margins of ice streams and are suggested to be formed subglacially of mostly subglacial till (Dyke and Morris, 1988; Stokes and Clark, 2001; Stokes and Clark, 2002; Batchelor et al., 2016). ISLMs can be formed in the shear zone between fast-flowing and slow-flowing sections of an ice sheet, which are termed ice stream lateral shear moraines (Bentley, 1987; Dykes and Morris, 1988; Dyke et al., 1992; Stokes and Clark, 2001; Stokes and Clark, 2002; Ottesen et al., 2005; Batchelor et al., 2016). When formed at the lateral boundary between an ice stream and an ice-free terrain, these moraines are called ice stream lateral marginal moraines (Batchelor et al., 2016). The presence of ISLMs are thus important indicators of paleo ice stream behaviors. Examples of marine ISLMs can be seen in Canada (e.g. Batchelor et al., 2014; Batchelor and Dowdeswell, 2015), Greenland (e.g. Batchelor et al., 2016; Arndt et al., 2015), Antarctica (Shipp et al., 1999), the UK (Golled and Stoker, 2008), Norway (Rydningen et al., 2013; Batchelor et al., 2016), and the Barents Sea (Ottesen et al., 2005; 2007).

Differentiating between a moraine and a GZW can be difficult. Batchelor and Dowdeswell (2015) state that while a moraine would require “considerable vertical accommodation space or sediment derived from point-sourced subglacial meltwater streams”, a GZW is formed where floating ice constrains the vertical accommodation space. GZWs are also limited to marine environments, whereas moraines can exist on terrestrial and marine landscapes (Demet et al., 2018). Simkins et al., (2018) suggest that GZWs are found where the grounding line retreat was irregular with longer standstills, and a larger-magnitude retreat event. On the other hand, a steady grounding line retreat comprised of smaller-magnitude retreat events would be marked rather by moraine sequences. GZWs are considered to have more subdued relief and higher length:height ratios than moraines, which tend to have a higher amplitude (Dowdeswell and Fugelli, 2012; Batchelor and Dowdeswell, 2015, 2016).

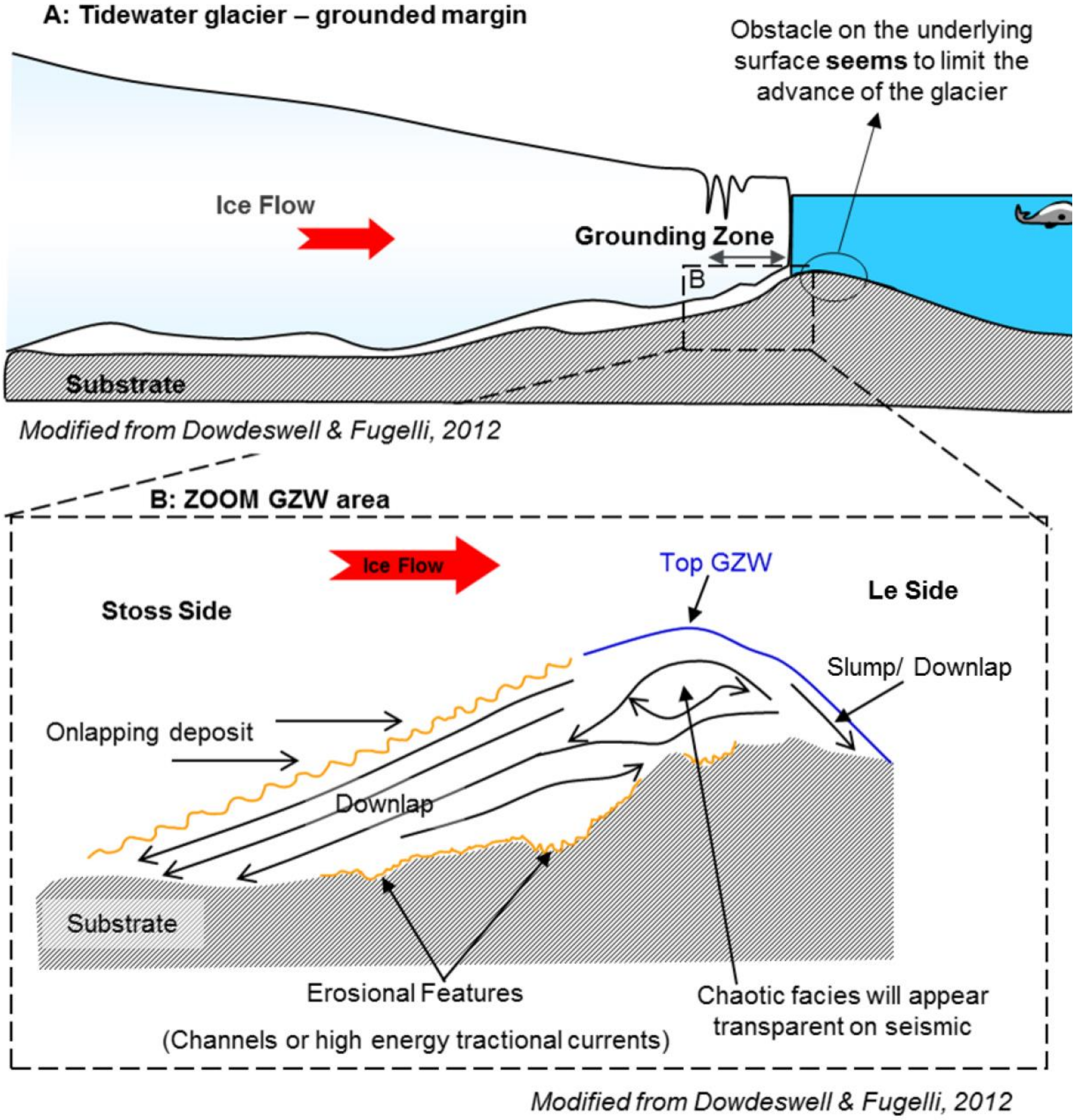

Figure 6. GZW formation diagram from Decalf, et al. 2012

1.3.3 Subglacial Meltwater Channels

The method of incision of subglacial meltwater channels is not entirely known but generally thought to be through meltwater abrasion, till slurry abrasion, or ice abrasion (Glasser and Hambrey, 1998). There are several types of subglacial channels: Rothlisberger (R) channels, Nye (N) channels, and p-forms. In the situation in Eyjafjarðaráll basin, where there is no longer any ice, we do not care about R-channels as these are channels which are carved into the ice itself. N-channels and p-forms are carved into the bedrock or substrate below the ice sheet (Bell et al., 2016).

Tunnel valleys are elongate depressions that have been incised into sediment or bedrock parallel to the direction of former ice flow by subglacial meltwater erosion (Ussing, 1903; Wright, 1973; Attig et al., 1989; Wingfield, 1990;, Piotrowski, 1994; Patterson, 1997; Huuse and Lykke-Anderson, 2000; Jörgensen and Sandersen, 2006; Livingstone and Clark, 2016). Whether tunnel valleys are formed by an outburst of subglacial meltwater or a gradual and steady state formation is still debated (Livingstone and Clark, 2016). Understanding the formation of tunnel valleys is important to understanding subglacial hydrological systems and drainage routeways (Livingstone and Clark, 2016).

1.3.4 Eskers

Understanding ice sheet hydrology is a very important aspect of understanding ice dynamics and for refining ice sheet models (Burke et al., 2015). Eskers are ridges which typically form perpendicular to the ice margin, which can be straight or sinuous in shape, which are created in meltwater drainage conduits on, within, or under the glacier, and are composed of stratified glaciofluvial sand and gravel (Banerjee and McDonald, 1975; Burke et al., 2015; Storrar et al., 2013). Eskers have a wide range of sizes based on their morphology (Storrar et al., 2013): Eskers are used as an alternative method to better understand modern day ice sheet meltwater drainage systems, being that it is much easier to study these paleo ice sheet landforms than it is to study modern ice sheet meltwater drainage systems through dye tracing, remote sensing, or modeling (Fricker and Scambos, 2009; Storrar et al., 2013). While numerical models typically assume steady state esker formation, there is still debate on the genesis of eskers as recent studies have shown that glacial hydrologic systems are never in steady state (e.g. Gray, 2005; Bell, 2008; Bartholomaus et al., 2011).

1.3.5 Crevasse Squeeze Ridges

Crevasse squeeze ridges are, as the name implies, ridges which are caused by top-down, basal, or straight through crevassing at the glacier margin where there is soft, easily deformable sediments to enter the crevasses, which are then imprinted on the landscape when the ice melts, though their formation is not completely understood (Evans and Rea, 1999; Rea and Evans, 2011; Bell et al., 2016; Farnsworth et al., 2016). The composition of CSRs is mainly matrix supported diamict sediments and form perpendicular to ice flow (Sharp, 1985; Rea and Evans, 2011; Farnsworth et al., 2016). The preservation potential of CSRs is higher in marine environments than on terrestrial environments, as there is not extensive reworking of the ridges as the ice melts out as there is when terrestrial CSR which lose lateral support with ice melt. This also leads to higher relief CSRs in marine environments than in terrestrial environments (Rea and Evans, 2011).

The presence of these ridges is typically used as evidence of surging in a glacier or ice stream, though that is not always the case as CSRs have occurred in modern non-surging temperate glaciers (Evans et al., 2016). According to Evans et al., (2016), the pattern of a CSR is crucial to determining whether they were created by a surging versus non-surging glacier, and the paper goes on to suggest that ice stream dynamics control the pattern and distribution of CSRs in a ridge network, analyzing specifically the bed of a paleo ice stream from the southwest margin of the Laurentide Ice Sheet. This paper interprets CSRs from the Maskwa paleo-ice stream to be caused by fracturing during the final stages of ice stream shut down rather than of a surging glacier.

1.3.6 Murtoos

Murtoos are only recently described from Finland and Sweden. Previously considered dead ice moraines (Johnson et al., 2018), a murtoo is a subglacially formed triangular or V-shaped landforms which a typically between 30-200 m long, 30-200 m wide, and have a relief less than 5 m, though much larger murtoos have been found, specifically in Sweden (Ojala et al., 2018). Due to their recent discovery, very little research has been done on these features and thus there are very few sources to describe them. Detailed studies on the sedimentology of murtoos is currently being carried out, but preliminary analysis show that these landforms are composed of primarily loose diamicton with some sorted beds and surface boulders (Ojala et al., 2018; Johnson et al., 2018; Kajuutti et al., 2018; Makinen et al., 2018; Peterson et al., 2018)

Murtoos are considered to be created during rapid ice retreat phases (during the Bølling-Allerød and early Holocene as determined by Ojala et al., 2018). They are also considered to be created under warm-based glaciers and during periods of significant subglacial meltwater flows and in non-channelized environments (Ojala et al., 2018).

1.3.7 Iceberg scours

Iceberg scours, also called iceberg ploughmarks, iceberg furrows, and ice-keel ploughmarks, are grooves or furrows which are found on sea or lake floors of currently or previously glaciated areas across the world (Bell et al., 2016). When ice calves from an ice sheet, a variety of forces including tides, ocean currents, and storms drive the icebergs movement throughout the sea. Iceberg scours are formed when these icebergs becomes partially or completely grounded to the seafloor, thus creating a scour where it is grounded (Brown et al., 2017). They are typically limited to the relatively shallow banks surrounding a trough, where the sediments are disturbed by the scouring (Domack and Powell, 2016).

1.4 Subglacial Sediments

Ice transported sediments are reflective of the underlying and surrounding bedrock geology and vice versa. Understanding the subglacial sedimentology is key to understanding the movement and sediment flux to the glacier margin, and to understand the sediment transport in a glacial system requires understanding the supra-, pro-, and subglacial environments (Menzies et al., 2013).

Several sediment cores have been obtained within the EB (Figure7) over the past 30 years (i.e. Knudsen and Eiríksson, 2002; Knudsen et al. 2004; Kristjánsdóttir, 1999), however few in depth sedimentological analysis have been carried out on the cores. These cores consist of two seismic units: unit A and unit B. Unit A is the uppermost unit and is from 1-46 m thick, horizontally layered, and has a weak seismic reflection. This unit is Holocene mud, which is soft, olive green with low magnetic susceptibility, high carbon content. Unit B is the lower unit with a strong regional reflector, debris flows, and faulting. This unit is a glacial marine mud which is stiff, grey with higher magnetic susceptibility, low carbon content and IRD.

Analysis of cores (Figure 7) along the EB (Kristjánsdóttir, 1999) revealed a transition zone between 15 – 20 cm thick at varying depths in cores which most likely represents a debris flow. Sediments above this transition zone date younger than 3885+-35 BP, and below to 6440-8490 or 11140 BP. The cores are also missing the primary Vedde (12100 BP) and Saksunarvatn (10300 BP); the absence of the latter could be explained by erosion caused by the debris flow.

Unfortunately, very little is known about the sedimentary composition of the glacial geomorphological features in EB. In addition, none of these cores are directly within any of the geomorphological features such as moraines, eskers, or V-shaped ridges meaning that their internal structure and composition is mostly unknown. The closest core to the V-shaped ridges is B9-97-317PC1. What can be said about these ridges is that they are composed of hardened till. We also do not understand how much the debris flow which is represented in each of the cores by a transition zone effected the features which are seen in the basin. Questions such as how much of the ridges was eroded, or how many features were destroyed must be considered.

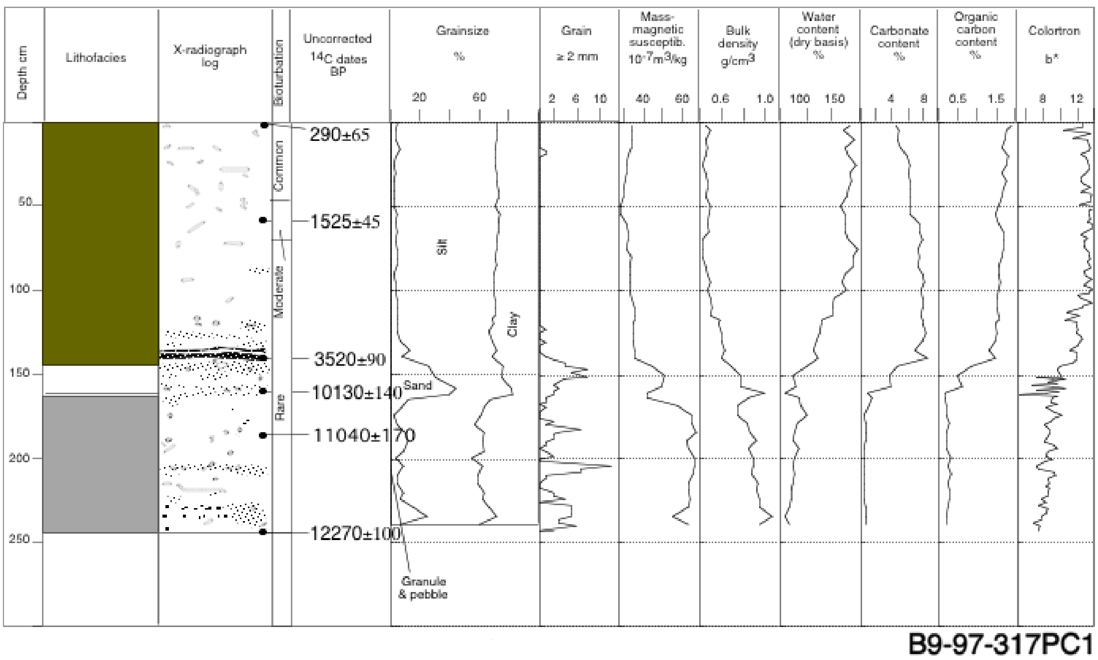

Figure 7. Sedimentary core analysis from Kristjánsdóttir, 1999 on three shallow cores collected withing the EB, onboard R/V Bjarni Sæmundsson. Noticeable in all three cores is the presence of a transition zone and the different lithofacies above and below it. At least 3ky has been eroded from within the cores. Locations of cores shown

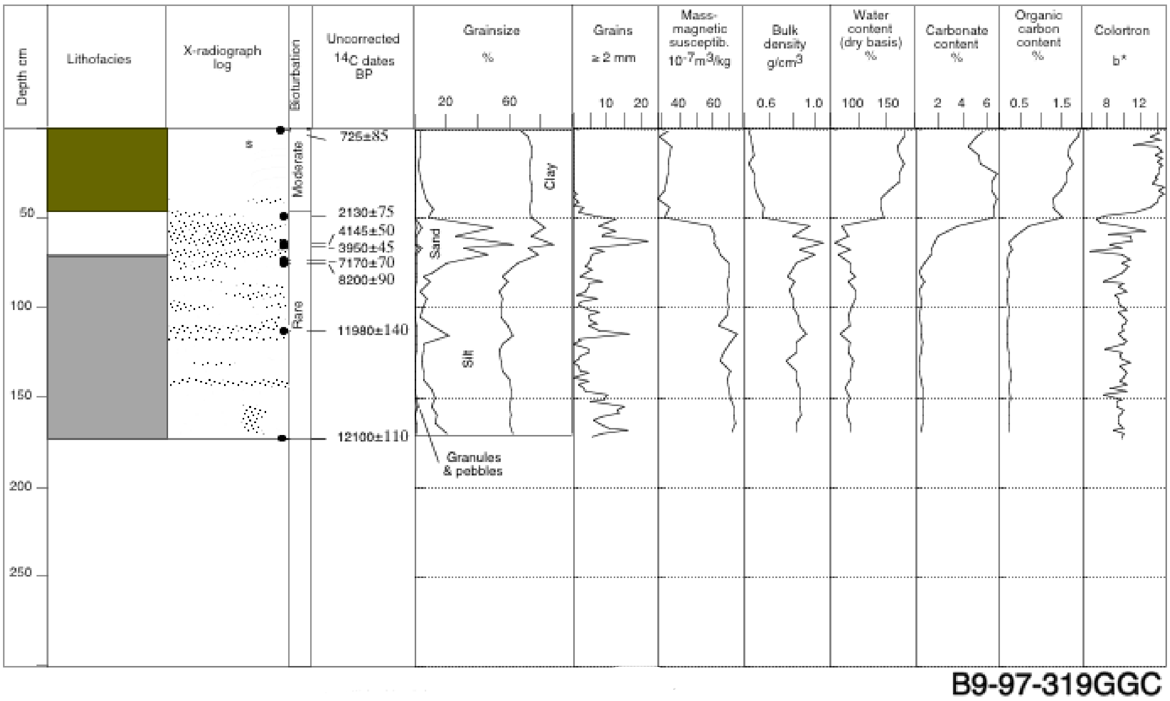

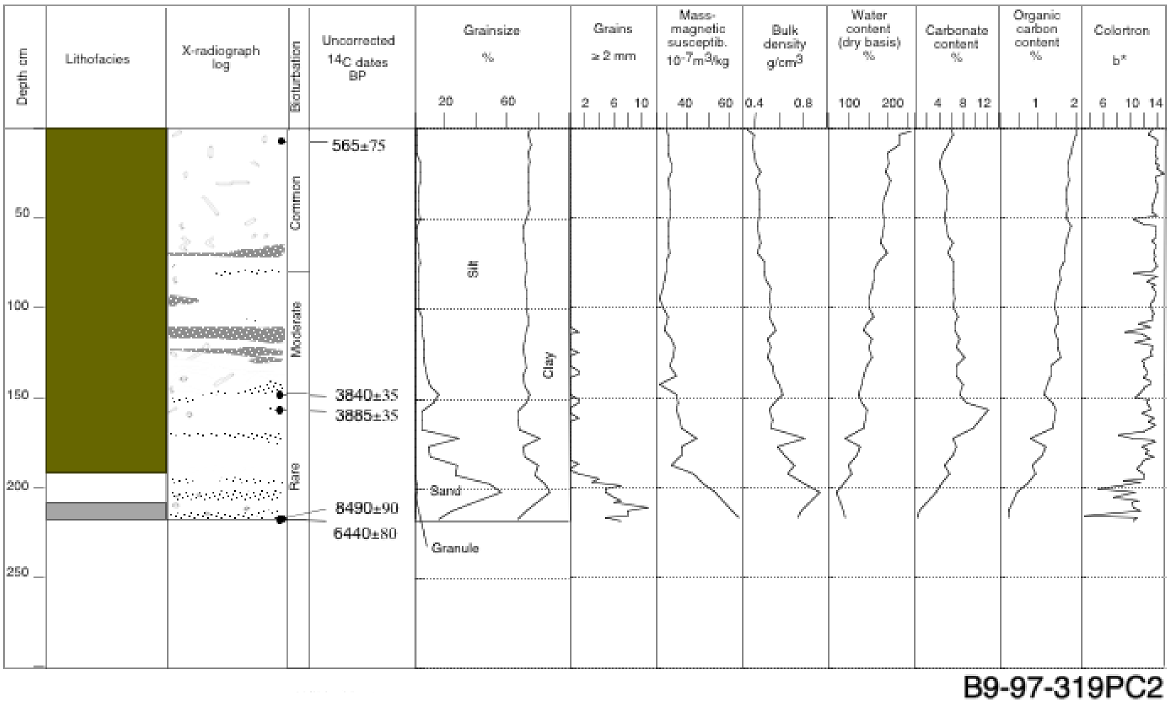

Figure 7. (cont.)

2 Methodology

The multibeam bathymetric and high-resolution seismic reflection data was acquired during five Tjörnes Fracture Zone surveys in 2001-2005. Data collection commenced in July 2001 using the Scripps Institution of Oceanography's (SIO) Edgetech subscan Chirp system and a portable High-Resolution Multichannel Seismic Acquisition System onboard the *R/V Bjarni Sæmundsson* cruise TFZ-B9. The Chirp system emits 1- to 6-kHz signal with a 50-ms sweep, providing, at best, a 30–50 m penetration into the sediments with sub-meter resolution. Positions were provided by GPS. Approximately 1600 km of data were collected across Eyjafjarðaráll, Skjálfandadjúp, Skjálfandi, and Öxarfjörður. A second Chirp mapping campaign, focusing on Skjálfandi Bay and southern Eyjafjarðaráll was conducted between 21 July and 1 August 2003 on *R/V Bjarni Sæmundsson* (6 days of data collection). The campaign in 2003 also included side scan of the HFF and bottom photographs of the study areas in Skjálfandi Bay using the WHOI TowCam system (Brandsdóttir et al., 2003).

Multibeam bathymetric mapping was carried out using the Simrad EM-300 System onboard *R/V Árni Friðriksson* in 2002 and 2005 and *R/V Baldur* (5 days of data collection) in 2003. The bathymetric data were gridded with a resolution of 10 m. On the *R/V Baldur* a Reason 8101 shallow water swath mapping system was used to obtain higher resolution maps of inshore areas along the HFF in SE-Eyjafjarðaráll, Skjálfandi bay, and Öxarfjörður.

The bathymetric data were processed using the open-source MBSystem software package (Caress and Chayes, 1995) and converted using ERDAS Imagine before being interpreted in Esri GIS platform ArcMap 10.6.1. The Generic Mapping Tool software was used to generate figures (Wessel and Smith, 1991). The Chirp data were converted into standard SEG-Y format and processed using the Seismic Unix seismic processing software (Cohen and Stockwell, 2006). Data results were interpreted using Adobe Illustrator.

The data was loaded in ArcMap in order to begin identifying glacial features and ice stream behavior in the study area. I used a hillshade filter with Z factor 7 and azimuth 315° at 50% transparency and 20% contrast to clarify the results and emphasize the features present. I created several hillshades with Z factors 1-10 and experimented with the azimuth angle in order to find the clearest map to identify the features. Features were identified and transects were created to identify qualities such as width, length, relief from sea floor, and abundance using the 3D analyst tools interpolate line and profile graph. These characteristics along with their location relative to the known ice streams were used to identify features and identifications were based on similar described landforms from literature.

A more detailed analysis was conducted on the V-shaped ridges found throughout the basin. I used ArcMap to identify the relief width, and length of each arm of the V-shaped ridges (top value) and then found the values after eliminating outliers (bottom values), including when the value was zero because one arm was not visible (either buried or destroyed) so no accurate measurement could be taken. The relief was taken from the highest point and the length measured from the crest to the bottom of each arm.

3 Results

The bathymetric data collected in the Eyjafjarðaráll basin (Figure 8) has revealed a complex glaciation pattern generated by the Eyjafjörður-Eyjafjarðaráll ice stream which merged with the Skagafjörður ice stream offshore to the west, and the Skjálfandadjúp ice stream offshore to the east. This section will be split into subsections for different sections from northern Eyjafjörður and southern Kolbeinsey ridge where the IIS is considered to have had its terminal position during the LGM, to the southern Eyjafjörður extent of the IIS, probably occurring prior to the Younger Dryas, though possibly being the Younger Dryas extent.

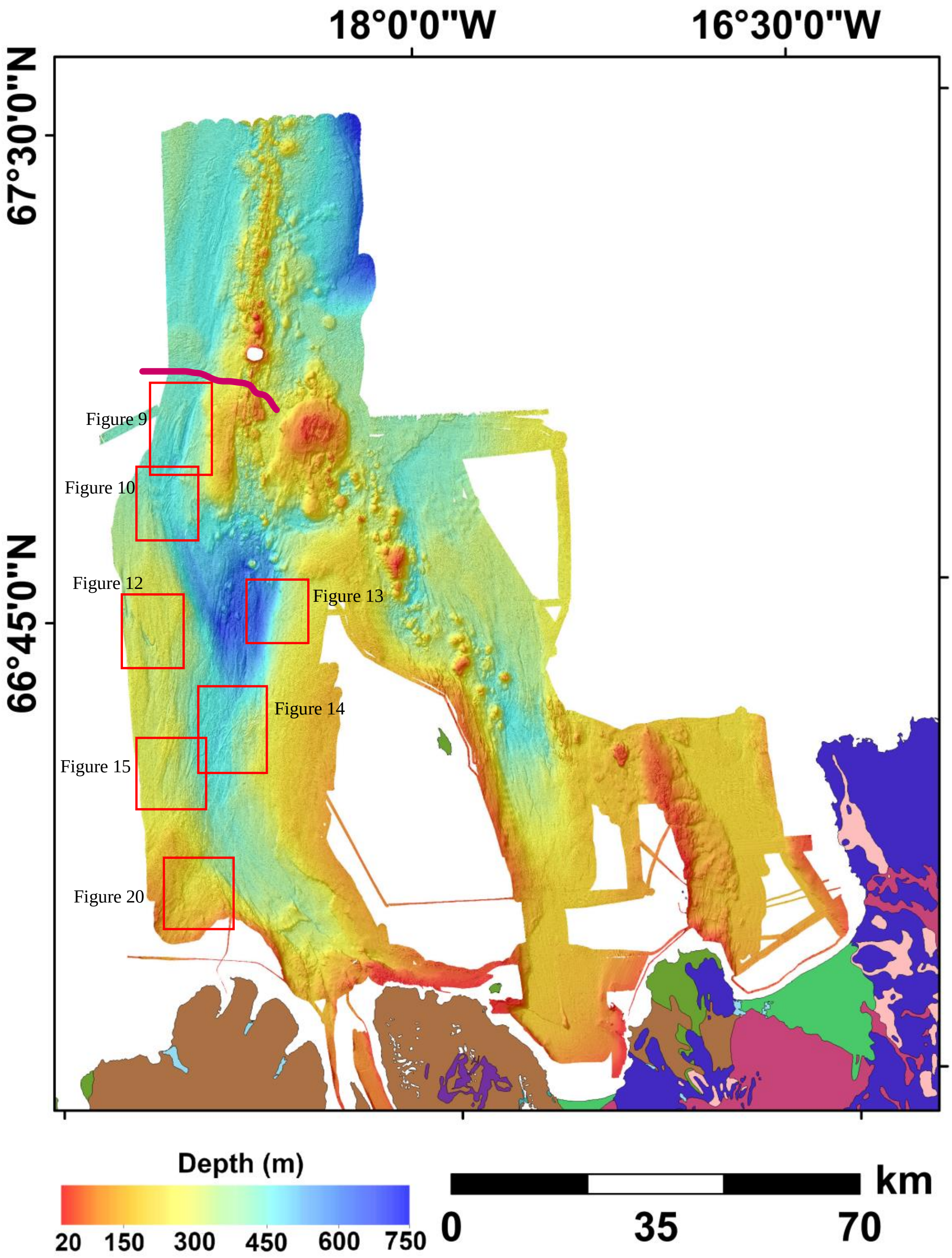

Figure 8. A multibeam bathymetric map of the study area. Red squares indicate locations of figures with the figure numbers next to them. Purple line above the location of Figure 9 shows the hypothesized terminal position of the IIS at the LGM.

3.1 Northern Eyjafjarðaráll

Previous models of the extent of the Icelandic Ice Sheet (IIS) at the Last Glacial Maximum (LGM) do not have the ice sheet extending as far onto the North Iceland Shelf as the northern-most glacial features in our data (e.g. Hubbard et al., 2006; Norðdahl et al., 2008; Patton et al., 2017). However, Patton et al., (2017) model the LGM extent of the IIS covering the southern KR at 22.9 ka BP, i.e. around 67.2ºN, which is still south of the northernmost feature we identify, around 67°50'N.

Although the northernmost Eyjafjarðaráll Basin and southern Kolbeinsey Ridge (KR) region are characterized by fewer glacial features than the region further south, glacial morphology along the flanks of the Kolbeinsey Ridge show that ice streams from the IIS could have extended as far as the southern Kolbeinsey Ridge (67.7ºN) during the LGM. Without sediment samples, seismic sections or other age constraining data for this region, it is not possible to determine their age, however, based on volcanic productivity along the KR, and postglacial sediment rates within the Tjörnes Basins (Knudsen and Eiríksson, 2002; Gudmundsdóttir et al., 2011) we conclude that the glacial features described below were created during the last ice age, most likely near the LGM.

The northernmost glacial landform assemblage in the bathymetric data lies directly southwest of Kolbeinsey island, approximately 105 km offshore (Figure 9). In this area is a subglacial channel, is just under 1 km wide, approx. 50 meters deep at its deepest point, and 6 km long. The channel lies parallel to ice flow. Several profiles across the channel show that the channel remains consistently deep (about 50 m) throughout the majority of its length but tapers off and becomes shallower along its northern and southern extents. The channel is symmetrical with steep walls creating a "U-shape", with the exception of the ends which have a steeper, higher eastern bank as compared to the western side. The southern portion of the channel connects with a basin which is similarly deep but wider and with shallower basin walls, which we do not define as a part of the subglacial channel.

Surrounding the channel are eskers, moraines, and several V-shaped ridges to the west of the channel, labeled E, M, and V, respectively (Figure 9). The V-shaped ridges run NNE and are approximately 5 m in relief, 600 m from arm to arm, with each arm ~200 m wide, and with lengths varying between 1-2 km. Several other ridges, SE of the channel (~2000 m into the southernmost profile in Figure 9), represent some sort of a moraine. The most prominent of these ridges which lies directly on the flank of the channel is approximately 3 km long, 5m in relief, and 150 m wide. We consider it to represent a discontinuous moraine that has been breached in the center. The northern end of the moraine ends in at least three winding ridges, approximately 2-3 m in relief, ~100 m wide, and 0.6 – 1 km long, which most likely represent a discontinuous end moraine or eskers (labeled E/M in Figure 9). Several other smaller but similarly winding ridges which are approximately 1-2.5 m in relief, 50-100 m wide and 1-2 km long are considered to be eskers (northern Es in Figure 9). Also present on the plateau to the east are roughly W-E trending iceberg scours which were likely created by icebergs coming from the Greenland ice sheet and caught in the eastward flowing branch of the Irminger Current.

In summary, the combination of glacial features in this area, indicate the they formed at a grounding zone of an ice stream along the western flank of the KR. The combination of eskers, V-shaped ridges, and moraines were likely formed during a minor advance of this ice stream and are no younger than ~21kya, as after this point the IIS began a rapid breakup and retreat. The channel had to have been created by a powerful force in order to explain its depth and size. Similar channels in the North Sea are thought to be derived from subglacial meltwater activity or jökulhlaups (Pearce et al., 2012). Sediment infill along the KR channel cannot be quantified, but the actual depth of the channel is possibly some meters deeper than what can be seen in the data. This channel could represent a tunnel valley, similar to those seen across Canada (Livingstone and Clark, 2016). It is possible that the channel was created by a jökulhlaup which flowed through this region, though no other evidence of a jökulhlaup occurring in this region during the LGM or earlier exists, yet. The channel could also have been formed by compression of the ice sheet by the plateau to the east causing increased pressure and erosion.

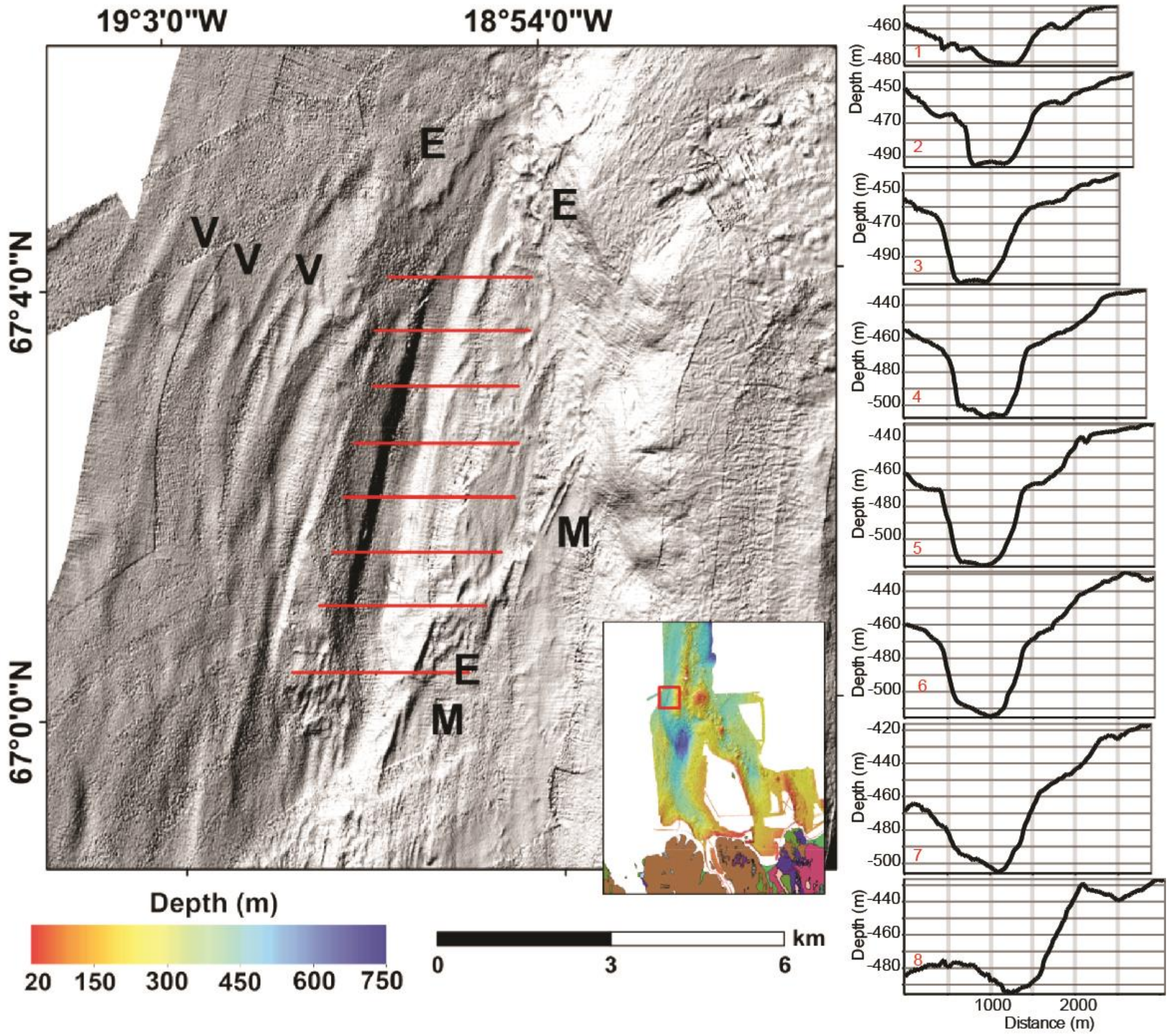

Figure 9. Subglacially formed channel along the southwestern margin of the Kolbeinsey Ridge, and moraines (M), eskers (E), and V-shaped ridges (V), attributed to a grounding zone wedge. The profiles show that the main channel is just under 1 km wide, approx. 50 meters deep at its deepest point, 6 km long with a symmetrical transect. The transects are labeled 1-8 from northern most to southern most transect.

Further south there is an abundance of N-NE trending ridges representing eskers, V-shaped ridges, MSGLs, and moraines (Figure 10). There is also some faulting in this region.

Two areas where the V-shaped ridges are most prominently seen (northern Vs on transects 4-5, and southern Vs on transects 8-12, Figure 10). In the northern section, there are at least 5 ridges, possible more which have either been eroded or were simply less developed than the others. They have reliefs ranging from 2.5 - 10 m and are all roughly 500 - 600 m in width from arm to arm, with some of the ridges overlapping one another.

The southern V-shaped ridge cluster is ~4.5 km south of the northern cluster V-shaped ridges and there are at least 9 visible ridges. Similar to the northern cluster, there are some ridges which are overlapping one another and some ridges which are obviously better preserved or better developed than others. These ridges are similar in size to each other, all of them are around 4 m in relief, around 400 m wide arm to arm, and range from 0.5 - 1 km in length. There are also at least 2 V-shaped ridges which are ~5 km in length (transects 10 and 11, Figure 10). These are the longest V-shaped ridges which are found in EB.

To the north, there are several NE-SW trending ridges (transects 1-3 and the upper M label, Figure 10) which are somewhat curved and end in the east where they are disrupted by a plateau. They have varying widths and lengths. The larger ridges are 5 – 10 m in relief, ~400 m wide, and 1 – 1.5 km long. The smaller ridges are 2 – 4 m in relief, ~100 m wide and up to 600 m long. I propose that these ridges represent recessional moraines, with the possibility that the smaller, curved ridges represent eskers due to their winding shape (Labeled E in Figure 10).

Also prominent in this region are several NE-SW trending ridges (transects 7-12 and labeled M, Figure 10). These ridges vary in length between 1.5 - 4.5 km, and in at least one instance one of the ridges cuts through the southern cluster of V-shaped ridges. These ridges range from 3 - 5 m in relief and are 100 - 200 m wide. The ridges are roughly straight and parallel to one another. They are also parallel to sub-parallel to the ice stream flow direction. They appear to be recessional moraines.

In the southern part of this region, there are dozens lineations trending SSE-NNW, approximately 8 km long in total. The ridges are at most 2.5 m tall and up to 50 m wide. The ridges are on the small side, but I considered them to be MSGLs due to their dimensions and shape. There is an iceberg scoured plateau in between two depressions in this area.

There are two ridges with a small, spherical depression between them running perpendicular to ice flow direction (seen in transects 5-9, Figure 10) at approximately 66°56’ and 66°57’ with N-S trending ridges draping them. These ridges both have the V-shaped ridges draping them. The southern ridge is approximately 1.5 km wide and the northern ridge is approximately 2 km wide. These ridges could represent large end moraines which were then overridden and draped by V-shaped ridges and recessional moraines.

To the southeast, (above the inset, Figure 10), there are a few elongated, round hills which narrow in the down ice direction which are labeled CT. There are at least three prominent hills, which are approximately 10 m in relief and wider in the up-ice direction vs the down ice direction. These features are a part of the volcanic system in the KR which existed prior to the LGM and were overridden by the ice streams in this area, creating crag-and-tail like features.

There are also iceberg scours on the plateau in the northeastern portion of this area, and on the elevated section near the moraines and MSGLs, the majority of which trend ENE-WSW.

Due to the assemblage of landforms present in this area, I hypothesize that this is a grounding zone and that the IIS experienced a readvance and/or minor standstill in this region. This could possibly represent the extent of the IIS at the LGM, though like the region north of this, without better age constraining data it is not possible to say whether the ice sheet extended further north. Most models do not have the IIS extending this far north during the LGM, however the model created by Patton, et al., 2017 does project the ice sheet extending to about this point meaning it is possible that this was the terminal position and a grounding zone of the IIS during the LGM. The presence of the lineations leading up to the grounding zone indicate the ice stream was fast flowing as it approached terminal position.

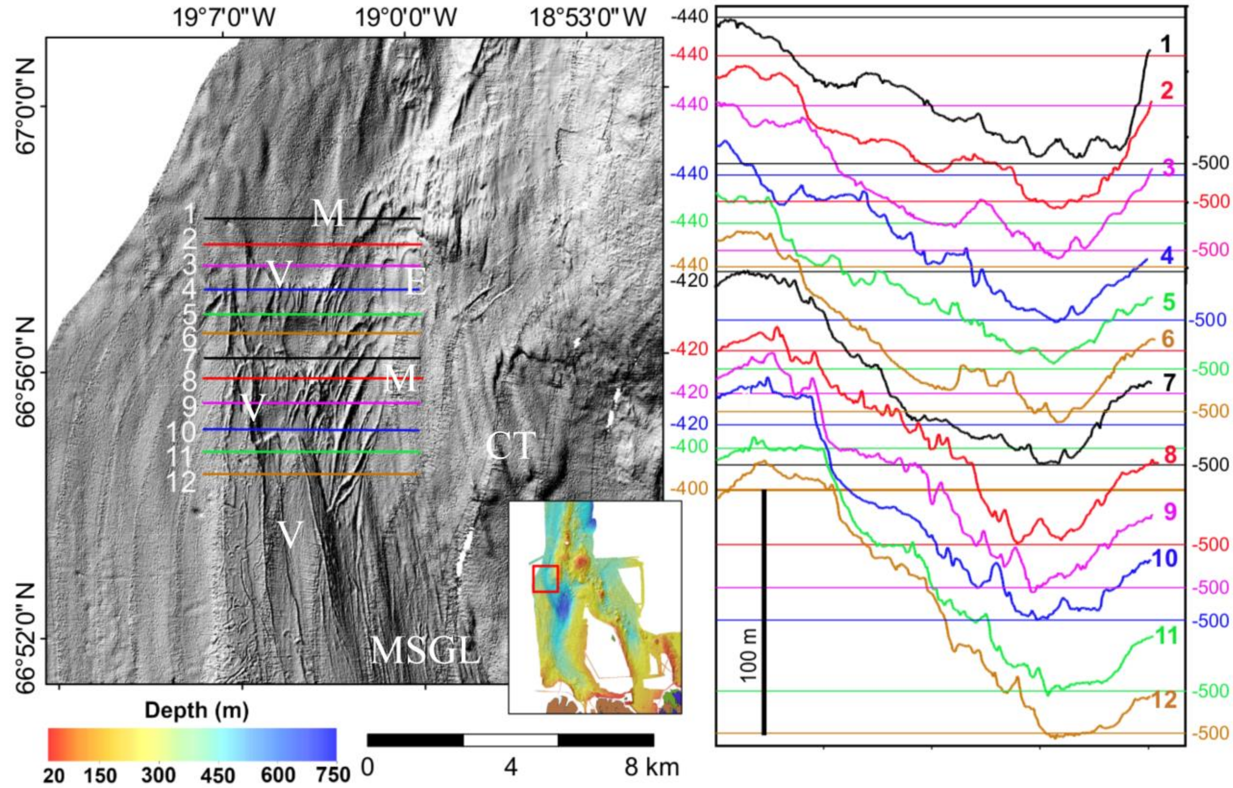

Figure 10. V-shaped ridges (V), eskers (E), moraines (M), MSGLs, Crag-and-Tails (CT) iceberg plough marks, and faulting present in the Northern portion of EB, just south of KR. Transects taken across the ridges are shown to the right, labeled 1-12. The transects are color coded, from North to South in the following order: Black, red, purple, blue, green, and brown, and then repeated in that order.

3.2 Central Eyjafjarðaráll

This paper defines the central part of EB between 66°50’N and 66°23N. Within this region lie the majority of the glacial features found in EB. It is also the location of dozens of faults which have been created since the end of the last ice age. A map with several transects taken across it which show that the faulting has caused subsidence of 100 - 140 m throughout the basin (Figure 11). The next paragraphs will describe the features found in this region from north-most to south-most, which is inferred to be oldest features to youngest features.

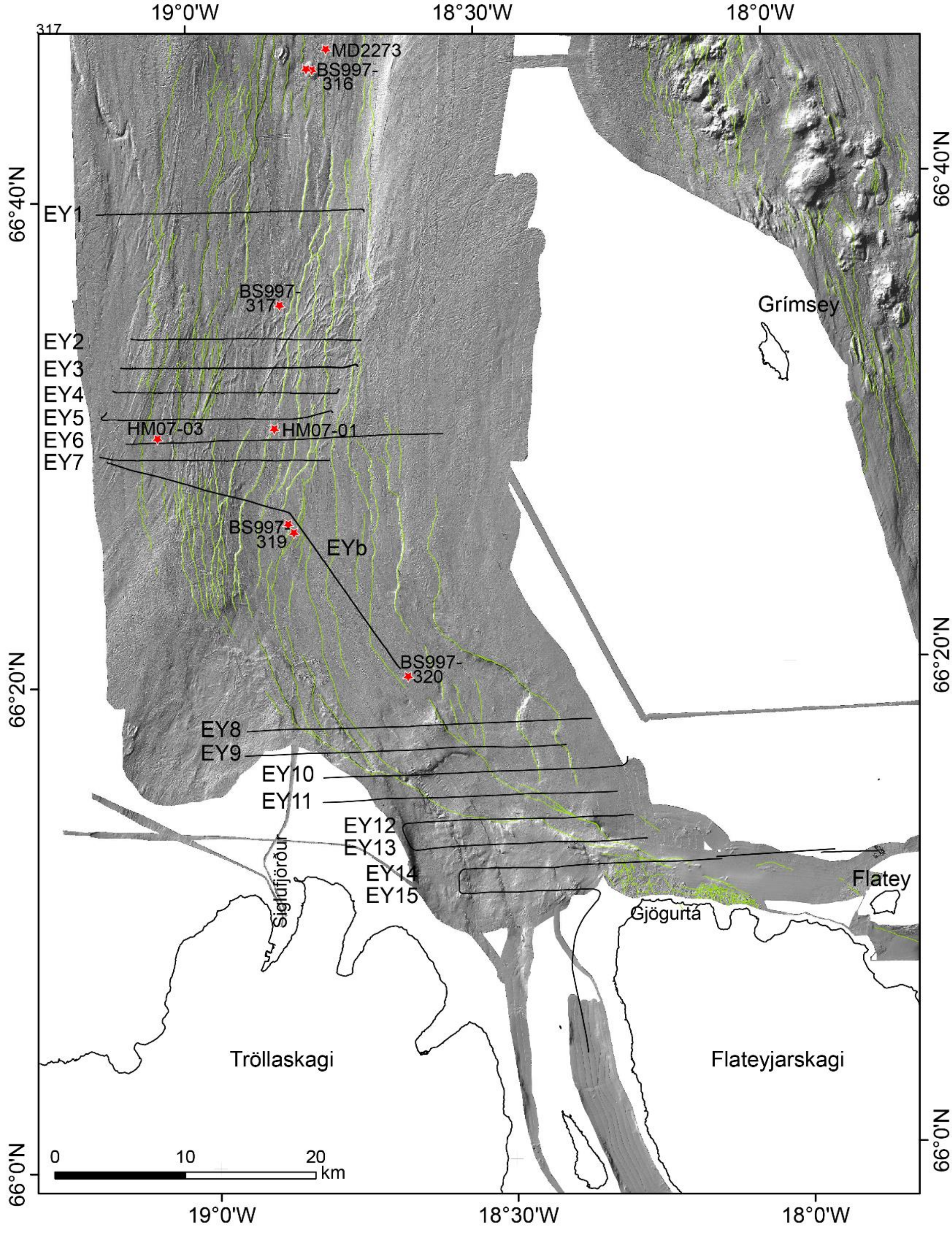

Figure 11. The central and southern portion of the Eyjafjarðaráll Basin. Green lines represent normal faults, and black lines Chirp seismic profiles. Red dots represent Bjarni Sæmundsson (BS) and Håkon Mosby (HM) core sites.

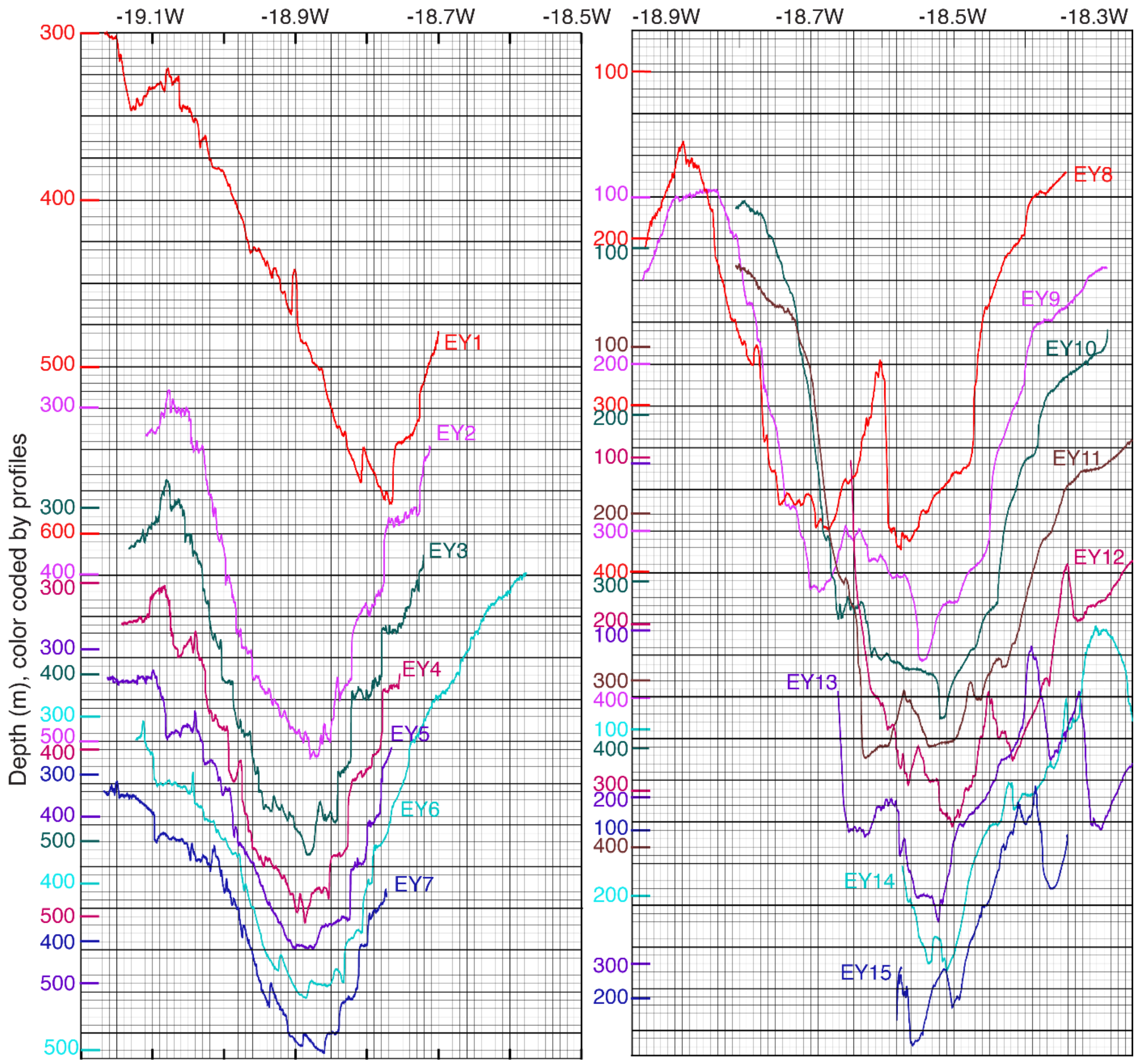

Figure 11 (cont.). Transects across EB showing a cumulated subsidence of more than 100 m by normal faulting throughout both the northern (left) and southern (right) basin. Different coloured numbers refer to the same coloured profiles.

Starting around 66°50'N there are two sections that will be discussed: one on the western flank of EB and one on the eastern flank.

To the west, there are two large subglacial channels, around 66°45'N by 19°10'W (Figure 12). Transects across both of these channels reveal that they are U-shaped, symmetrical, and deeply incised. The fully visible eastern channel (Labeled B on Figure 12) is just under 1 km wide at its widest point, approximately 4.7 km long, and up to 60 m deep. The western channel (Labeled A on Figure 12) is only partially visible but appears to be of similar length. This channel is approx. 50 m deep and 400 m wide. Both channels runs NNW-SSE. Without cores or seismic data through the channels, it is not certain how much sediment infill has occurred within them. The shape of it appears to be similar, either in comma form or *sichelwanne* (crescent shaped). “Comma form” channels are considered to be part of a continuum of transverse subglacial channels with *sichelwanne* forms, having one well developed arm and one missing or poorly developed arm as is the case with these channels (Kor et al., 1991). Chirp data taken just south of the two channels shows a sediment filled basin which is leading up to the channels (Figure 12D). Within this channel are several ridges which are not easily visible on the bathymetric data which could represent eskers or flutes.

I identify these as hook-shaped channels, though the western most channel is not fully visible as the data does not extend far enough west to show its entire structure. The hook shape is considered to represent a transition from transverse to longitudinal channel forms and are created through preferential erosion around a median ridge and horseshoe vortices in the subglacial meltwater (Kor et al., 1991; Benn and Evans, 2010).

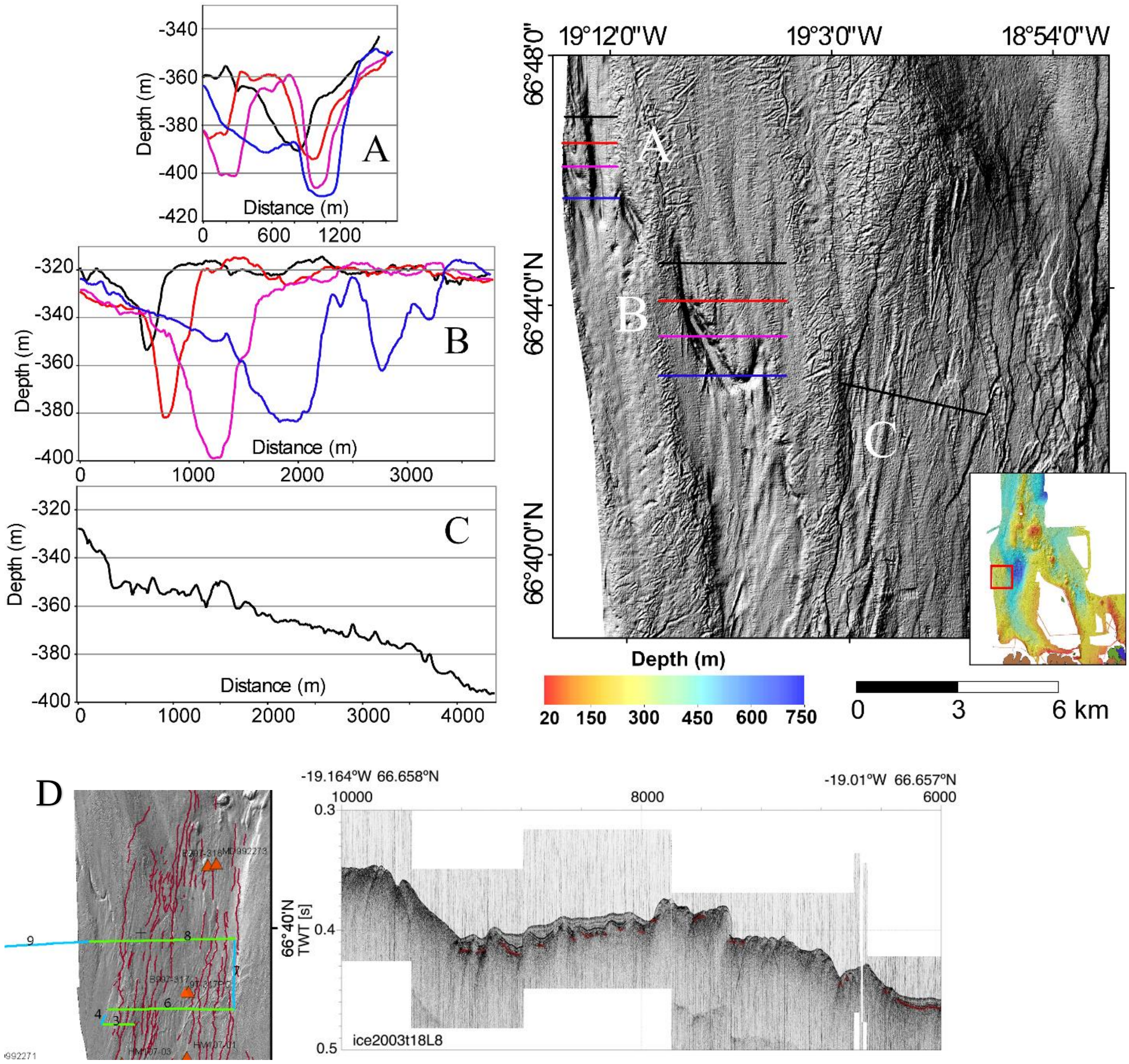

Figure 12. Subglacial channels on the western flank of EB, as well as lineations, iceberg scours, and several faults. Nine transects taken across these figures are shown to the left, and are labeled A-C based on their location on the map. D. Chirp data taken across the area just south of the channels showing a sediment filled basin with several buried ridges. Transect color legend as in Figure 10.

Directly east of these channels, there exists a number of NNE-SSW flowing ridges on the wall of the over deepened part of EB (Labeled C on Figure 12). They appear to be related to the MSGLs to the north (Figure 10). Transects taken across these ridges show that they are all of similar size, between 2 and 5 m in relief and 100 m wide, but with varying lengths. The largest lineation is 6 km long, 300 m wide, and 6 m in relief. It is unclear how the faulting in this region impacted these ridges, though it is clear that the ridges predate the faults as they intersect the ridges in places. These ridges are small compared to the standard size of MSGLs, however they possibly fit the standard 15:1 length to width ratio as described by Clark (1993). I consider that these ridges were formed by fast flow and that they could therefore be representative of MSGLs. These MSGLs were created during the retreat of the IIS sometime after 23 kya but predate the faulting in the region as the faults crosscut some of the ridges.

Another set of ridges can be found in the eastern part of the Eyjafjarðaráll basin where the EB nearly meets the Grímsey Oblique Ridge (GOR) to the east and KR to the north (Figure 13). The ridges run in the NNE-SSW direction, parallel to subparallel to the hypothesized direction of the ice sheet. As seen in the transects, these ridges exist on a steep basin wall and from the northern end (transect 1) to the southern end (transect 6) there is over a 50 m depth change. It is unclear how this steepness has changed since these ridges were deposited. These lineations are of varying lengths, with the longest lineation running approximately 6 km. Other lineations have lengths from approximately 1 km to 3.5 km. These lineations have reliefs ranging between 2 and 7 m and widths ranging between 50 and 100 m. It is possible that the lineations have been partially buried or destroyed by the faulting in the area, but without seismic data it is difficult to tell. Due to their size and shape, I describe these ridges as either a set of lateral moraines or MSGLs, which would be indicative of fast flow conditions in this region.

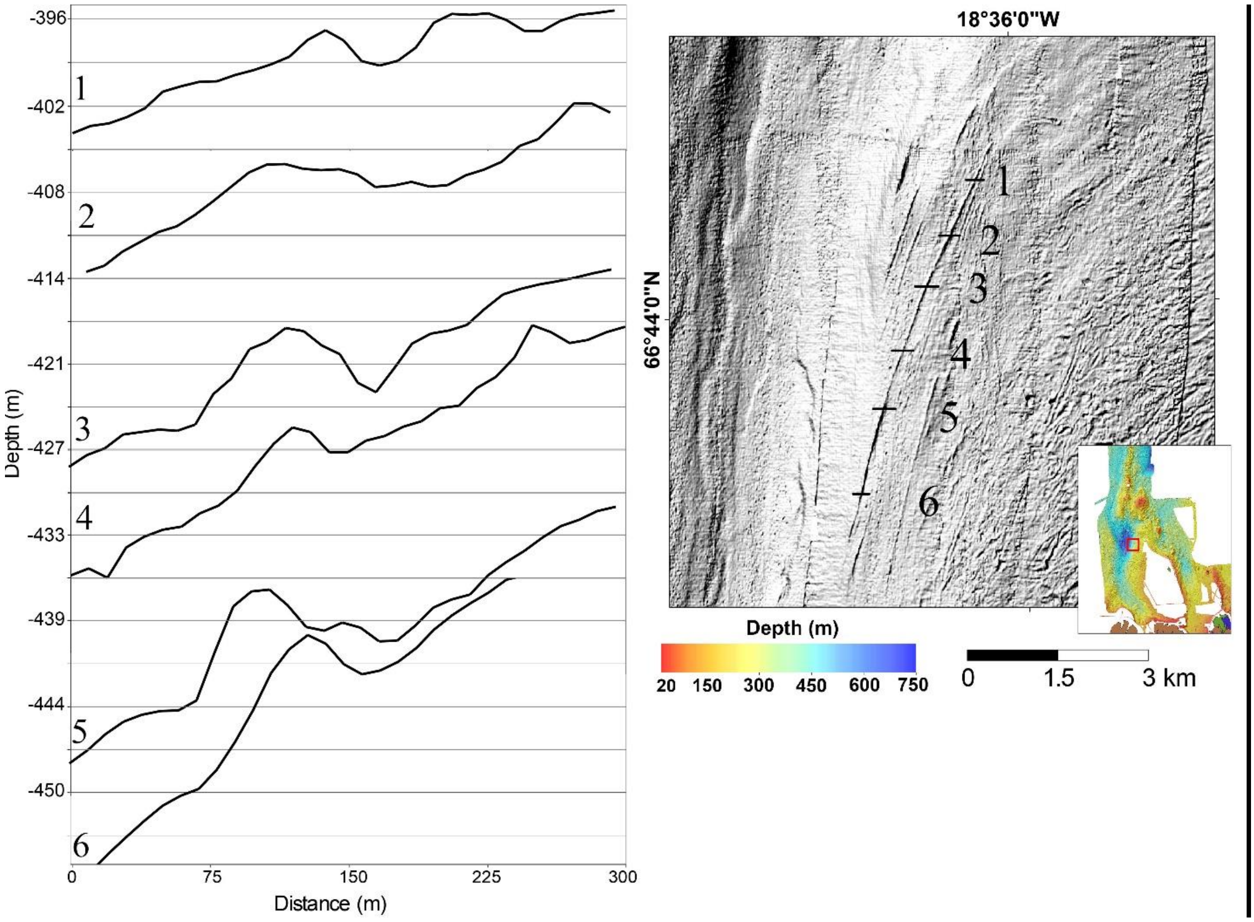

Figure 13. MSGLs on the eastern flank of EB near the GOB. Transects are labeled 1-6 and show the largest ridge in this area. These ridges are on the basin wall and there is over 50 m drop between the beginning and end of the ridges.

Just south of the previous area (Figure 13) is an area which shows one of two large clusters of the V-shaped ridges found in EB, along with eskers, moraines, MSGLs, and iceberg scours, as well as intense faulting (Figure 14). Section 3.2.1 will be dedicated to analysis of the V-shaped ridges within the EB.

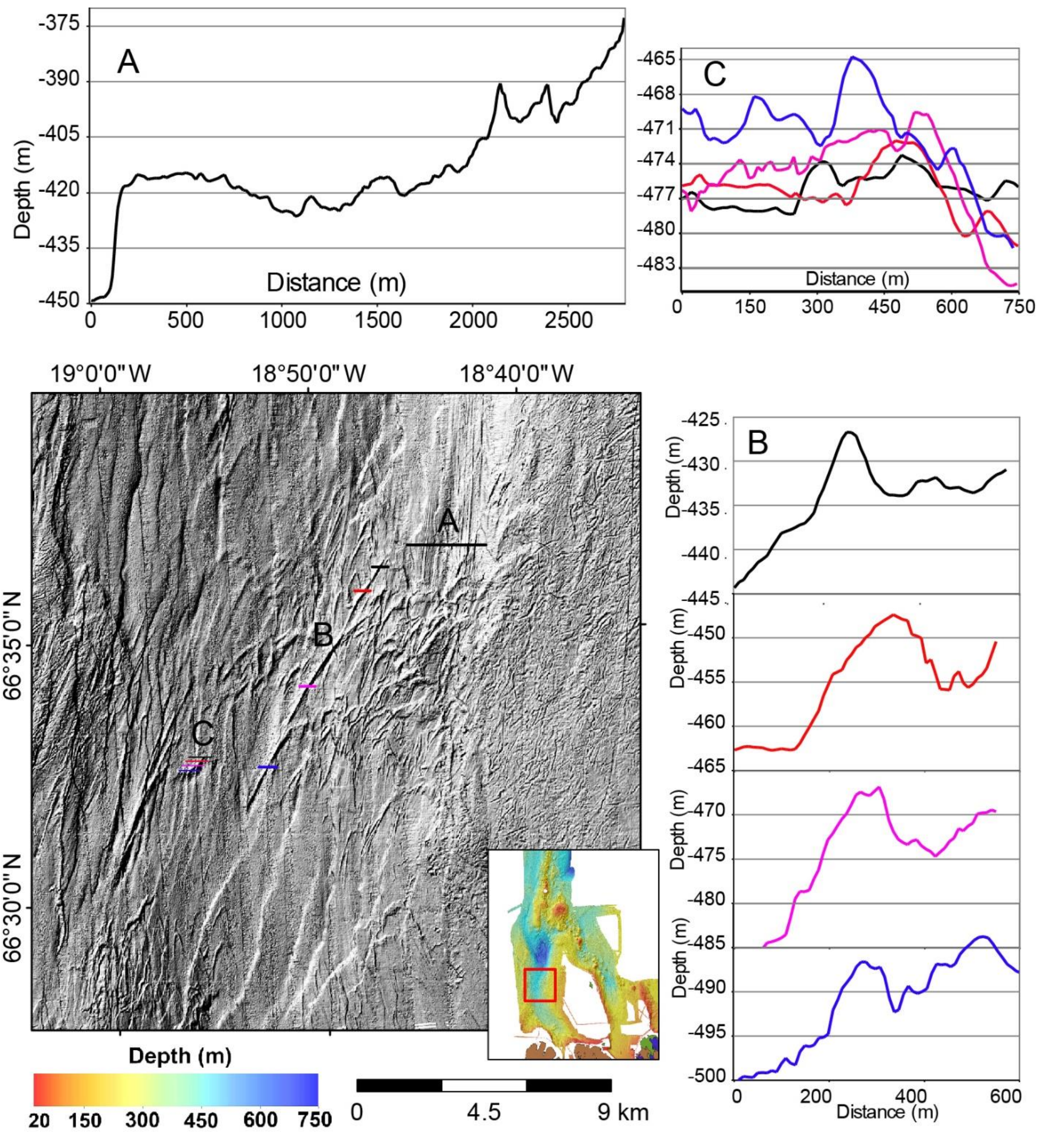

Figure 14. V-shaped ridges, moraines, eskers, and iceberg scours in Central EB. A. MSGLs extending N-S, and interuppted in the south by ridges created during a readvancement after the MSGLs were created. B. a medial moraine. C. a terminal or recessional moraine. Transect color legend as in Figure 10.

To the northeast there are several streamlined ice parallel ridges (Figure 14A) which are at least 7 km in length, further south it is not possible to determine their length as other V-shaped ridges and moraines overlap these ridges. These ridges have reliefs ranging from ~3-4 m in the west and up to ~10 m in the west and are 100-300 m wide. Due to their shape and size, I describe these ridges as MSGLs which formed during fast flow as the ice stream advanced to its terminal position at the LGM. These MSGLs predate the moraines and V-shaped ridges to its south which disrupt the southern extensions of the MSGLs.

An elongated ridge (Figure 14B) is found at approximately 66°32' north and 18°50' west at a depth of 435 – 500 m bsl. It has a length of approximately 10 km, a width of 100-150 m, and a relief of 5-10 m. This feature is located between where the larger Skagafjörður ice stream and smaller Eyjafjörður ice stream likely met, we describe this as a medial moraine. There is also several faults running N – S which cut through the moraine and thus show the faulting postdates the deposition of this moraine. There are no obvious signs of the moraine disrupting any of the V- shaped ridges.

West of the moraines southern extension is a short ridge flowing parallel to subparallel to ice flow direction (Figure 14C). Several transects taken across it which shows that the ridge is about 150 m wide, and over 6 m in relief. The ridge is just under 2 km long. The dimensions of this ridge are similar to those of the moraines in the area, and it is larger than the V-shaped ridges described in section 3.2.1. There are some similar short ridges in this area which could have been formed during the same event. This ridge could represent a short push moraine or esker.

A group of ridges are present at approximately 66°31'N by 19°6'W. This location is thought to be in the flow path of the ice stream which came from Skjálfandadjúp, flowing NE into Eyjafjarðaráll basin. Transects going across these ridges, as well as the hill above it (Figure 15, labeled GW) show the ridges range from 2 to 4 kilometers in length, 2 to 5 meters in relief and approximately 50 to 100 meters in width and are roughly symmetrical. While these features are shorter than the average length of MSGLs as described in Clark, et al. (2003), they do fit 4 the typical length:width ratio of 15:1 and thus I describe these features as MSGLs. There are at least 8 MSGLs in this area, though the exact count is hard to determine as some features are less obvious in the bathymetric maps and transects than others.

Just north of these MSGLs is an iceberg scoured hill which is approximately 30-40 meters in relief, ~1-3.5 km wide and 6-7 km long (Figure 15, transects labeled GW), though the faulting running through it could have shortened it since its deposition. This hill forms an inverted Δ-shape, thickening in the down ice direction, towards the NE. The faulting running through it indicates that this feature predates the faults. Due to its shape, location, and the surrounding features, I describe this feature as a grounding zone wedge. This feature displays a classic GZW shape (Dowdeswell and Ottesen, 2016; Ó Cofaigh et al., 2016). The existence of a GZW in this area would then point to a period of stagnation in either the retreat of the IIS or during a period of readvance.

Just east of the GZW there is a set of ridges running in the same ice parallel direction as the moraine and of similar relief (Figure 15, labeled M on the map and Moraine on the transects). There is a significant amount of faulting cutting through this area, most notably the fault which is located directly next to or possibly cutting through the western ridge. These ridges are 5 – 10 m in relief and 100 – 200 m wide. They run approximately 6 – 8 km long. There is also a winding ridge in this area that is approximately 8 meters in relief, 150 m wide, and

6.5 km long. This ridge could represent a moraine as well, or an esker as has a very typical esker shape (Figure 15, labeled E on the map and Esker on the transects).

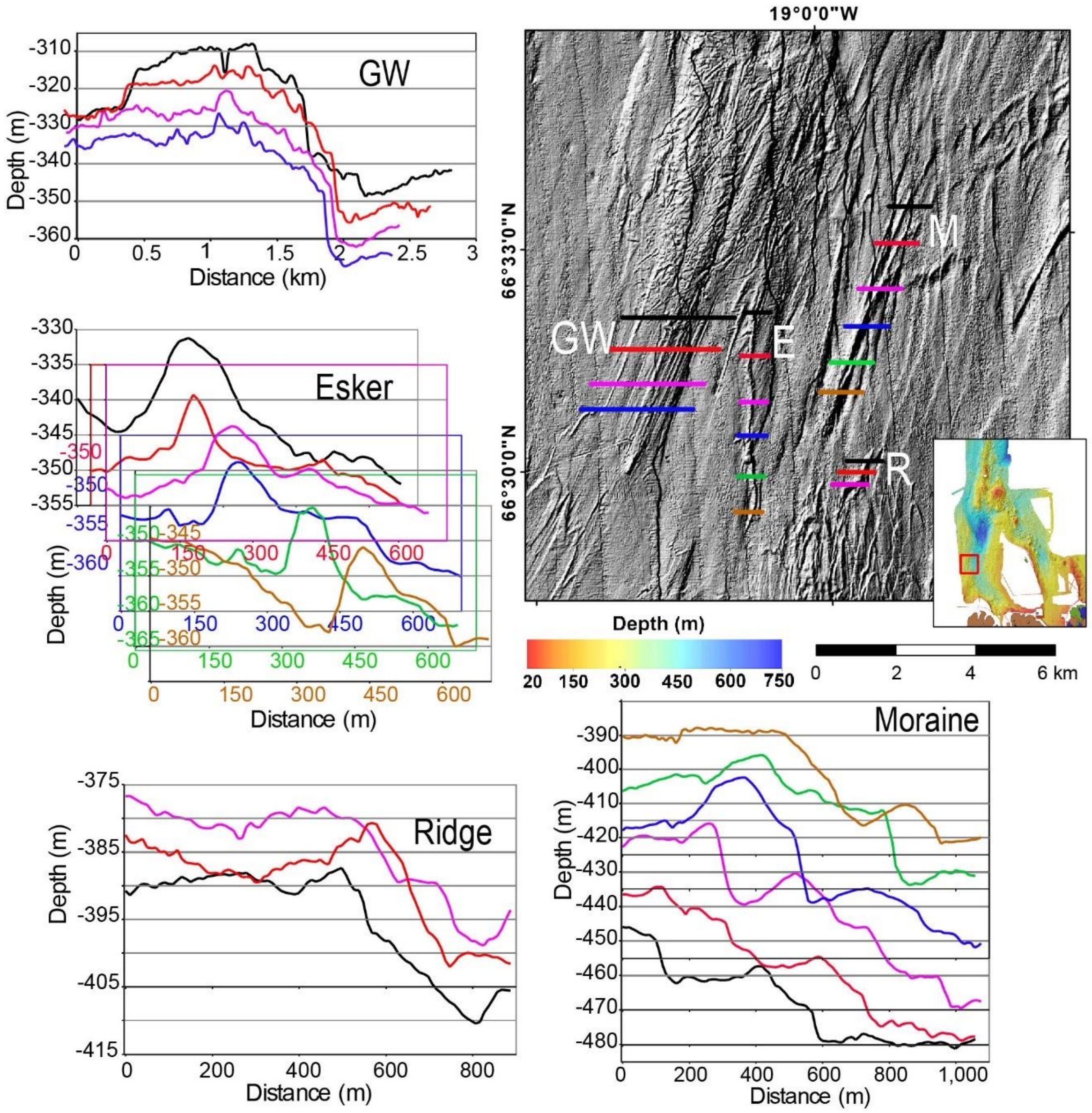

Figure 15. A grounding zone wedge (GW) with MSGLs, moraines (M), eskers (E), and iceberg scours surrounding it. Transect color legend as in Figure 10.

A small ridge can be seen south of the moraine (Figure 15, labeled R on the map and Ridge on the transects). This ridge is around 300 m wide, up to 20 m in relief and 1.7 km long. This ridge is directly north of a cluster of V-shaped ridges which will be discussed in section 3.2.1. This ridge is similar in size to the moraine and esker located just north, though it is shorter. It appears to be similar to the ridge to it east (Figure 14C). I describe this ridge as a short push moraine or esker and believe it is related to the eastern push moraine/esker (Figure 14C).

The landform assemblage (Figure 15) indicate that this was a grounding zone, likely for the ice stream coming from Skagafjörður rather than from Eyjafjörður. The data cuts off to the west of the features, which could possibly reveal more about this grounding zone and the direction that the ice stream was coming from.

The final collection of landforms in the central portion of EB begins at ~66°30N (Figure 16). The majority of these features are the V-shaped ridges, though just north of and in the center of this cluster of V-shaped ridges there also are several more arcuate shaped ridges which also have much wider crests than the V-shaped ridges which they lie among. Several transects taken through these ridges (Figure 16, labeled A and B) show that they possess similar qualities to the recessional moraines found to the north (Figures 14 and 15). Due to these similarities and relative proximity, I describe these ridges as either push moraines or eskers.

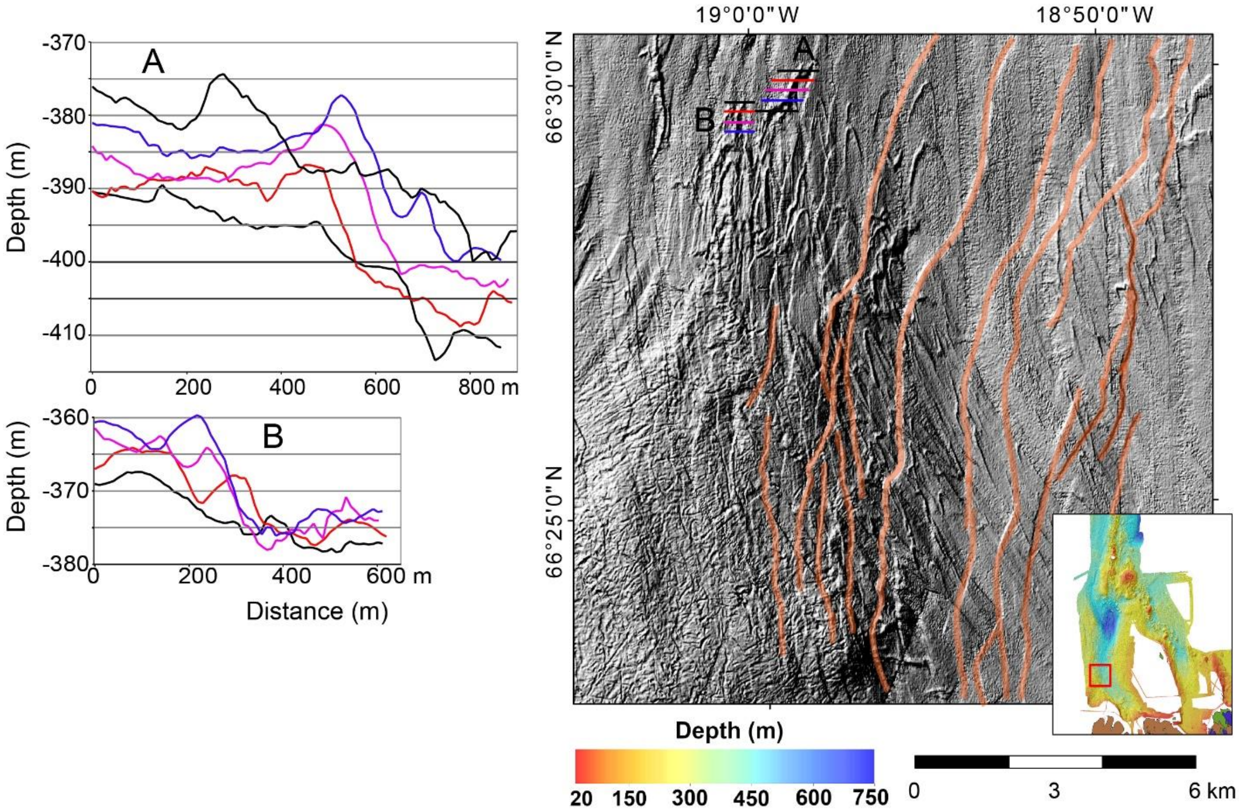

Figure 16. A cluster of V-shaped ridges cut by faults (represented by orange lines). Two ridges (Labeled A and B), just north of the V-shaped ridge cluster most likely represent recessional moraines. Transect color legend as in Figure 10.

Much of the sea floor in EB is iceberg scoured, with the scours somewhat chaotic but mostly trending SE-NW throughout the basin (Figures 12-16). These scours are present mostly at depths above 350 m bsl. Whether these scours were created by icebergs breaking off of the IIS or are from icebergs from the Greenland Ice Sheet (GIS) is not known. Some scours are overriding the subglacial features such as the V-shaped ridges when they occur at shallow enough depths indicating that these scours occurred sometime after the retreat of the IIS during the LGM.

3.2.1 V-shaped ridges

Clusters of V-shaped ridges exist in at least four distinct locations within the EB. These ridges are unlike any other features seen in marine paleo glacial environments which have been described in literature and are possibly unique to the paleo ice streams in Northern Iceland. Similar but not identical ridges have been described in the Bay of Fundy (Shaw et al., 2009). Terrestrial examples of similar ridges, identified as sawtooth or push moraines, can be seen across Iceland, described in section 4.1. At least 100 of these ridges are visible on the surface, though there are many more that are not as apparent due to being buried by sediment, seen in the seismic reflection data (Figure 17), and possibly more which have been altered/destroyed by faulting/tectonic activity.

Seismic reflection data taken over the basin shows that these features exist cross-basin, buried by sediment (Figure 17 A, B, and D). Unfortunately, ridges have not been specifically cored, so their internal structure and composition is not well understood. The ~10 kya marker (red line in Figure 17 B and D) shows that these features are older, and that this area had in fact been deglaciated by that time. The ridges are also highly reflective, indicating that they are composed of hardened sediments. The sediment drape in the central basin and other small depressions is transparent to semi-transparent representing an infill, consisting likely of marine mud. The dark, opaque reflector blanketing theses ridges and other glacial landforms represents tephra layers (Kristjánsdóttir, et al. 2007). Buried ridges are also identified by the reflection data, showing that there are potentially far more of these V-shaped ridges than is apparent in the bathymetric data, though these ridges could also represent MSGLs or moraines.

A

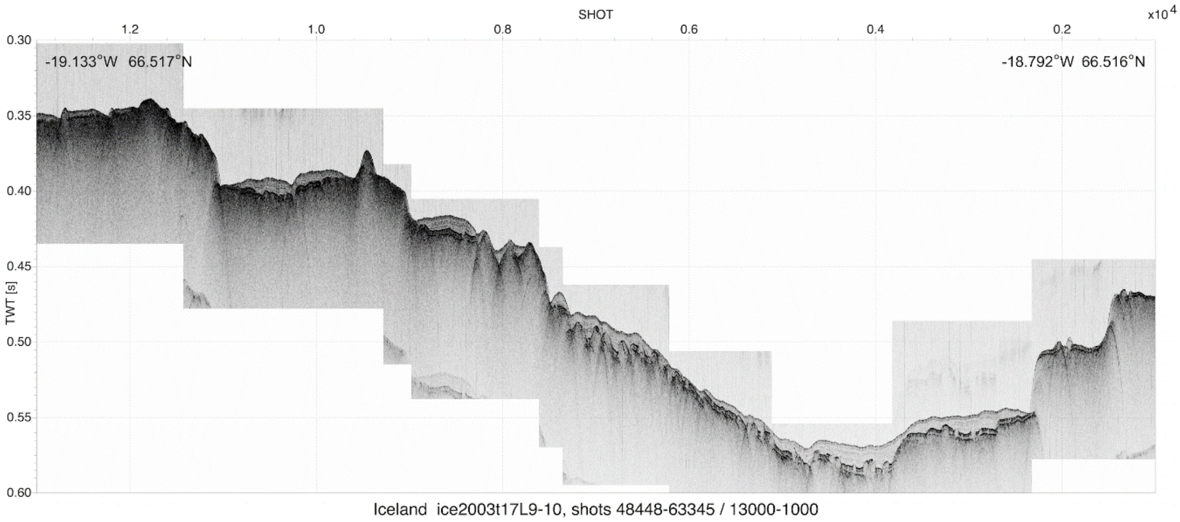

Figure 17. High-resolution Chirp seismic reflection data from the central Eyjafjaðaráll basin, showing that the V-shaped ridges are also buried beneath the sediment infill (light colored) at the center of the basin.

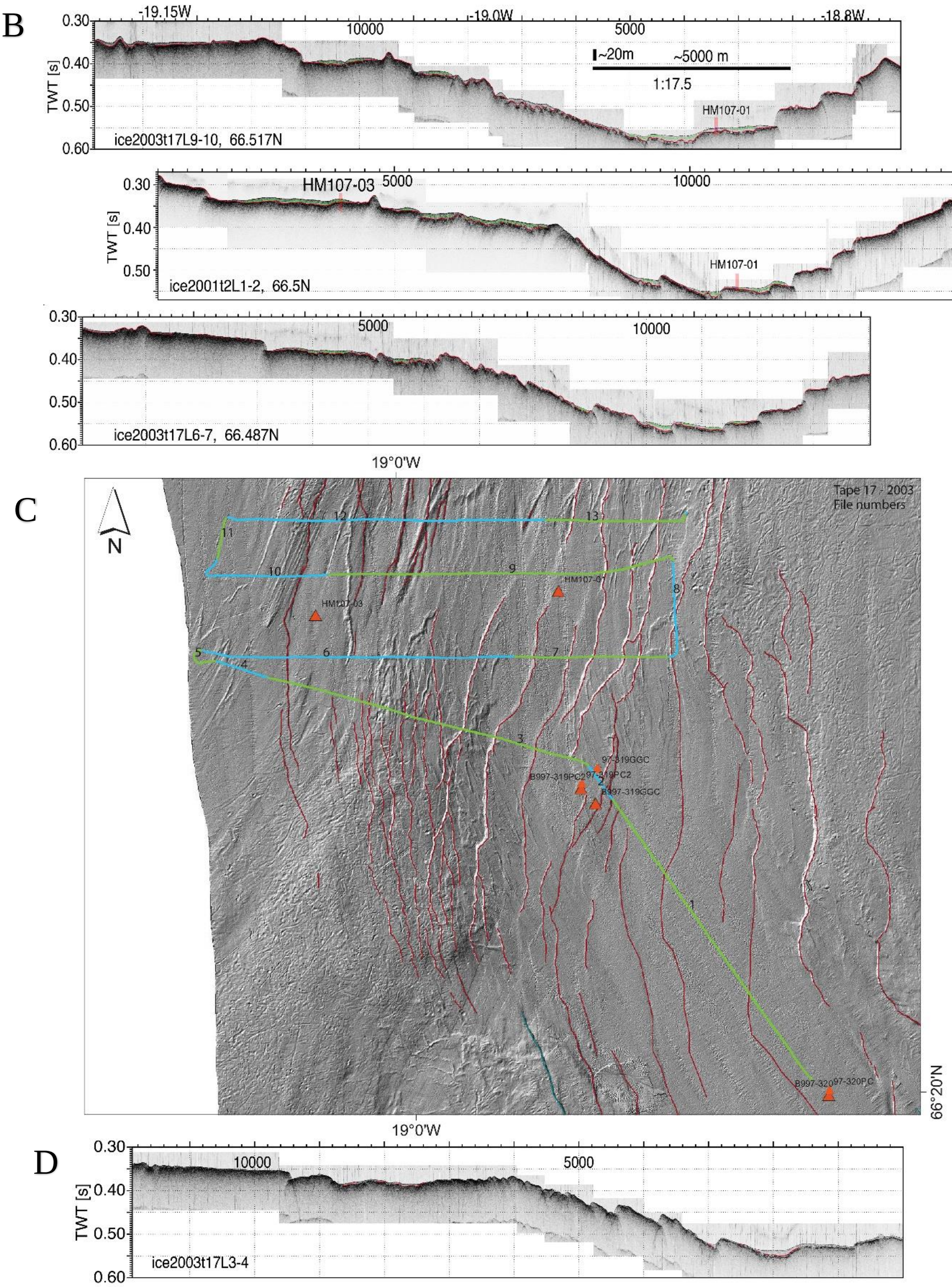
B
-19.15W
-19.0W
-18.8W
10000
5000
~20m
~5000 m
1:17.5
HM107-01
TWT [s]
0.30
0.40
0.50
0.60
ice2003t17L9-10, 66.517N
HM107-03
5000
10000
HM107-01
ice2001t2L1-2, 66.5N
5000
10000
ice2003t17L6-7, 66.487N
19°0'W
C
N
Tape 17 - 2003
File numbers
HM107-03
HM107-01
97-319GGC
B997-319PC2
97-319PC2
B997-319GGC
B997-320
97-320PC
66°20'N
19°0'W
D
10000
5000
ice2003t17L3-4

Figure 17 (cont.). B. Reflection data from survey lines 9 and 10, 1-2 (not displayed on the map, but located between 9-10 and 6-7), and 6-7. The red line represents a 10 ky marker in the sediment. Red rectangles are cores with their names labeled above them. C. Map of EB showing the locations of seismic data shot lines (green and blue lines). The red lines on the map are faults, and the red line running through the seismic reflection data is the 10k marker. D. Reflection data from shots 3-4. Notice in the reflection lines that the V-shaped ridges exist below the sediment in A, B, and D, meaning that there are even more V-shaped ridges than what can be seen with the multibeam data.

Analysis of the visible ridges was done to better understand the dimensions of these ridges (Table 1 and Figure 18). As can be seen in Table 1, the left arm is on average larger in every category compared to the right arm. The right arm was more often nonexistent compared to the left arm, which was almost always present. Out of 100 ridges analyzed, 21 had their right arm not visible versus five ridges which had their left arm not visible. Values of zero were considered in the average in the top row of Table 1 (highlighted yellow boxes) but removed as outliers for the average in the second row (white boxes).

Analysis of the ridges shows that they range from 0.5 – 10 m in relief, 100 - 5478 m in length, and 96 - 1296 m in width from arm to arm, and individual arms can range from 37 – 380 m wide or be completely absent.

Avg Width	Avg Width LA	Avg Width RA	Avg Relief LA
381.7979798	105.4646465	79.24242424	3.791414141
371.4947368	102.4	76.94736842	3.719473684

Avg Relief RA	Avg Length LA	Avg Length RA
3.105555556	744.4141414	503.7878788
3.036315789	733.9263158	447.1473684

Table 1. Values from analysis of 100 V-shaped ridges in EB. The top, yellow row represents all values, and the bottom, white row represents values with outliers removed. LA = Left Arm, RA = Right Arm.

I graphed these values to see how they relate to one another (Figure 18, A-I). I excluded the outliers from these graphs. All of the graphs show an overall positive trend, though not many of them show a good line fit. The first plot, Plot A, shows the left arm width vs. total ridge width with an R^2 value of 0.4272. Plot B shows the right arm width vs. total ridge width with an R^2 value of 0.3766. Plot C shows right arm relief vs right arm width with an R^2 value of 0.5796. Plot D shows left arm length vs left arm width with an R^2 value of 0.103. Plot E shows right arm relief vs left arm relief with an R^2 value of 0.304. Plot F shows right arm width vs left arm width with an R^2 value of 0.4669. Plot G shows left arm length vs right arm length with an R^2 value of 0.321. Plot H shows left arm relief vs. left arm length with an R^2 value of 0.6024. Plot I shows right arm relief vs right arm length with an R^2 value of 0.1771.

The relationships with the highest correlation are the relief vs length for both arms (Figure 18C and H), and the width of the right arm vs width of the left arm (Figure 18F). There appears to be less of a relationship the widths of individual arms and the total width of the V-shaped ridge (Figure 18A and B). There appears to be little relationship between the characteristics when comparing left vs right arm (Figure 18D, E, G, and I). Thus there seems to be a strong relationship between the relief and length of either arm of these ridges, and for the relief and width of the right arm, but the relief and length of the arms appear to develop individually and the data does not reveal a strong relationship.

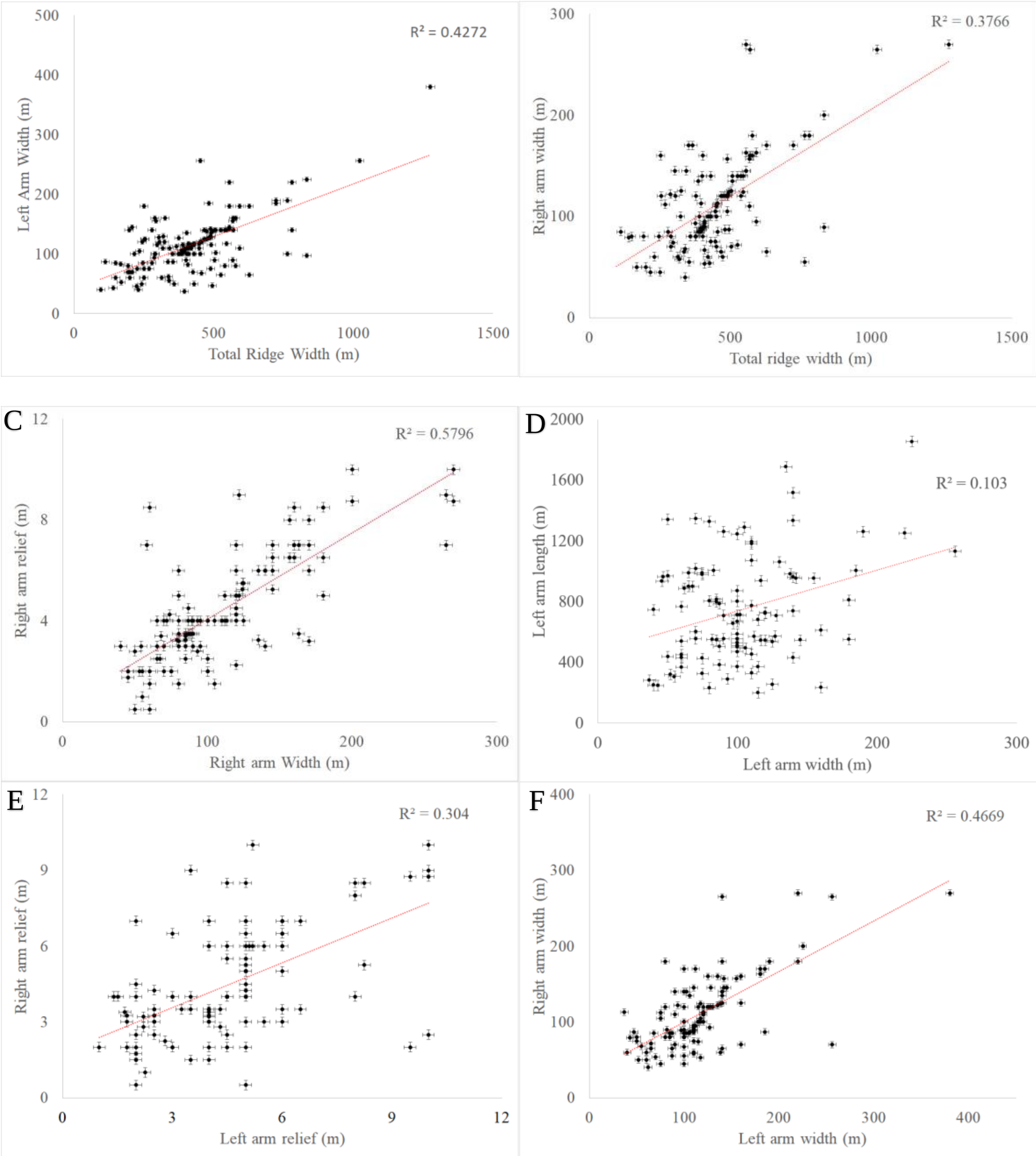

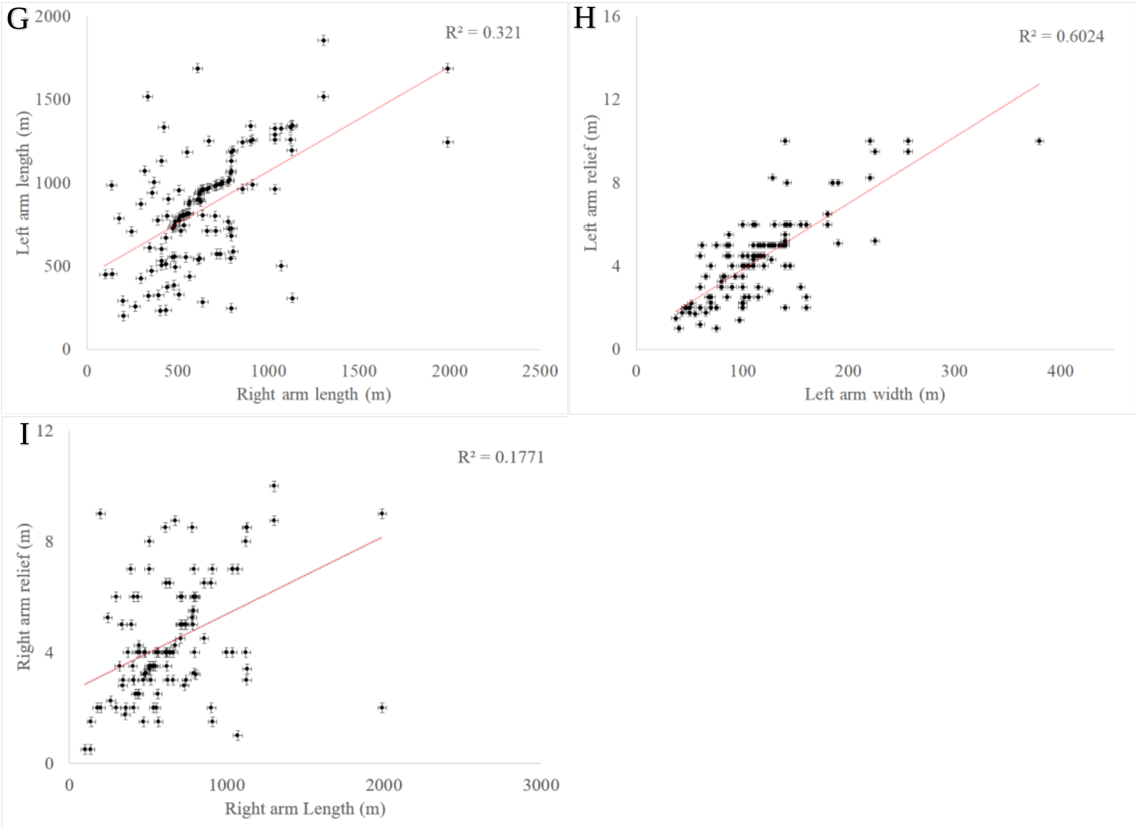

Figure 18. Comparison between the length, width, and relief of V-shaped ridges.

The V-shaped ridges appear to occur where the flow direction of the ice stream(s) is being altered. The southern-most ridges appear to occur where the Eyjafjörður ice stream collided with the much larger Skagafjarðardjúp ice stream, diverting the Eyjafjörður ice stream to the east. Then, the northern-most ridges appear to occur where the ice stream(s) divert to the north due to the presence of an over deepened basin. This change of flow direction is potentially an influence on their creation, as they do not seem to occur elsewhere throughout the basin, including at the potential LGM extent

Transects were taken across three ridges which were easily identified (Figure 19). These have a variety of sizes and often exist between faults. They are found both on level ground (Figure 19A) and on steep slopes (Figure 19B and C). The ridges exist both overlapping other ridges and among moraines and other ridges. The first map (Figure 19A) shows transects taken across two overlapping ridges, where the northern ridge was created and then slightly overridden by the southern ridge. The fault to the east cuts through the southern ridges right arm, which can be seen as an ~2 m on the eastern side of the fault. With these ridges, it appears that both arms are similar in size (~7-10 m) and that both the northern and southern V-shaped ridge also have similar sizes. The next ridge (Figure 19B) shows a ridge surrounded by other ridges, moraines, and lineations, as well as faulting to the southeast and northwest. The ridge is located on a steep slope. The transects taken across this ridge show that the left arm is better developed than the right arm. Whether this is due to the right arm never developing or being poorly preserved over time is not certain. The left arm is ~6 m in relief at its tallest point. The third ridge (Figure 19C) is also located on a steep slope, though less steep than Figure 19B. This ridge is easily identified as there is not many features overlapping or surrounding it. This ridge is similar to the ridge in Figure 19B; as seen in the transects it has a better developed left arm versus right is ~6m in relief.

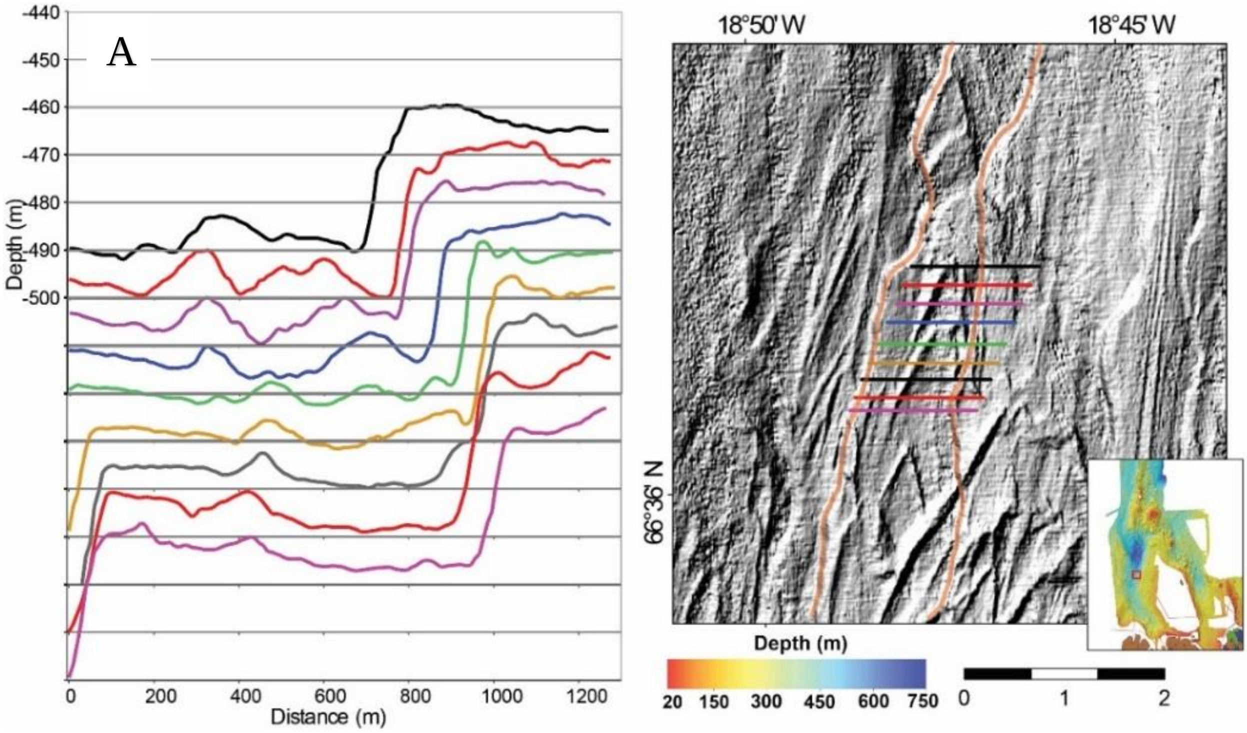

Figure 19. Transects across V-shaped ridges A, B, and C. Color legend as in Figure 10.

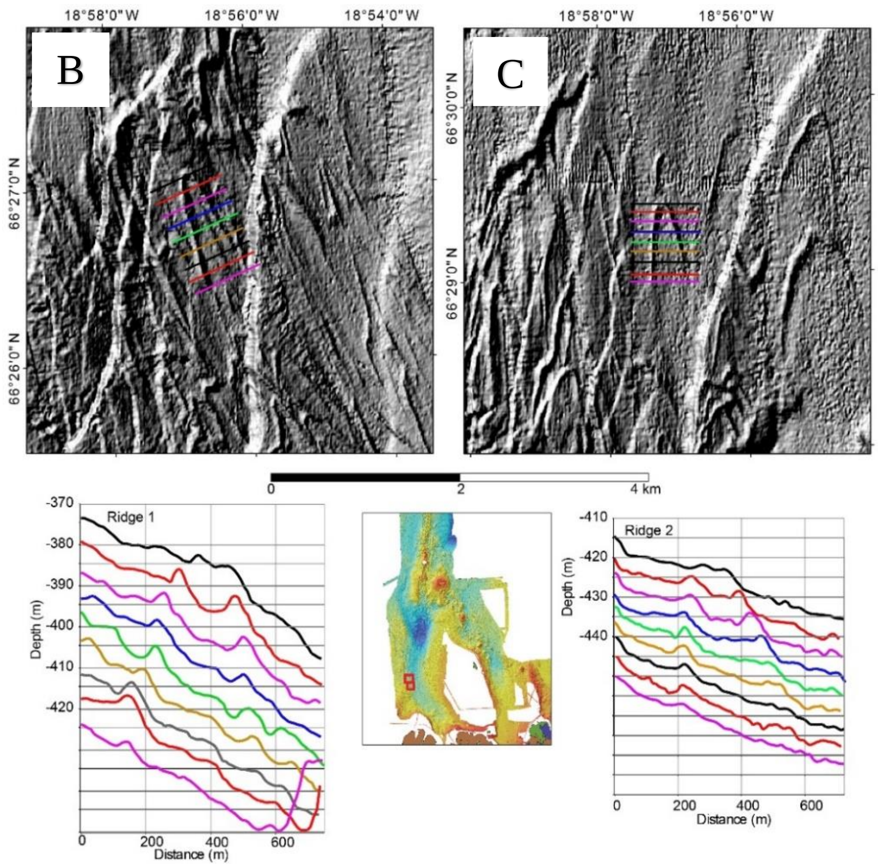

Figure 19. Cont.

3.3 Southern Eyjafjarðaráll

The southern portion of EB, from 66°23" to the opening of Eyjafjörður does not contain any visible V-shaped ridges. There are however several moraines and a potential grounding zone in this region. There is also intense faulting cutting through the region with cumulative subsidence of up to 140 m similar to the faulting in the central EB.

A set of features can be seen in the southwestern part of our study area around 66°18'N and 19°1'W (Figure 20). In this area there is the beginning of a trough-like feature which are oriented roughly SW-NE into the main EB trough. The trough is approximately 6 km wide at its widest point and up to 50 m deep (Transect 1 in Figure 20). Within this trough are numerous ridges which are oriented both parallel and perpendicular to the trough's NE-SW axis (transects 2-9 in Figure 20).

The ridges shown in transects 2 and 3 lie just next to the trough wall, flowing roughly SW-NE. There are at least 3 ridges, though the third ridge (the southeastern most ridge) is much smaller and shorter than the other two. They are between 3 and 10 meters in relief, up to 400 m wide and just over 1 km long. They are discontinuous, being split into two sections each by a gap in the middle. They lie parallel to the proposed ice flow direction in this trough. Due to these properties, I consider these ridges to represent an ice stream lateral moraine.

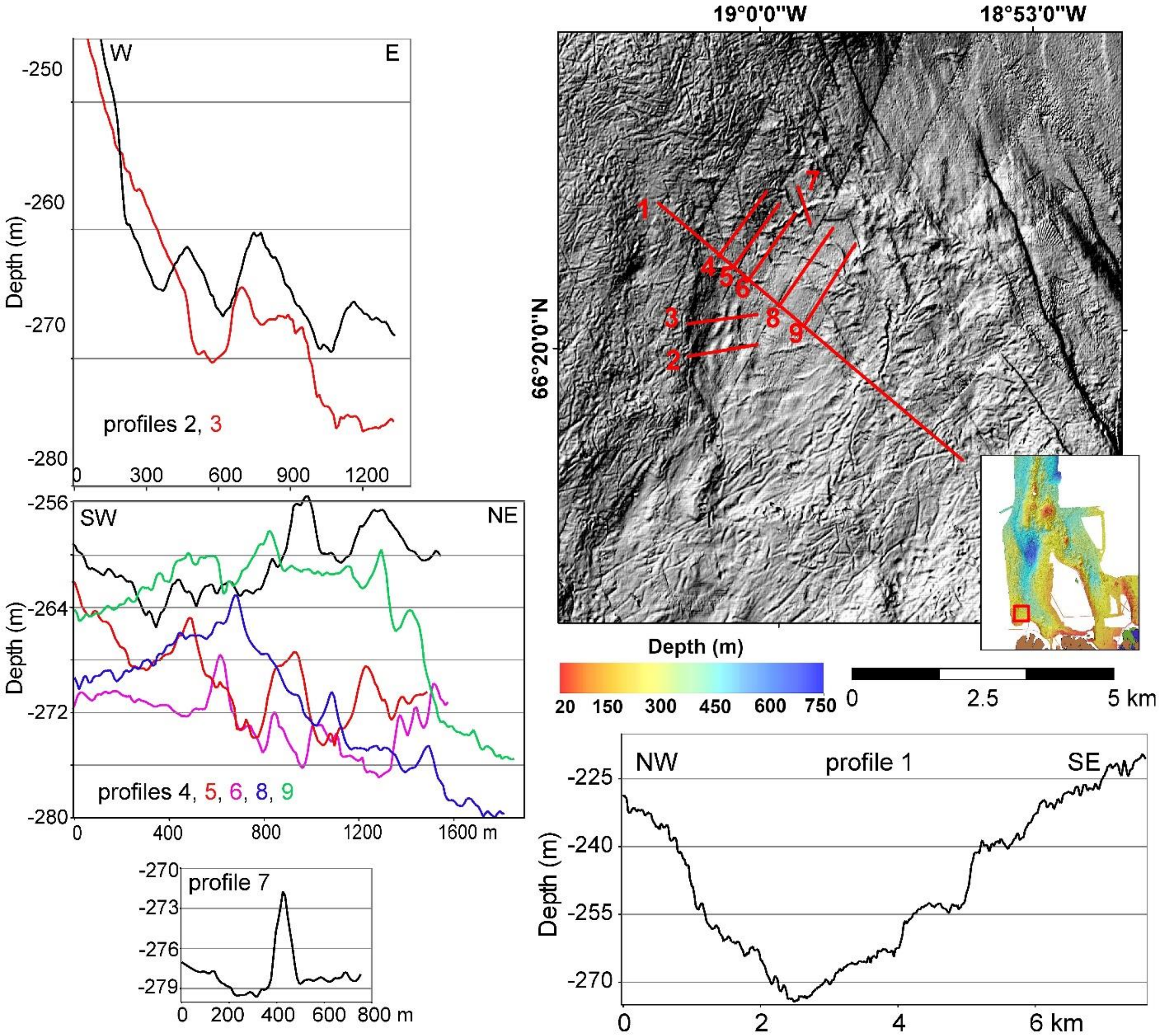

Figure 20. A possible moraine or grounding zone wedge from an ice stream coming from the southwest, possibly Skagafjörður (or a small ice stream coming from Siglufjörður?). Also shown are transects taken across the feature. Transect color legend as in Figure 10.

The ridges shown in transects 4-9 (excluding transect 7) are oriented perpendicular across the trough and are much smaller than the ridges in transects 2-3. These ridges have reliefs between 2 and 5 m, are 150-200 m wide, and 800-1500 m long. The ridge shown in transect 7 is more parallel to the ice flow direction and appears to be disrupted by one of the ice-perpendicular ridges from transect 4-9 in the southwest. This ridge is approx. 7 m in relief, 100 m wide and 1500 m long. Due to their positioning and size, I describe the ridges shown in transects 4-9 as recessional moraines, and ridge 7 as an esker, as it is oriented approximately parallel to the ice flow direction near the proposed terminal position this ice stream/outlet glacier.

Southwest of the ridges (Figure 20) is another, larger ridge which spans the distance of the trough. This feature is easily identified in ArcScene (Figure 21). The feature has somewhat of a sinusoidal shape which gives it a total length of approximately 6.5 km. It is approximately 200 m wide and has a 6 m relief. This feature is perpendicular to the basin and could represent a grounding zone wedge or large recessional moraine. The landform is overridden by iceberg scours, which have a dominant ENE-WSW direction (Figure 20). This ridge and the trough have light scouring compared to the elevated shelf to the northwest of the trough. I find it likely that in this area there was a smaller outlet glacier coming from the west, probably from Skagafjörður, which advanced through this area creating this trough and terminating once it reached EB, creating a hanging valley feature. As it retreated, it created a series of recessional moraines and experienced a readvance which created the larger sinuous ridge (Figure 21).

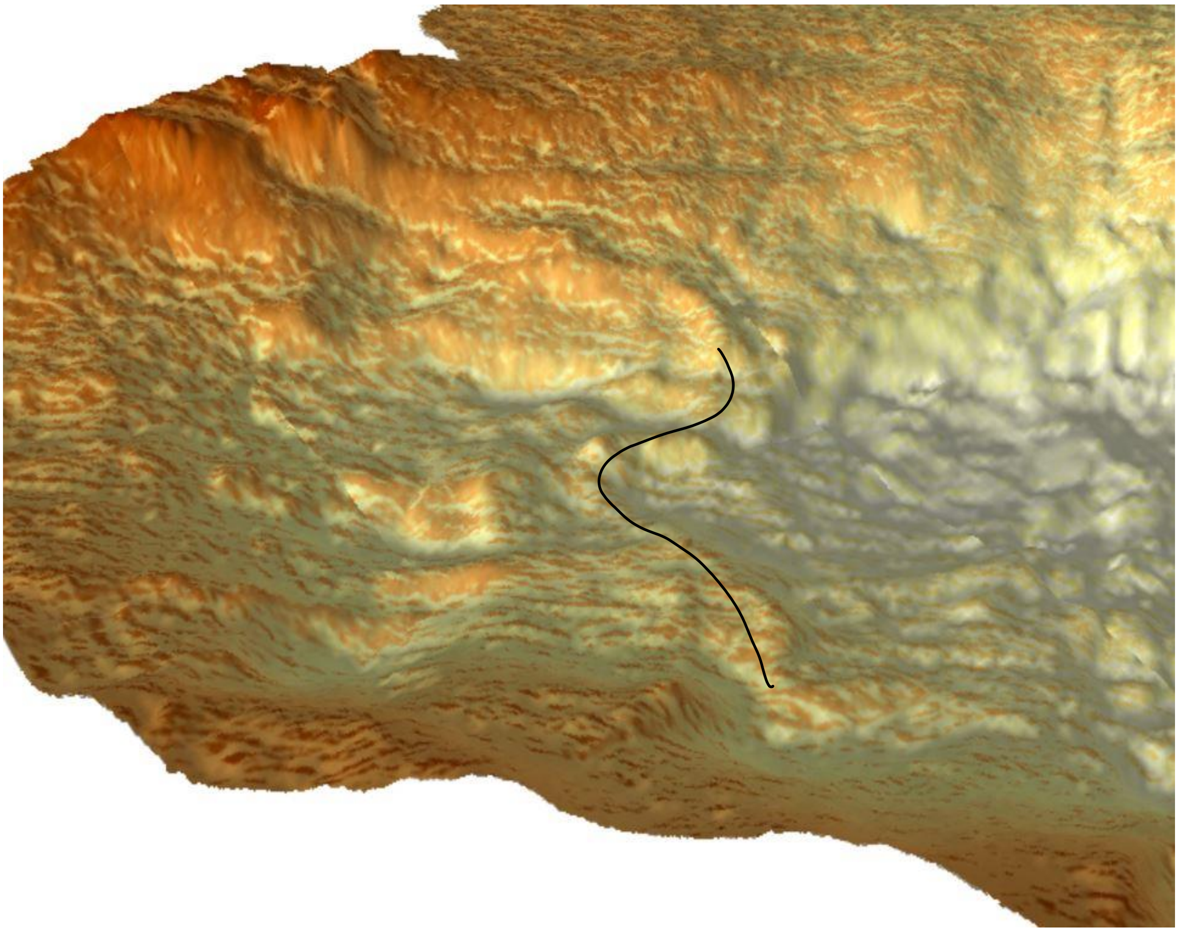

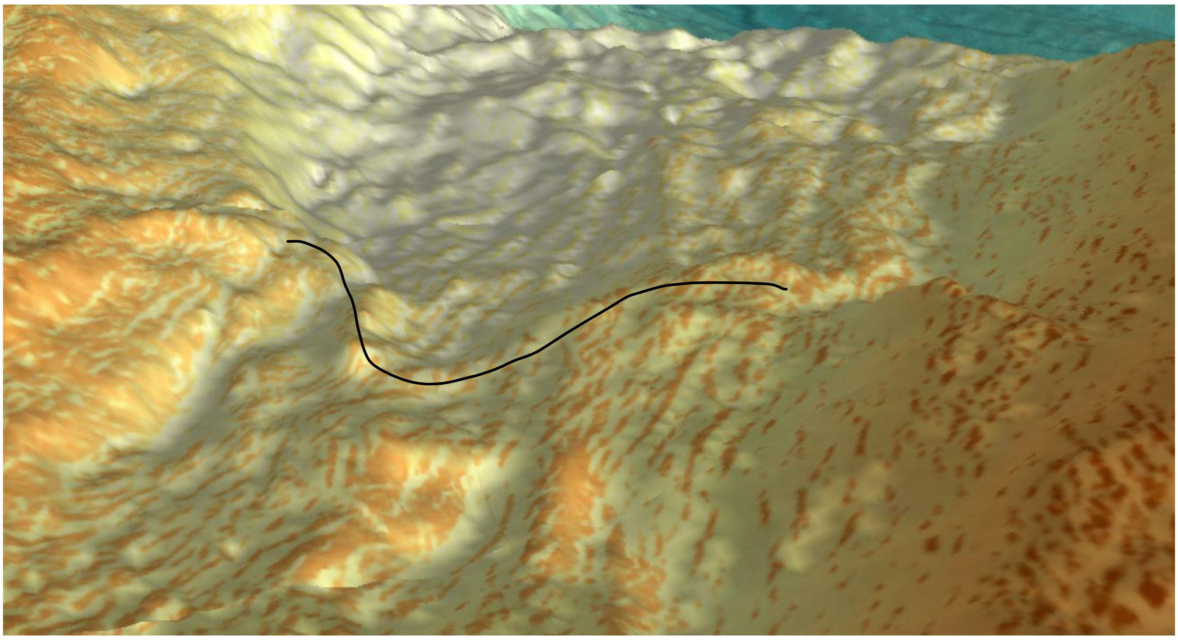

Figure 21. An ArcScene 3D figure showing the sinuous ridge flowing across the trough from Figure 20. The black line is outlining the ridge. A. Looking NW at the ridge from SE. B. Looking NE at the ridge from SW.

4 Discussion

The multibeam bathymetric data has revealed a complicated seafloor imprinted with tectonics cutting a variety of glacial landforms. In order to fully understand these V-shaped ridges, it is important to analyze and describe the entire landform assemblages, or what these features being found together says about the behavior of the ice sheet. Looking at the overall landform assemblages and limited sediment data in EB, a fast-moving ice stream within the EB retreated and left the basin ice-free by at least 13 kya, in line with models by Norðdahl et al., (2008) and Patton et al., (2017), among others. The locations and orientations of MSGLs, moraines, and grounding zone features indicate that there were several ice streams merged on the northern insular shelf on Iceland. The Eyjafjarðaráll ice stream, from the south, and the Skagafjarðardjúp from the west, met at approximately 66°30'N. The impact of the Skagafjarðardjúp ice stream with the smaller EB ice stream caused the EB ice stream to divert flow direction the east, reflected by the change of direction of the long axis of the fjord as well as a change in orientation of the V-shaped ridges. Similarly, a cluster of V-shaped ridges where the EB ice stream diverts to the west to flow into the over deepened basin which begins at approx. 66°38'N. The change in the flow direction of the ice stream would thus seem to be related to the formation of the V-shaped ridges. However, their apparent proximity to grounding zones and GZWs would imply that they are formed during periods of standstill or minor readvances.

There is a possibility that this ice stream was a surging glacier. If we considered the typical landform assemblages which are seen in modern and paleo marine terminating surging glacier landscapes, we would expect to see landforms such as overridden recessional moraines, MSGLS, terminal moraines, eskers, push moraines, and crevasses squeeze ridges (Sharp, 1985; Ottesen et al., 2008; Streuff et al., 2015). Several of these features can be found throughout the EB in close association with one another. Based on the typical descriptions of landform assemblages seen at modern and paleo marine terminating surging glaciers, I find it possible that the Eyjafjarðaráll ice stream was a surging glacier.

The V-shaped ridges do not necessarily resemble crevasse squeeze ridges found in places such as Iceland (Evans et al., 2007), Svalbard (Aradóttir et al, 2019), or Canada (Evans et al., 2016), though that does not entirely rule out the possibility of them originating as a type of crevasse squeeze ridge. Most literature about crevasse squeeze ridges from paleo ice streams/surging glaciers are terrestrial which are not identical to crevasse squeeze ridges in marine environments. Ottesen and Dowdeswell (2006) write about submarine landform assemblages in Svalbard, including rhombohedral ridges which they identify as crevasse squeeze ridges, which still are not very similar to the V-shaped ridges seen in EB.

De Geer moraines are found in palaeo glacial landscapes across the world (Lundqvist, 2000). They are small moraines occurring in clusters, parallel to the ice margin (though they have also been known to be perpendicular, winding, or anastomosing) and are usually 100s of meters long, 10-20 meters wide, and a few meters high (De Geer, 1940; Lundqvist, 2000). As seen in areas such as Kongsfjorden, Svalbard, De Geer moraines can display a “sawtooth” pattern in planform (Streuff, et al. 2015). The V-shaped ridges in EB can be described as having a sawtooth pattern, though they are morphologically dissimilar to De Geer moraines (e.g. Lundqvist, 2000; Streuff, et al. 2015; Ojala, 2016). Thus, I do not describe the V-shaped ridges found in EB as De Geer moraines.

The arcuate V-shaped ridges within the EB do not clearly fit available data on murtoos (Section 1.3.6). Murtoos are more triangular than the V-shaped ridges. The average size of murtoos as described by Ojala et al., (2018) is also much smaller than the average size of the V-shaped ridges. Though they may ultimately have a similar genesis, we do not believe they are the same features but without further research on both, this cannot be confirmed.

Relating the V-shaped ridges to push moraines would suggest that the ice stream in EB experienced periods of standstill and minor readvancement throughout the basin where the V-shaped ridges are present. The V-shaped thus had to form as the IIS was retreating as they would have been overridden and destroyed if they had formed prior to the IIS reaching its LGM position. Push moraines have a variety of characteristic shapes/sizes, and the V-shaped ridges are not necessarily morphologically similar to other push moraines described in Iceland, nor other glacial regions (i.e. Norway, Greenland, Antarctica) (Chandler et al., (2016); Johnson et al., (2013)). However there are some moraines in the forefields of several Icelandic glaciers which appear similar to these ridges which will be discussed in section 4.1.

The ridges were not influenced or created by tides or waves as they are too deep in the ocean. We can likely conclude that these features were formed at a significant depth that they could not be influenced by either of these (Norrman, 1964).

4.1 Modern Analogues?

Several glacial forefields exist with ridges that are somewhat similar to the V-shaped ridges in EB. The western tongue of the Breiðamerkurjökull outlet, on the southern margin of Vatnajökull, has retreated by several hundred meters in recent decades revealing a unique spiked, finger-like extensions (Figure 22) which are likely due to crevassing caused by outward splaying of the ice (Chandler et al., 2016; Evans et al., 2016). A series of arcuate ridges and several V-shaped ridges can be seen in the forefield from at least as far back as 1988 (the earliest time they are visible on aerial photos). Evans and Twigg (2002) state that these moraines have been forming since 1965. The arcuate ridges in the outer forefield represent recessional push moraines. As noticed by Evans and Twigg (2002), the V-shaped ridges in the forefield seem to align very well with the spiked edges of the glacier margin. These ridges are occasionally superimposed, which points to a winter readvancement which extended beyond the previous readvancement (Evans and Twigg, 2002). The push moraines are formed either by squeezing of water-soaked subglacial sediments or pushing of proglacial materials (Howarth, 1968; Price, 1970; Evans and Twigg, 2002). An aerial photo taken from 1988 which shows these V-shaped ridges (Figure 22). They are smaller in size than those found in EB, though that could be due to the ice stream which flowed through EB in the LGM being significantly larger than the Breiðamerkurjökull outlet glacier.

Similar V-shaped ridges are present in the forefield of Skaftafellsjökull, an outlet glacier of western Öræfajökull. An aerial photo from 1988 (Figure 22) shows a similar finger-like extensions coming from the glacier, likely producing the ridges seen in the forefield of the photos. Similar to that at Breiðamerkurjökull, the snout of Skaftafellsjökull is crevassed into a radial pectin pattern which influences the sawtooth shape of the push moraines in its forefield (Evans et al., 2018).

Similar ridges can also be seen in the forefields of Skálafellsjökull and Fláajökull outlet glaciers of SE-Vatnajökull, discussed in detail by Evans et al., (2016), Chandler et al., (2016), and Evans and Orton (2015). The snouts of Skálafellsjökull and Fláajökull are heavily crevassed into a radial pectin formation. The ridges in their forefields are hypothesized to be created through a combination of push and infill between these finger-like extrusions (Chandler et al., 2016; Evans et al., 2016). There are also superimposed ridges found where the crevasses are closely spaced (Evans and Orton, 2015). These sawtooth moraines are common and well developed in recently deglaciated (last 50 years) forefields of glaciers in South Iceland (Chandler et al., 2015, 2016; Evans et al., 2015; Price, 1970; Evans et al., 2018).

These glacial forefields of Vatnajökull are also similar to the forefield of Bødalen glacier in Western Norway (Matthews et al., 1979; Lien and Rye, 1988; Burki et al., 2009). Research done on these ridges has shown that their genesis is not entirely clear but thought to be caused by a combination of thrusting and bulldozing, and variations in stress and strain caused by changes in valley width creating splaying crevasses on the glacier tongue (Burki et al., 2009). Burki et al., (2009) also point out that heavily crevassed glacier tongues are not uncommon, so in addition to this crevassing, an interaction between glacier dynamics and valley geometry must be controlling factors in whether these sawtooth moraine ridges are created. One major difference between the sawtooth moraines in front of Bødalen glacier and those in EB are that those in EB are discontinuous and the sawtooth moraines form a continuous ridge with notches and teeth extending the width of the valley.

If these modern V-shaped ridges have a similar genesis to the ridges in EB, then that would point to similar behavior in the LGM ice stream and these outlet glaciers. A modern analogue can easily be observed and used in models for the LGM IIS to better understand its size and behavior.

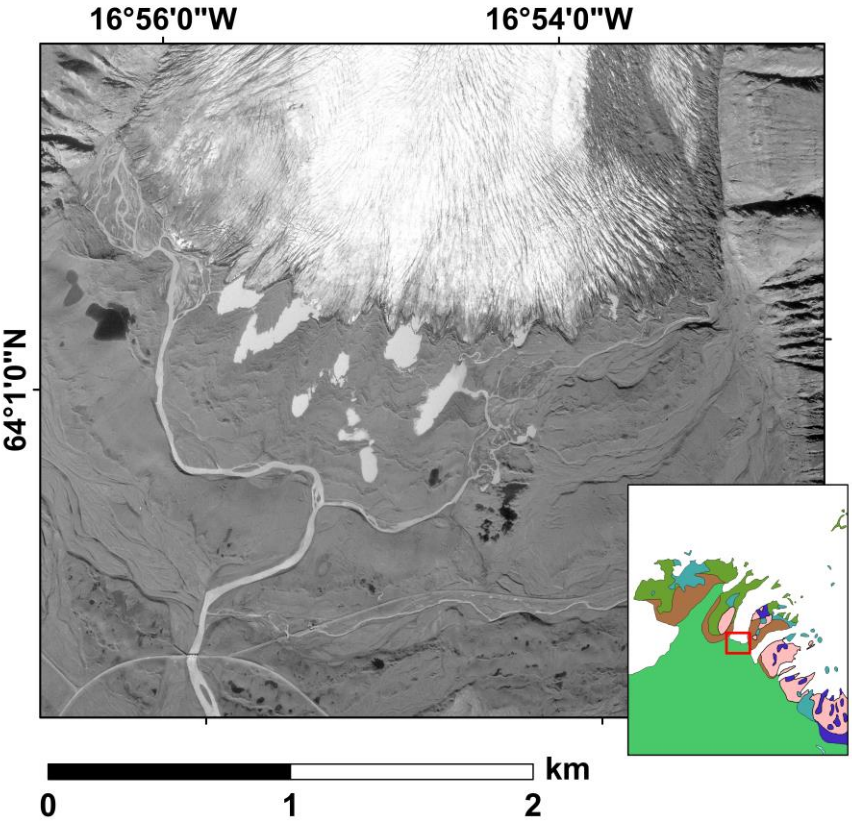
16°56'0"W
16°54'0"W
64°1'0"N
km
0
1
2

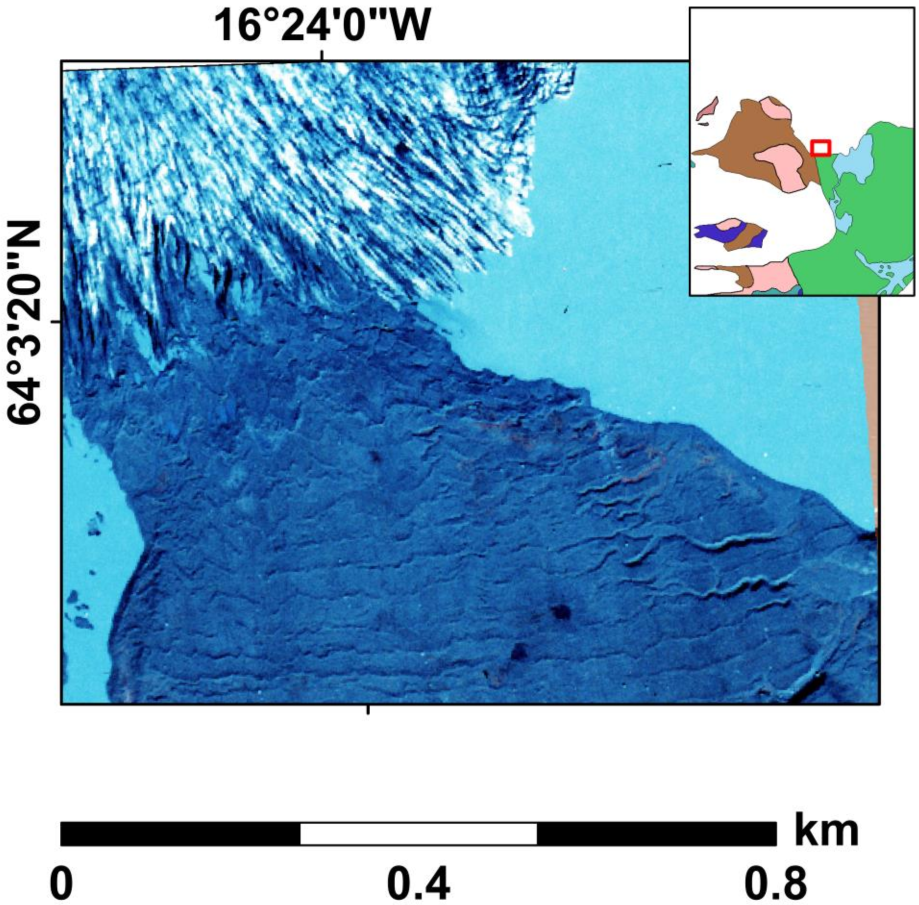
16°24'0"W
64°3'20"N
km
0
0.4
0.8

Figure 22. Aerial photos of Skaftafellsjökull in 1988 (top) and western Breiðamerkurjökull, by Breiðamerkurfjall in 1988 (below) showing the development on sawtooth moraines in the forefield overtime as well as the radial pectin pattern of the snout. Source: The National Land survey of Iceland.

A diagram on the hypothesized genesis of the V-shaped ridges found in EB was created (Figure 23). Without age constraints, we cannot say for certainty what events (i.e. warming of ocean water and increased sea level during Bølling-Allerød) caused the breakup, retreat, and readvances in the Eyjafjarðaráll ice stream, other than these ridges were created during the retreat of the IIS. We hypothesize that the Eyjafjarðaráll ice stream terminated at about 85 km offshore North Iceland at the LGM. The IIS began to retreat rapidly approx. 18.6 kya and was rapid but step like (Geirsdóttir et al., 2007; 2009; Norðdahl and Ingólfsson, 2015; Patton et al., 2017; Pétursson et al., 2015). During the retreat, the ice sheet experienced periods of stand still and readvanced, and the stress caused by rapid retreat, mixed with being topographically confined to the basin and forced change of direction caused pectin like crevasse patterns at the ice streams terminus (Figure 23A) which, through a combination of push and infill, created the V-shaped ridges which are seen throughout the basin. We hypothesize that the V-shaped ridges found in EB have a similar genesis to those found in the forefield of Skálafellsjökull, Fláajökull, and Breiðamerkurjökull. We also hypothesize that the size of the V-shaped ridges vary based on the extent of the ice stream readvancement, i.e. longer flanks are created through further advances and shorter flanks are created through smaller advances. This is similar to the landforms seen at Bødalen glacier in Norway, described as saw-tooth moraines, where the heavily crevassed glacier tongue is similar to those seen at Fláajökull, Skálafellsjökull, and Skaftafellsjökull (Burki et al., 2009).

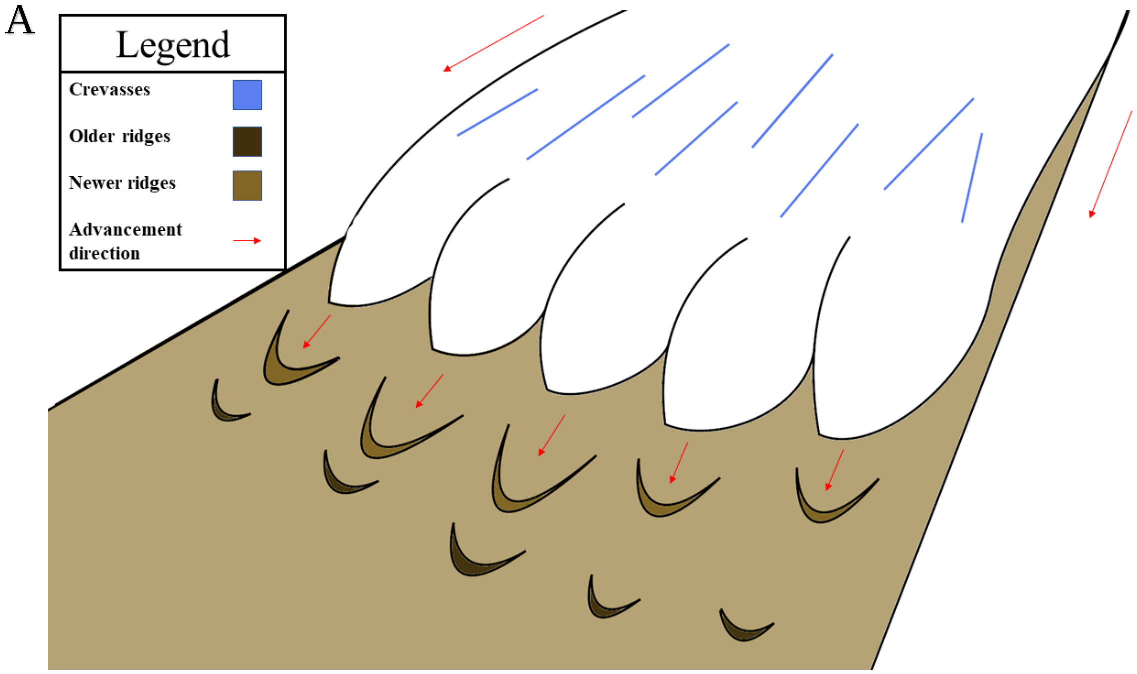

B

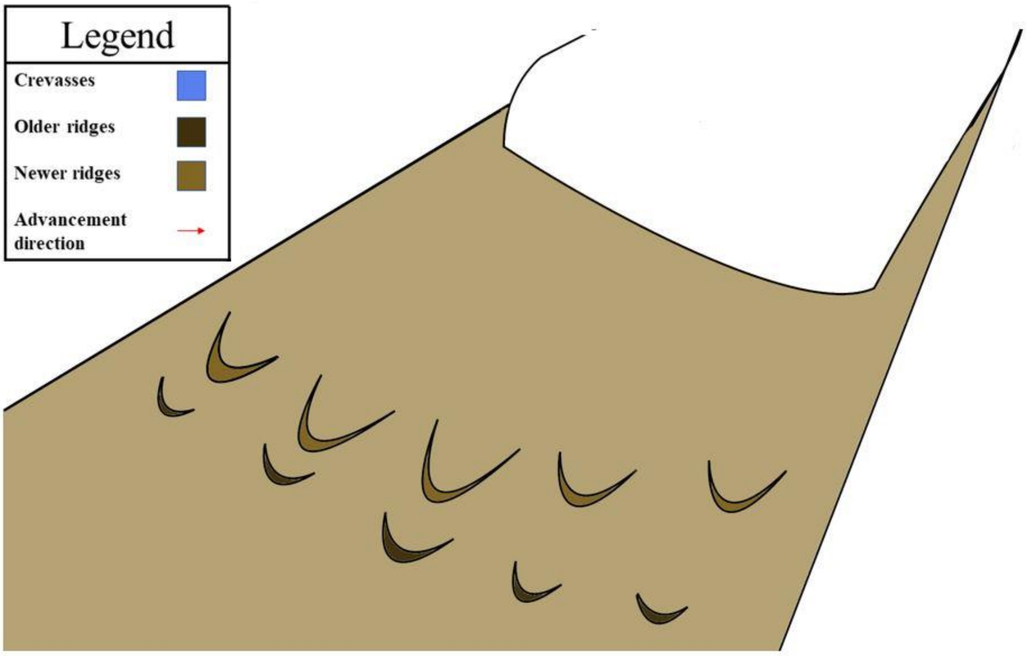

C

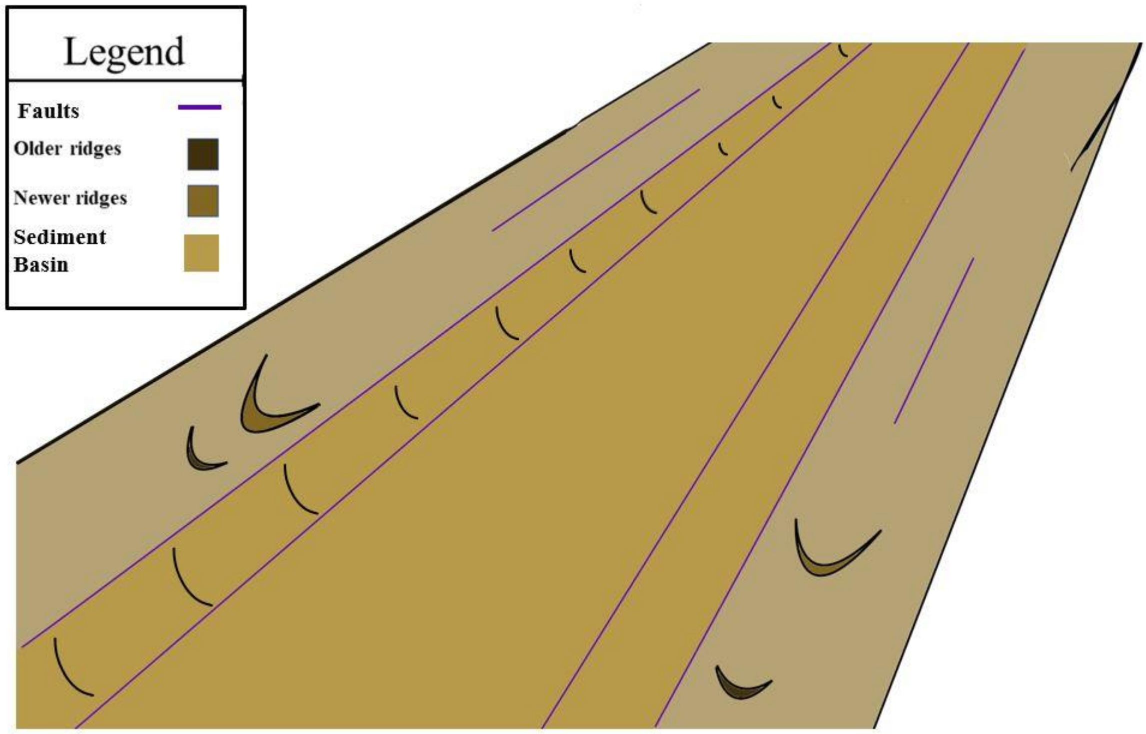

Figure 23. Diagram of creation of V-shaped ridges in EB in 3 steps: A) a readvance of the ice stream causes stress on the ice, resulting in a radial pectin crevassing on the snout. Through a combination of push and infill, the V-shaped ridges are created. In the down-ice direction, a prior readvance created B) Rapid breakup of the ice stream causes intense

calving, resulting in a more arcuate snout. A standstill occurs and the grounding of the ice stream at the southernmost portion of EB creates a large GZW or moraine. C) modern day EB has been faulting, resulting in over deepening of the basin by approx. 120 meters and sediment infill has obscured many of the V-shaped ridges, as well as other glacial relics. The outer most ridges and flanks of moraines can still be seen on the east and west sides of the basin.

5 Conclusion

During the last ice age, the IIS could have extended ~100 km north of the current coastline within the Eyjafjarðaráll and Skjálfandadjúp basins. Stepwise readvancements during the retreat have been mapped in detail withing these basins. The presence of several grounding zones throughout the EB are indications of where the ice streams experienced standstills (Dowdeswell et al., 2008), and minor readvancements during the breakup of the IIS. The presence of these indicators in the EB confirms the idea that the IIS experiences a rapid but step like retreat (Geirsdóttir et al., 2007; 2009; Norðdahl and Ingólfsson, 2015; Patton et al., 2017; Pétursson et al., 2015).

Evidence of the extent of the IIS at the LGM in the EB can be found as far north as 67°4'N, possibly further (Figure 9). Studies of paleo glacial landforms in Skjálfandi basin shows that the LGM ice stream extended to a similar position (Figure 24). Based on these features, the ice streams extending into the North Iceland insular shelf and merged just south of the Kolbeinsey Ridge. The EB ice stream and Skjálfandi ice stream also have grounding zones at similar positions in the middle of the basins.

The overall landscape assemblage which is revealed through the data points to a fast-moving ice stream which had fully receded onto land by at least 10kya. The features seem to match those of a typical surging marine terminating glacier foreground as described by Streuff et al., 2015 which could indicate that this was the location of a surging glacier.

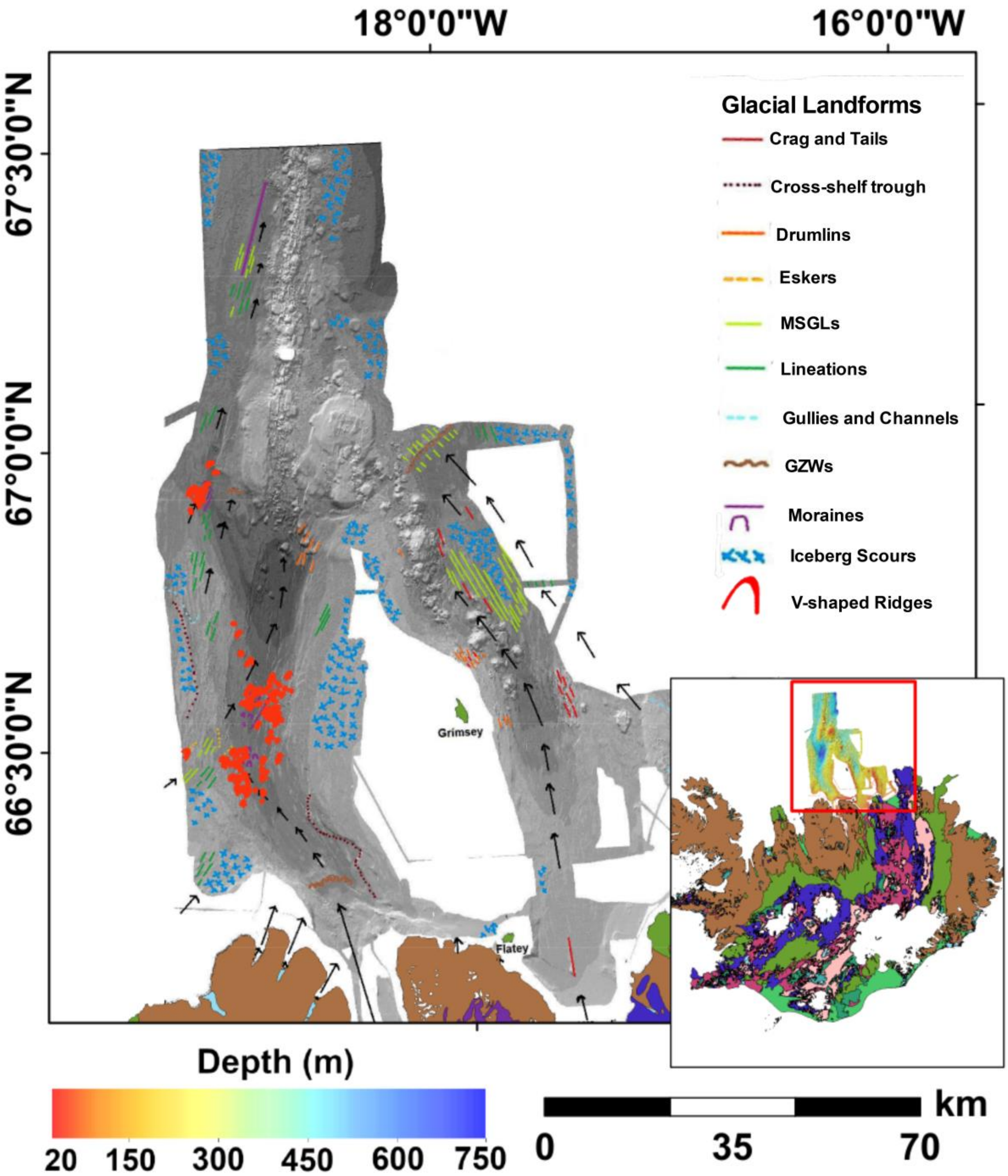

Figure 24. Glacial landforms found on the North Iceland Insular Shelf. Modified from Höfer, 2019 to include V-shaped ridges.

Further analysis of the V-shaped ridges which are present throughout EB help further refine models of the extent and behavior of the IIS during the last glaciation. The locations and genesis of the V-shaped ridges could indicate that the IIS was grounded up to 100 km offshore north Iceland and experienced surging. What is currently known about the V-shaped ridges are as follows:

- They are formed at grounding zones of fast-moving ice stream.
- Are often found in association with MSGLs and eskers.

- Exist cross basin, with an unknown number of ridges buried beneath sediment.
- Have a wide range of lengths, reliefs, and widths, and tend to have a better developed left arm compared to their right, and many ridges are lacking a right arm altogether.
- Exist in areas where there is a disruption in the flow of the ice stream.
- Exist in distinct areas throughout the basin beginning at about 35 km from the mouth of Eyjafjörður and extending as far out as approx. 92 km (directly west of Stóragrunn).

To understand how and why these ridges formed, we must first attempt to understand the basal ice dynamics, interface thermal conditions, and sediment rheologies of the basal load (Hart, 1997; Hindmarsh, 1999; Schoof, 2007; Dunlop, et al. 2008; Menzies and Hess, 2013; Vreeland, et al., 2015; McCracken, et al. 2016; Menzies, et al. 2016). Without further investigation of this area and the composition of these ridges, it is difficult to gain a complete understanding of these processes and thus their genesis cannot be known with certainty.

5.1 Future Research

Further studies on these ridges are required to better constrain their formation. An analysis of their internal composition and structure need to be done before there is any conclusive answer on the genesis of these ridges. Also, better mapping offshore Iceland could also uncover more of these V-shaped ridges in other locations, helping us to understand what conditions these ridges form under. Further studies should aim to answer the following questions: 1) What process(es) create these V-shaped ridges? 2) What is the structure/composition of these feature?

Cores of the ridges or other features could be very useful in helping understand the genesis and properly identifying them. I have marked on the map areas where further cores could be collected (Figure 25).

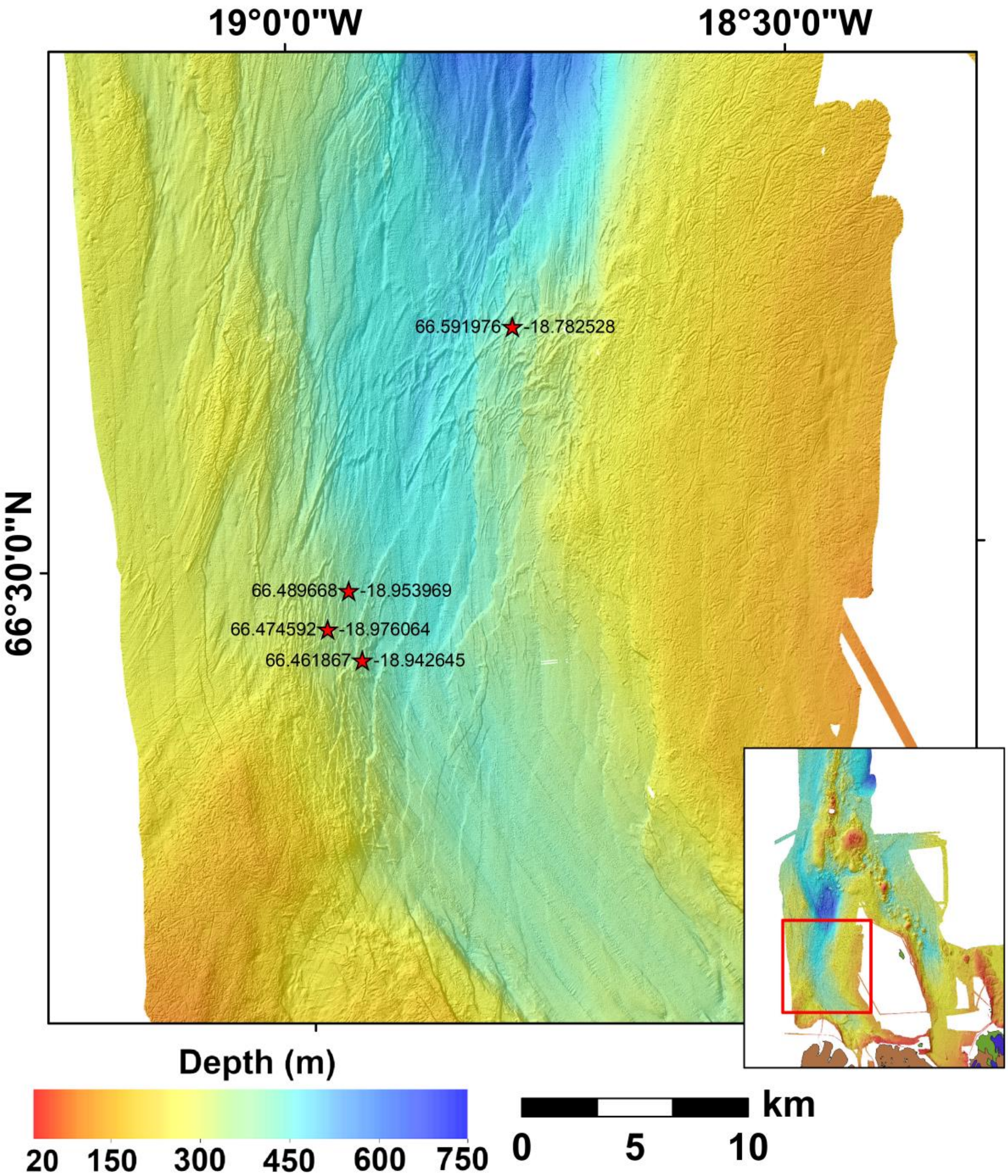

Figure 25. Potential core sites (red stars) in the EB

References

Alley, R.B., Blankenship, D.D., Bentley, C.R., Rooney, S.T., 1986. Deformation of till beneath ice stream B, West Antarctica. *Nature 322 (6074),* 57–59.

Andrews, J.T., Harðardóttir, J., Helgadóttir, G., Jennings, A.E., Geirsdóttir, Á., Sveinbjörnsdóttir, Á.E., Schoolfield, S., Kristjánsdóttir, G.B., Smith, L.M., Thors, K., Syvitski, J.P.M. (2000). The N and W Iceland Shelf: insights into Last Glacial Maximum ice extent and deglaciation based on acoustic stratigraphy and basal radiocarbon AMS dates. *Quaternary Science Reviews 19,* 619-631.

Aradóttir, N., Ingólfsson, Ó, Noormets, R., Benediktsson, Í.Ö., Ben-Yehoshua, D., Håkansson, L., Schomacker, A. (2019). Glacial geomorphology of Trygghamna, western Svalbard – Integrating terrestrial and submarine archives for a better understanding of past glacial dynamics. *Geomorphology 334:* 75-89. doi:10.1016/j.geomorph.2019.07.007

Arndt, J.E., Jokat, W., Dorschel, R., Myklebust, R., Dowdeswell, J.A., Evans, J. (2015). A new bathymetry of the Northeast Greenland continental shelf: constraints on glacial and other processes. *Geochemistry, Geophysics, Geosystems, 16,* 3733-3753

Ashwell, I.Y. (1996). The geomorphology of Fnjóskadalur, N. Iceland: Reinterpretation in terms of sub-glacial hydrologic processes, with the introduction *"The deglaciation of Iceland".* Personal publications.

Attig, J. W., Mickelson, D. M., Clayton, L. (1989) Late Wisconsin landform distribution and glacier-bed conditions in Wisconsin, *Sediment. Geol., 62,* 399–405.

Axelsdóttir, H. (2002). Búðaröðin: Landmætunarfræðileg kortlagning jökulgarða milli Þjórsár og Eystri-Rangár. Unpublished B.S. Thesis, University of Iceland, Reykjavík, 41 pp.

Bamber, J.L., Vaughan, D.G., Joughin, I. (2000). Widespread complex flow in the interior of the Antarctic Ice Sheet. *Science 287 (5456),* 1248–1250.

Banerjee, I., McDonald, B.C. (1975). Nature of esker sedimentation. *Glaciofluvial and Glaciolacustrine Sedimentation, Society of Economic Paleontologist and Mineralogists,* 304-320

Barcheck, C.G., Schwartz, S.Y., Tulaczyk, S. (2019). Icequake streaks linked to potential mega-scale glacial lineations beneath an Antarctic ice stream. *Geology, v. 48,* doi: 10.1130/G46626.1

Bart, P.J., Owolana, B. (2012). On the duration of West Antarctic Ice Sheet grounding events in Ross Sea during the Quaternary. *Quaternary Science Reviews, 47*, 101-115.

Bartholomaus, T.C., Anderson, R.S., Anderson, S.P. (2011). Growth and collapse of the distributed subglacial hydrologic system of Kennicott Glacier, Alaska, USA, and its effects on basal motion. *Journal of Glaciology, 57,* 985-1002.

Batchelor, C.L., Dowdeswell, J.A., Pietras, J.T. (2014). Evidence for multiple Quaternary ice advances and fan development from the Amundsen Gulf cross-shelf trough and s ope, Canadian Beaufort Sea margin. *Marine Petroleum Geology, 52*, 125-143.

Batchelor, C.L., Dowdeswell, J.A. (2015). Ice-sheet grounding-zone wedges (GZWs) on high-latitude continental margins. *Marine Geology 363*, 65-92.

Batchelor, C.L., Dowdeswell, J.A. (2016). Lateral shear-moraines and lateral marginal moraines of palaeo-ice streams. *Quaternary Science Reviews 151,* 1-26.

Bell, R.E. (2008). The role of subglacial water in ice-sheet mass balance. *Nat. Geoscience, 1*, 297-304.

Bell, T., Cooper, A.K., Solheim, A., Todd, B.J., Dowdeswell, J.A., Canals, M., Jakobsson, M., Dowdeswell, E.K., Hogan, K.A. (2016). Glossary of glaciated continental margins and related geoscience methods. From: Dowdeswell, J.A., Canals, M., Jakobsson, M., Todd, B.J., Dowdeswell, E.K., Hogan, K.A. (eds) 2016. *Atlas of Submarine Glacial Landforms: Modern, Quaternary, and Ancient*. Geological Society, London, Memoirs, 46, 49-50, 2016, 555-574. doi:10.1144/M46.177

Benn, D.I., Evans, D.J.A. (1998). Glaciers and Glaciation. *Arnold, London,* 734 pp.

Benn, D.I., Evans, D.J.A. (2010). Glaciers and Glaciation, 2nd edition. *London: Routledge*, doi: 10.4324/9780203785010

Bennett, M.R. (2001). The morphology, structural evolution and significance of push moraines. *Earth-Science Reviews 53,* 197–236.

Bennett, M.R. (2003). Ice streams as the arteries of an ice sheet: their mechanics, stability and significance, *Earth-Science Reviews*, *61*, 309–339, doi:10.1016/S0012 8252(02)00130-7.

Bennett, M.R. (2011). Ice-Marginal Processes. In: Singh V.P., Singh P., Haritashya U.K. (eds) *Encyclopedia of Snow, Ice and Glaciers. Encyclopedia of Earth Sciences Series.* Springer, Dordrecht.

Bennett, M.R., MacLean, B., Blasco, S., Hughes Clark, J.E. (2016) Glacial lineations in Navy Board Inlet, Nunavut, Canada. From: Dowdeswell, J.A., Canals, M., Jakobsson, M., Todd, B.J., Dowdeswell, E.K., Hogan, K.A. (eds) 2016. *Atlas of Submarine*

Glacial Landforms: Modern, Quaternary, and Ancient. Geological Society, London, Memoirs, 46, 49-50, 2016, doi:10.1144/M46.56

Bentley, C.R. (1987). Antarctic ice streams: a review. *J. Geophys. Res., 92,* 8843-8858.

Boulton, G.S. (1986). Push-moraines and glacier-contact fans in marine and terrestrial environments. *Sedimentology 33,* 677–698.

Boulton, G.S., Van der Meer, J.J.M., Beer, D.J., Hart, J.K., Ruegg, G.H.J. (1999). The sedimentary and structural evolution of a recent push moraine complex: Holmstrømbreen, Spitsbergen. *Quaternary Science Reviews 18,* 339–371.

Bourgeois, O., Dauteuil, O., van Vliet-Lanoe, B. (2000). Geothermal control of flow patterns in the last glacial maximum ice sheet of Iceland. *Earth Surface Processes and Landforms (25),* 59–76.

Brandsdóttir, B., Detrick, R., Driscoll, N., Fornari, D., Richter, D., Mayer, L., Calder, B. (2003). Shallow water multibeam bathymetry, high resolution Chirp Sonar and photographic investigation of pockmarks within the Tjörnes Fracture Zone, Northern Iceland. *Cruise Report:* 40 pp.

Brown, C.S., Newton, A.M.W., Huuse, M., Buckley, F. (2017). Iceberg scours, pits, and pockmarks in the North Falkland Basin. *Marine Geology 386:* 140-152. doi:10.1016/j.margeo.2017.03.001

Burke, M.J., Brennand, T.A., Sjogren, D.B. (2015). The role of sediment supply in esker formation and ice tunnel evolution. *Quaternary Science Reviews 115,* 50-77. doi:10.1016/j.quascirev.2015.02.017

Burki, V., Larsen, E., Fredin, O., Margreth, A. (2009). The formation of sawtooth moraine ridges in Bødalen, western Norway. *Geomorphology (105),* 182-192.

Caress, D.W., Chayes, D.N. (1995). New software for processing sidescan data from sidescan-capable multibeam sonars. *Proceedings of the IEEE Oceans 95 Conference,* 997-1000.

Chandler, B. M. P., Evans, D. J. A., Roberts, D. H. (2016). Characteristics of recessional moraines at a temperate glacier in SE Iceland: Insights into patterns, rates and drivers of glacier retreat. *Quaternary Science Reviews, 135,* 171–205.

Chandler, B.M.P., Evans, D.J.A., Roberts, D.H., Ewertowski, M., Clayton, A.I. (2015). Glacial geomorphology of the Skálafellsjökull foreland, Iceland: A case study of 'annual' moraines, *Journal of Maps, 12:5*, 904-916, doi: 10.1080/17445647.2015.1096216

Clark, C.D. (1993). Mega-scale glacial lineations and cross-cutting ice-flow landforms. *Earth Surface Processes and Landforms,* 18(1): 1-29. doi:10.1002/esp.3290180102

Clark, C.D. & Spagnolo, M. (2016) Glacially eroded cross-shelf troughs surrounding Iceland from Olex data. From: Dowdeswell, J.A., Canals, M., Jakobsson, M., Todd, B.J., Dowdeswell, E.K., Hogan, K.A. (eds) 2016. *Atlas of Submarine Glacial Landforms: Modern, Quaternary, and Ancient*. Geological Society, London, Memoirs, 46, 165 -166. doi:10.1144/M46.86

Clark, C., Tulaczyk, S., Stokes, C., Canals, M. (2003). A groove-ploughing theory for the production of mega-scale glacial lineations, and implications for ice-stream mechanics. *Journal of Glaciology, 49(165)*, 240-256. doi:10.3189/172756503781830719

Cohen, J., Stockwell Jr., J.W. (2006). CWP/SU: Seismic Unix Release No. 39: A Free Package for Seismic Research and Processing. *Center for Wave Phenomena*, Colorado School of Mines.

Decalf, C., Fugelli, E., Dowdeswell, J. (2013). The Seismic Architecture and Geometry of Glacial Grounding-Zone Wedges from Greenland and North Africa. [Abstarct]. Adapted from an oral presentation given at AAPG 3P Arctic Polar Petroleum Potential Conference & Exhibition, Stavanger, Norway, October 15-18, 2013. doi:10.13140/RG.2.1.4955.6242.

De Geer, G. (1940). Geochronologia Suecica Principles. Kungl. *Svenska Vetenskapsakademiens Handlingar III: 18: 6*, 367pp.

Demet, B. P., Nittrouer, J. A., Anderson, J. B., Simkins, L. M. (2018). Sedimentary processes at ice sheet grounding-zone wedges revealed by outcrops, Washington State (U.S.A.). *Earth Surface Processes and Landforms*. doi:10.1002/esp.4550

Domack, E.W., Powell, R. (2016). Modern glaciomarine environments and sediments, an Antarctic perspective. *Past Glacial Environments (2),* 181-272.

Dowdeswell, J.A., Jakobsson, M., Hogan, K.A., O'Regan, M., Backman, J., Evans, J., Hell, B., Löwemark, L., Marcussen, C., Noormets, R., Ó Cofaigh, C., Sellén, E., Sölvsten, M. (2010). High-resolution geophysical observations of the Yermak Plateau and northern Svalbard margin: implications for ice-sheet grounding and deep-keeled icebergs. *Quaternary Science Reviews, 29,* 3518-3521.

Dowdeswell, J.A., Fugelli, E.M.G. (2012). The seismic architecture and geometry of ground zone wedges formed at the marine margins of past ice sheets. *Geological Society of America Bulletin 124(11-12),* 1750-1761. doi:10.1130/B30628.1

Dowdeswell, J.A., Ottesen, D. (2016). A set of grounding-zone wedges in Vestfjorden, North Norway. From: Dowdeswell, J.A., Canals, M., Jakobsson, M., Todd, B.J., Dowdeswell, E.K., Hogan, K.A. (eds) 2016. *Atlas of Submarine Glacial Landforms: Modern, Quaternary, and Ancient*. Geological Society, London, Memoirs, 46, 229 -230. doi:10.1144/M46.135

Dowdeswell, J., Powell, R. (1996). Instruments and methods: Submersible remotely operated vehicles (ROVs) for investigations of the glacier-ocean-sediment interface. *Journal of Glaciology, 42(140),* 176-183. doi:10.3189/S002214300003063X

Dunlop, P., Clark, C.D., Hindmarch, R.C.A. (2008). Bed ribbing instability explanation: testing a numerical model of ribbed moraine formation arising from coupled flow of ice and subglacial sediment. *Journal of Geophysical Research 113,* F03005.

Dyke, A.S., Morris, T.F. (1988). Drumlin Fields, Dispersal trains and ice streams in Arctic *Canada. Can. Geogr., 32,* 86-90.

Dyke, A.S., Morris, T.F., Green, E.C., England, J. (1992). Quaternary geology of Prince of Wales Island, Arctic Canada*. Geol. Surv. Can. Mem., 433*.

Einarsson, Th. (1967). Zu der ausdehnung der weichselzeitlichen vereisung Nordislands. *Sonderveröffentlichungen des Geologischen Institutes der Universität Köln 13,* 167 -173.

Einarsson, P. (1991). Earthquakes and present-day tectonism in Iceland. *Tectonophysics, 189*, 261–279.

Einarsson, P. (2008). Plate boundaries, rifts and transforms in Iceland. *Jökull 58,* 35–58.

Einarsson, P., Sæmundsson, K. (1987). Earthquake epicenters 1982–1985 and volcanic systems in Iceland, map. In: *Sigfússon, Th. (Ed.),* Í hlutarins edli, Festschrift for Thorbjörn Sigurgeirsson, Menningarsjódur, Iceland.

Eiríksson, J. (2008). Glaciation events in the Pliocene – Pleistocene volcanic succession of Iceland. *Jökull (58),* 315-329.

Engelhardt, H., Kamb, B. (1997). Basal hydraulic system of a West Antarctic ice stream: constraints from borehole observations. *Journal of Glaciology 43 (144),* 207–230.

Etzelmuller, B., Hagen, J.O., Vatne, G., Ødegard, Sollid, J.L. (1996). Glacier debris accumulation and sediment deformation influenced by permafrost: examples from Svalbard. *Annals of Glaciology 22,* 53–62.

Evans, D.J.A. (1989). The nature of glaciotectonic structures and sediments at sub-polar glacier margins, northwest Ellesmere Island, Canada. *Geografiska Annaler 71A*, 113-123.

Evans, D. J. A., Ewertowski, M., Orton, C. (2015). Fláajökull (north lobe), Iceland: Active temperate piedmont lobe glacial landsystem, *Journal of Maps.* doi:10.1080/17445647.2015.1073185

Evans, D.J.A., Orton, C. (2015). Heinabergsjökull and Skálafellsjökull, Iceland: active temperate piedmont lobe and outwash head glacial landsystem, *Journal of Maps, 11:3,* 415-431, doi:10.1080/17445647.2014.919617

Evans, D.J.A., Rea, B.R. (1999). Geomorphology and sedimentology of surging glaciers: a land-systems approach. *Annals of Glaciology 28,* 75-82.

Evans, D.J.A., Roberts, D.H., Hiemstra, J.F., Nye, K.M., Wright, H., Steer, A. (2018). Submarginal debris transport and till formation in active temperate glacier systems: The southeast Iceland type locality. *Quaternary Science Reviews 195,* 72-108. doi:10.1016/j.quascirev.2018.07.002

Evans, D.J.A., Storrar, R.D., Rea, B.R. (2016). Crevasse-squeeze ridge corridors: Diagnostic features of late-stage palaeo-ice stream activity. *Geomorphology 258,* 40-50. doi:10.1016/j.geomorph.2016.01.017

Evans, D.J.A., Twigg, D.R. (2002) The active temperate glacial landsystem: a model based on Breiðamerkurjökull and Fjallsjökull, Iceland. *Quaternary Science Reviews 21 (20 21),* 2143-2177

Evans, D.J.A., Twigg, D.R., Rea, B.R., Shand, M. (2007). Surficial geology and geomorphology of the Brúarjökull surging glacier landsystem. *Journal of Maps, 3:1,* 349-367. doi:10.1080/jom.2007.9710850

Farnsworth, W.R., Ingólfsson, Ó., Retelle, M., Schomacker, A. (2016). Over 400 previously undocumented Svalbard surge-type glaciers identified. *Geomorphology 264,* 52-60. doi:10.1016/j.geomorph.2016.03.025

Fricker, H.A., Scambos, T. (2009). Connected subglacial lake activity on lower Mercer and Whillans Ice Streams, West Antarctica, 2003-2008. *Journal of Glaciology 55,* 303 315.

Geirsdóttir, Á. (2004). Extent and chronology of glaciations in Iceland; a brief overview of the glacial history. *Developments in Quaternary Sciences 2.* 175-182. doi: 10.1016/S1571-0866(04)80067-8

Geirsdóttir, Á., Eiríksson, J. (1994). Growth of an intermittent ice sheet in Iceland during the late Pliocene and early Pleistocene. *Quaternary Res. 42,* 115–130.

Geirsdóttir, Á., Eiríksson, J. (1996). A review of studies of the earliest glaciations in Iceland. *Terra Nova 8,* 400–414.

Geirsdóttir, Á., Harðardóttir, J., Eiriksson, J. (1997). Depositional history of the Younger Dryas(?)—Preboreal sediments, South Central Iceland. *Arctic, Antarctic, and Alpine Research. 29,* 13–23.

Geirsdóttir, Á., Harðardóttir, J., Sveinbjörnsdóttir, A.E. (2000). Glacial extent and catastrophic meltwater events during the deglaciation of southern Iceland. *Quaternary Science Reviews 19,* 1749-1761.

Geirsdóttir, Á., Miller, G.H., Andrews, J.T. (2007). Glaciation, erosion, and landscape evolution of Iceland. *Journal of Geodynamics 43:* 170-186. doi:10.1016/j.jog.2006.09.017

Geirsdóttir, Á., Miller, G.H., Axford, Y., Ólafsdóttir, S. (2009). Holocene and latest Pleistocene climate and glacier fluctuations in Iceland. *Quaternary Science Reviews 28.* 2107–2118

Glasser, N.F., Hambrey, M.J. (1998). Subglacial meltwater channels at Thurstaston Hill, Wirral and their significance for Late Devensian ice sheet dynamics. *Proceedings of the Geologists' Association*, *109,* 139-148.

Golledge, N.R., Stoker, M.S. (2008). A palaeo-ice stream of the British Ice Sheet in eastern Scotland. *Boreas, 35,* 231-243

Gudmundsdóttir E.R. (2010). Tephra stratigraphy and land-sea correlations: a tephrochronological framework based on marine sediment cores off North Iceland. PhD thesis, University of Iceland.

Gudmundsdóttir, E.R., Eiríksson, J., Larsen, G. (2011). Identification and definition of primary and reworked tephra in Late glacial and Holocene marine shelf sediments off North Iceland. *Journal of Quaternary Science 26,* 589–602. doi:10.1002/jqs.1474

Gray, L. (2005). Evidence for subglacial water transport in the West Antarctica Ice Sheet through three-dimensional satellite radar interferometry. *Geophysical Research Letters, 32.*

Hart, J.K. (1997). The relationship between drumlins and other forms of subglacial deformation. *Quaternary Science Reviews 16,* 93-108.

Hindmarsh, R.C.A. (1999). Coupled ice-till dynamics and the seeding of drumlins and bedrock forms. *Annals of Glaciology 28,* 221-230.

Hjartardóttir, Á.R., Einarsson, P., Magnúsdóttir, S., Björnsdóttir, Þ., Brandsdóttir, B. (2015) Fracture systems of the Northern Volcanic Rift Zone, Iceland: an onshore part of the Mid-Atlantic plate boundary. *Magmatic Rifting and Active Volcanism. Geological Society, London, Special Publications, 420,* doi:10.1144/SP420.1

Hjartarson, Á., Ingólfsson, Ó. (1988). Preboreal glaciation of southern Iceland. *Jökull 38,* 1-16.

Howarth, P.J. (1968). Geomorphological and Glaciological Studies, Eastern Breiðamerkurjökull, Iceland. Unpublished Ph.D. Thesis, University of Glasgow.

Hubbard, A., Sugden, D., Dugmore, A., Norðdahl, H., Pétursson, H.G. (2006). A modelling insight into the Icelandic Last Glacial Maximum ice sheet. *Quaternary Science Reviews 25:* 2283-2296. doi:10.1016/j.quascirev.2006.04.001

Hubbard, T.D., Reid, J.R. (2006). Analysis of flute forming conditions using ice sheet reconstructions and field techniques. *Geomorphology 74 (1-4),* 137-151. doi:10.1016/j.geomorph.2005.07.013

Huuse, M., Lykke-Andersen, H. (2000). Overdeepened Quaternary valleys in the eastern Danish North Sea: Morphology and origin, *Quat. Sci. Rev., 19,* 1233–1253.

Höfer, P. (2019). Morphodynamic features of Palaeo Ice Streams offshore N-Iceland based on Multibeam Bathymetric and High Resolution Chirp Seismic Data. MS Thesis, Faculty of Earth Sciences, University of Iceland, pp. 71.

Ingólfsson, Ó., Björck, S., Hafliðason, H., Rundgren, M. (1997). Glacial and climatic events in Iceland reflecting regional North Atlantic climatic shifts during the Pleistocene Holocene transition. *Quaternary Science Reviews 16*, 1135-1144.

Ingólfsson, Ó., Norðdahl, H. (1994). A review of the environmental history of Iceland, 13,000-9000 yr BP. *Journal of Quaternary Science 9*, 147-150.

Ingólfsson, Ó., Norðdahl, H., Schomacker, A. (2010). Deglaciation and Holocene Glacial History of Iceland. *Developments in Quaternary Sciences 13,* 51-68. doi:10.1016/S1571-0866(09)01304-9

Johnson, M.D., Benediktsson, Í.Ö, Björklund, L. (2013). The Ledsjö end moraine – a subaquatic push moraine composed of glaciomarine clay in central Sweden. *Proceedings of the Geologists' Association 124 (5),* 738-752. doi:10.1016/j.pgeola.2012.08.001

Johnson, M.D., Makinen, J.K., Peterson, G., Ojala, A.E.K., Palmu, J.K., Kajuutti, K., Öhrling, C., Ahokangas, E. (2018) Geomorphology and distribution of subglacial triangular hummocks (murtoos) in Sweden and Finland. *Abstracts of the Nordic Geological Winter Meeting 2018, 10–12.1.2018*, 172.

Joughin, I., Gray, L, Bindschadler, R., Price, S., Morse, D., Hulbe, C., Mattar, K., Werner, C. (1999). Tributaries of West Antarctic ice streams revealed by RADARSAT interferometry. *Science 286 (5438),* 283-286.

Joughin, I., Smith, B.E., Howat, I.M., Scambos, T., Moon, T. (2010). Greenland flow variability from ice-sheet-wide velocity mapping. *Journal of Glaciology. 56 (197),* 415–430.

Jóhannesson, H. (1985). Um endaleppu hraunin undir Eyjafjöllum og jökla síðasta jökulskeiðs. *Jökull, 35,* 83-95.

Jóhannesson, H. and Sæmundsson, K., 1998. Geological map of Iceland. Bedrock geology. Icelandic Inst Natur Hist, Reykjavík.

Jørgensen, F. and Sandersen, P. B. E. (2006). Buried and open tunnel valleys in Denmark erosion beneath multiple ice sheets, *Quat. Sci. Rev., 25,* 1339–1363.

Kajuutti K, Mäkinen J.K., Ahokangas E, Ojala, A., Palmu J.P. (2018). New subglacial landforms detected from LiDAR data. *Abstracts of the Nordic Geological Winter Meeting 2018, 10–12.1.2018,* 175.

Kaldal, I., Víkingsson, S. (1991). Early Holocene deglaciation in Central Iceland. *Jökull 40,* 51-66.

Kalin, M. (1971). The active push moraine of the Thompson Glacier, Axel Heiberg Island, Canadian Arctic Archipelago. *McGill University, Axel Heiberg Island, Research Report. Glaciology, vol. 4*. McGill University, Montreal.

King, E., Hindmarsh, R., Stokes, C. (2009). Formation of mega-scale glacial lineations observed beneath a West Antarctic ice stream. *Nature Geoscience 2(8),* 585–588

Knudsen, K.L., Eiríksson, J. (2002) Application of tephrochronology to the timing and correlation of palaeoceanographic events recorded in Holocene and Late Glacial shelf sediments off North Iceland. *Marine Geology 191,* 165-188.

Knudsen, K.L., Jiang, H., Jansen, E., Eiríksson, J., Heinemeier, J., Seidenkrantz, M.-S. (2004). Environmental changes off North Iceland during the deglaciation and the Holocene: foraminifera, diatoms and stable isotopes. *Marine Micropaleontology 50,* 273-305.

Kor, P.S.G., Shaw, J., Sharpe, D.R. (1991). Erosion of bedrock by subglacial meltwater, Georgian Bay, Ontario: A regional view. *Canadian journal of Earth Sciences 28(4),* 623-642. doi:10.1139/e91-054

Kristjánsdóttir, G.B., Geirsdóttir, Á, Harðardóttir, J., Helgadóttir, G., Andrews, J.T., Jennings, A.E., Sveinbjörnsdóttir, Á.E. (1999). Loftslags- og umhverfisbreytingar norðan Íslands frá 12.300 BP. *Vorráðstefna 1999*, Ágrip erinda og veggspjalda. Jarðfræðafélag Íslands bls. 19-20.

Kristjánsdóttir, G.B., Stoner, J.S., Jennings, A.E., Andrews, J.T., Grönvold, K. (2007). Geochemistry of Holocene cryptotephras from the North Iceland Shelf (MD99-2269): intercalibration with radiocarbon and palaeomagnetic chronostratigraphies. *The Holocene 17, 2,* 155-176.

Lien, R., Rye, N. (1988). Formation of saw-toothed moraines in front of the Bødalsbreen glacier, western Norway. *Norsk Geologisk Tidsskrift (68),* 21–30.

Livingstone, S.J., Ó Cofaigh, C., Stokes, C.R., Hillenbrand, C.D., Vieli, A., Jamieson, S.S.R. (2013). Glacial geomorphology of Marguerite Bay Palaeo-Ice stream, western Antarctic Peninsula, *Journal of Maps, 9,* 558-572.

Livingstone, S.J., Clark, C.D. (2016). Morphological properties of tunnel valleys of the southern sector of the Laurentide Ice Sheet and implications for their formation. *Earth Surface Dynamics, 4*, 567-589.

Lundqvist, J. (2000) Palaeoseismicity and De Geer Moraines. *Quaternary International 68 71*, 175-186. doi:10.1016/S1040-6182(00)00042-2

MacLean, B., Blasco, S., Bennett, R., Hughes Clarke, J.E., Patton, E. (2016). Mega-scale glacial lineations, Peel Sound, Canadian Arctic Archipelago. From: Dowdeswell, J.A., Canals, M., Jakobsson, M., Todd, B.J., Dowdeswell, E.K., Hogan, K.A. (eds) 2016. *Atlas of Submarine Glacial Landforms: Modern, Quaternary, and Ancient*. Geological Society, London, Memoirs, 46, 47-48, doi:10.1144/M46.89

Magnúsdóttir, S., Brandsdóttir, B., Driscoll, N., Detrick, R. (2015). Postglacial tectonic activity within the Skjálfandadjúp Basin, Tjörnes Fracture Zone, offshore Northern Iceland, based on high resolution seismic stratigraphy. *Marine Geology 367, 159-170*. doi:10.1016/j.margeo.2015.06.004

Makinen, J, Kajuutti, K, Ahokangas, E, Ojala, AEK and Palmu, J-P (2018) Sedimentology of murtoos – new subglacial landforms detected from LiDAR data in SW Finland. In Belmonte, L and 16 others (eds), *Abstracts of the Nordic Geological Winter Meeting 2018*, 10–12.1.2018, Copenhagen, Denmark: Geological Society of Denmark, pp. 176–177.

Margold, M., Stokes, C.R., Clark, C.D. (2015). Ice streams in the Laurentide Ice Sheet: Identification, characteristics and comparison to modern ice sheets. *Earth-Science Reviews 143,* 117-146.

Matthews, J.A., Cornish, R., Shakesby, R.A. (1979). "Saw-tooth" moraines in front of Bødalsbreen, southern Norway. *Journal of Glaciology (88),* 535–546.

McCracken, R.G., Iverson, N.R., Benediktsson, Í.Ö., Schomacker, A., Zoet, L.K., Johnson, M.D., et al. (2016). Origin of the active drumlin field at Múlajökull, Iceland: New insights from till shear and consolidation patterns. *Quaternary Science Reviews 148*, 243-260.

Menzies, J., Hess, D.P. (2013) Depositional features. In: *Shroder, J.F. (Ed.), Treatise on Geomorphology. Academic Press, San Diego*, 127-140.

Menzies, J., Hess, D.P., Rice, J.M., Wagner, K.G., Ravier, E. (2016). A case study in the New York Drumlin Field, an investigation using microsedimentology, resulting in the refinement of a theory of drumlin formation. *Sedimentary Geology 338,* 84-96.

Morgan, V. I., Jacka, T.H., Akerman, G.J., Clarke. A.L. (1982). Outlet glacier and mass budget studies in Enderby, Kemp, and MacRobertson Lands, Antarctica, *Annals of Glaciology, 3*, 204 – 210.

Norrman, J.O. (1964). Lake Vattern. Investigation on shore and bottom morphology, hydrology, *Geografiska Annaler 46 (1-2)*, 53-69. (Abstr.)

North Greenland Ice Core Project members. (2004). North Greenland Ice Core Project Oxygen Isotope Data. *IGBP PAGES/World Data Center for Paleoclimatology Data Contribution Series # 2004-059.* NOAA/NGDC Paleoclimatology Program, Boulder CO, USA.

Norðdahl, H. (1991). A review of the glaciation maximum concept and the deglaciation of Eyjafjörður, North Iceland. In J.K. Maizels and C Caseldine (eds.), *Environmental Changes in Iceland: Past and Present,* Kluwer Academic Publishers, Dordrecht, 31 47.

Norðdahl, H., Hafliðason, H. (1992). The Skógar tephra, a Younger Dryas marker in North Iceland. *Boreas 21*, 23-41.

Norðdahl, H., Ingólfsson, Ó., Pétursson, H.G., Hallsdóttir, M. (2008). Late Weichselian and Holocene environmental history of Iceland. *Jökull 58:* 343-364.

Norðdahl, H., Ingólfsson, Ó. (2015) Collapse of the Icelandic ice sheet controlled by sea level rise? *Arktos, 1-13*. doi:10.1007/s41063-015-0020-x

Norðdahl, H., Pétursson, H.G. (2005). Relative sea-level changes in Iceland: new aspects of the Weichselian deglaciation of Iceland. *Developments in Quaternary Science 5*, 25-78.

Ó Cofaigh, C., Pudsey, C.J., Dowdeswell, J.A., Morris, P. (2002) Evolution of subglacial bedforms along a paleo-ice stream, Antarctic Peninsula continental shelf. *Geophysical Research Letters 29(8).* doi:10.1029/2001GL014488

Ó Cofaigh, C., Stoke, C.R., Lian, O.B., Clark, C.D., Tulacyzk, S. (2013). Formation of mega-scale glacial lineations on the Dubawnt Lake Ice Stream bed: 2. Sedimentology and stratigraphy. *Quaternary Science Reviews 77:* 210-227. doi:/10.1016/j.quascirev.2013.06.028

Ó Cofaigh, C., Livingstone, S.J., Dowdeswell, J.A. (2016). Mega-scale glacial lineations in Marguerite Trough, Antarctic Peninsula. From: Dowdeswell, J.A., Canals, M., Jakobsson, M., Todd, B.J., Dowdeswell, E.K., Hogan, K.A. (eds) 2016. *Atlas of Submarine Glacial Landforms: Modern, Quaternary, and Ancient*. Geological Society, London, Memoirs, 46, 175-176. doi:10.1144/M46.72

Ojala, A.E.K. (2016). Appearance of De Geer moraines in southern and western Finland Implications for reconstructing glacier retreat dynamics. *Geomorphology 255,* 16-25. doi:10.1016/j.geomorph.2015.12.005

Ojala, A.E.K., Peterson, G., Makinen, J., Johnson, M.D., Kajuutti, K., Palmu, J.P., Ahokangas, E., Öhrling, C. (2018). Ice-sheet scale distribution and morphometry of triangular-shaped hummocks (murtoos): a subglacial landform produced during rapid retreat of the Scandinavian Ice Sheet. *Annals of Glaciology,* 1-12. doi:10.1017/aog.2019.34

Ottesen, D., Dowdeswell, J.A., Rise, L. (2005). Submarine landforms and the reconstruction of fast-flowing ice streams within a large Quaternary ice sheet: the 2500-km-long Norwegian-Svalbard margin (57° to 80°N). *Geological Society of America Bulletin, 117,* 1033-1050

Ottesen, D., Dowdeswell, J.A. (2006). Assemblages of submarine landforms produced by tidewater glaciers in Svalbard. *Journal of Geophysical Research Atmospheres 111(F1),* F01016, doi:10.1029/2005JF000330

Ottesen, D., Dowdeswell, J.A., Lanvik, J.Y., Mienert, J. (2007). Dynamics of the Late Weichselian ice sheet on Svalbard inferred from high-resolution sea-floor morphology, *Boreas, 36,* 286-306

Ottesen, D., Dowdeswell, J., Benn, D., Kristensen, L., Christiansen, H., Christensen, O., Vorren, T. (2008). Submarine landforms characteristic of glacier surges in two Spitsbergen fjords. *Quat Sci Rev 27(15),* 1583–1599.

Patterson, C. J. (1997). Southern Laurentide ice lobes were created by ice streams: Des Moines Lobe in Minnesota, USA, *Sediment. Geol.*, 249–261.

Patton, H., Hubbard, A., Bradwell, T., Schomacker, A. (2017). The configuration, sensitivity and rapid retreat of the Late Weichselian Icelandic ice sheet. *Earth-Science Reviews 166:* 223-245. doi:10.1016/j.earscirev.2017.02.001

Pearce, B., Tappin, D.R., Dove, D., Pinnion, J. (2012). 42-Benthos Supported by the Tunnel Valleys of the Southern North Sea. *GeoHAB Atlas of Seafloor Geomorphic Features and Benthic Habitats 2012,* 597-612.

Peterson, G., Johnson, M. and Öhrling, C. (2018). Sedimentological and morphological implications for the understanding of murtoo formation in Sweden. In Belmonte, L and 16 others (eds), *Abstracts of the Nordic Geological Winter Meeting 2018,* 10 12.1.2018, Copenhagen, Denmark, p. 177.

Pétursson, H.G., Norðdahl, H., Ingólfsson, O. (2015). Late Weichselian history of relative sea level changes in Iceland during a collapse and subsequent retreat of marine based ice sheet. *Cuadernos de Investigación Geográfica 41 (2),* 261-277.

Piotrowski, J. A. (1994). Tunnel-valley formation in northwest Germany–geology, mechanisms of formation and subglacial bed conditions for the Bornhöved tunnel valley, *Sediment. Geol*., 89, 107–141.

Price, R.J. (1970). Moraines at Fjallsjökull, Iceland, *Arctic and Alpine Research, 2*, 27-42.

Principato, S. M., Jennings, A. E., Kristjánsdóttir, G. B., Andrews, J. T. (2005). Glacial marine of subglacial origin of diamicton units from the southwest and North Iceland Shelf: implications for the glacial history of Iceland. *Journal of Sedimentary Research 75,* 698–983.

Principato, S.M., Moyer, A.N., Hampsch, A.G., Ipsen, H.A. (2016). Using GIS and streamlined landforms to interpret palaeo-ice flow in northern Iceland. *Boreas, Vol. 45*, 470–482. doi:10.1111/bor.12164. ISSN 0300-9483.

Rea, B.R., Evans, D.J.A. (2011). An assessment of surge-induced crevassing and the formation of crevasse squeeze ridges. *Journal of geophysical research 116, F04005*, doi:10.1029/2011JF001970

Rignot, E., Mouginot, J., Scheuchl, B. (2011). Ice flow of the Antarctic Ice Sheet. *Science 333 (6048),* 1427–1430.

Rydningen, T.A., Vorren, T.O., Laberg, J.S., Kolstad, V. (2013). The marine-based NW Fennoscandian ice sheet: glacial and deglacial dynamics as reconstructed from submarine landforms, *Quaternary Science Reviews, 68,* 126-141

Schoof, C. (2007). Ice sheet grounding line dynamics: Steady states, stability, and hysteresis. *Journal of Geophysical Research: Earth Surfaces 112 (F3),* 19.

Schoof C., Clarke G. K. C. (2008). A model for spiral flows in basal ice and the formation of subglacial flutes based on a Reiner-Rivlin rheology for glacial ice. *Journal of Geophysical Research 113,* B05024. doi:10.1029/2007JB004957

Sharp, M. (1985). Crevasse-fill ridges: a landform type characteristic of surging glaciers? *Geografiska Annaler Series A – Physical Geography 67 (3/4)*, 213-220.

Shaw, J., Pugin, A., Young, R.R. (2008). A meltwater origin for Antarctic shelf bedforms with special attention to megalineations. *Geomorphology 102,* 364-375. doi:10.1016/j.geomorph.2008.04.005

Shipp, S.S., Anderson, J.B., Domack, E.W. (1999). Late pleistocene-holocene retreat of the West Antarctic Ice-sheet system in the Ross sea: Part 1 – Geophysical results. *Geological Society of America Bulletin, 111,* 1486-1516.

Sigmundsson, F., Einarsson, P., Hjartardóttir, Á.R., Drouin, V., Jónsdóttir, K., Árnadóttir, T., Geirsson, H., Hreinsdóttir, S., Li, S., Ófeigsson, B.G. (2018). Geodynamics of Iceland and the signatures of plate spreading. *Journal of Volcanology and Geothermal Research.* doi:10.1016/j.volgeores.2018.08.014

Simkins, L.M., Greenwood, S.L., Anderson, J.B. (2018). Diagnosing ice sheet grounding line stability from landform morphology. *The Cryosphere 12(8),* 2707-2726. doi: 10.5194/tc-12-2707-2018

Slabon, P., Dorschel, B., Jokat, W., Myklebust, R., Hebbeln, D., Gebhardt, C. (2016). Greenland ice sheet retreat history in the northeast Baffin Bay based on high resolution bathymetry. *Quaternary Science Reviews, 154,* 182-198.

Søndergaard, M., Jeppesen, E., Jensen, J.P. (2005). Late glacial and Holocene palaeoclimatic fluctuations on the North Icelandic shelf – foraminiferal analysis, sedimentology and tephrochronology of core MD992275. PhD Dissertation, Aarhus Geoscience.

Spagnolo, M, Clark, C.D., Ely, J.C., Stokes, C.R., Anderson, J.B., Andreassen, K., Graham, A.G.C., King, E.C. (2014). Size, shape and spatial arrangement of mega-scale glacial lineations from a large and diverse datasat. *Earth Surface Processes and Landforms 39,* 1432-1448.

Stefánsson, R., Gudmundsson, G., Halldorsson, P. (2008). Tjörnes fracture zone. New and old seismic evidences for the link between the North Iceland rift zone and the Mid Atlantic ridge. *Tectonophysics 447,* 117-126. doi:10.1016/j.tecto.2006.09.019

Stokes, C., Clark, C. (1999). Geomorphological criteria for identifying Pleistocene ice streams. *Annals of Glaciology 28,* 67-74. doi:10.3189/172756499781821625

Stokes, C., Clark, C. (2001) Palaeo-ice streams. *Quaternary Science Reviews, 20,* 1437 1457.

Stokes, C., Clark, C. (2002). Ice stream shear margin moraines. *Earth Surf. Process. Landforms, 27*, 547-558.

Storrar, R.D., Stokes, C.R., Evans, D.J.A. (2013). A map of large Canadian eskers from Landsat satellite imagery. *Journal of Maps, 9:3,* 456-473. doi: 10.1080/17445647.2013.815591

Streuff, K., Forwick, M., Szczucinski, W., Andreassen, K., Ó Cofaigh, C. (2015). Submarine landform assemblages and sedimentary processes related to glacier surging in Kongsfjorden, Svalbard. *Arktos 1:14,* 1-19. doi:10.1007/s41063-015-0003-y

Tulaczyk, S., Scherer, R.P., Clark, C.D. (2001). A ploughing model for the origin of weak tills beneath ice streams: a qualitative treatment. *Quaternary International 86,* 59-70.

Ussing, N. V. (1993). Om Jyllands hedesletter og teorierne for deres Dannelse, Oversigt over Det Kongelige Danske Videnskabernes Selskabs Forhandlingar, 2, 1–152, (in Danish).

van den Broeke, M., Bamber, J., Ettema, J., Rignot, E., Schrama, E., van der Berg, W.J., van Meijgaard, E., Velicogna, I., Wouters, B. (2009). Partitioning recent Greenland mass loss. *Science 326 (5955),* 984–986.

Vreeland, N.P., Iverson, N.R, Graesch, M., Hooyer, T.S. (2015) Magnetic fabrics of drumlins of the Green Bay Lobe, southeastern Wisconsin. *Quaternary Science Reviews 112*, 33-44.

Wessel, P., Smith. W.H.F. (1991). Free software helps map and display data. *Eos, 72,* 441 448.

Winklemann, D., Jokat, W., Jensen, L., Schenke, H.W. (2010) Submarine end moraines on the continental shelf off NE Greenland – Implications for Late glacial dynamics. *Quaternary Science Reviews, 29,* 1069-1077. doi:10.1016/j.quascirev.2010.02.002

Wingfield, R. (1990). The origin of major incisions within the Pleistocene deposits of the Sea, *Mar. Geol., 91*, 31–52.

Winsborrow, M.C.M., Clark, C.D., Stokes, C.R. (2004). Ice streams of the Laurentide Ice Sheet. *Géographie Physique et Quaternaire 58 (2–3),* 269–280.

Winsborrow, M.C.M., Clark, C.D., Stokes, C.R. (2010). What controls the location of ice streams? *Earth-Science Reviews 103,* 45-59. doi:10.1016/j.earscirev.2010.07.003

Wright, H. E. (1973). Tunnel Valleys, Glacial Surges, and Subglacial Hydrology of the Superior Lobe, Minnesota, *Geol. Soc. Am. Mem., 136,* 251–276.